United Technologies

Research Center

Intensification of transport processes in fluid-filled porous media by sound waves. Application to Fuel Cell technology

ONR Contract N00014-02-C-0061

Final Report

Prepared By
United Technologies Research Center
411 Silver Lane
East Hartford, CT 06108

Prepared For
Office of Naval Research
800 North Quincy Street
Arlington, VA 22217-5660

Principal Investigator: Dr. Alexander Staroselsky

Research Team:
Dr. A. Staroselsky,
Dr. I. Fedchenia;
Dr. W. Lin;
L. Turner

31 January 2004

REPORT DOCUMENTATION PAGE

Form Approved
OMB No. 0704-0188

1. REPORT DATE *(DD-MM-YYYY)*	2. REPORT TYPE	3. DATES COVERED *(From - To)*
	31-Jan-2004	March 1, 2002 - October 31, 2003

4. TITLE AND SUBTITLE

Intensification of transport processes in fluid-filled porous media by sound waves. Application to Fuel Cell technology

5a. CONTRACT NUMBER

N00014-02-C-0061

5b. GRANT NUMBER

5c. PROGRAM ELEMENT NUMBER

6. AUTHOR(S)

Alexander Staroselsky (PI)

Igor Fedchenia,

Wenlong Li

5d. PROJECT NUMBER

5.600.0012

5e. TASK NUMBER

5f. WORK UNIT NUMBER

7. PERFORMING ORGANIZATION NAME(S) AND ADDRESS(ES)

United Technologies Research Center, East Hartford, CT, 06108

8. PERFORMING ORGANIZATION REPORT NUMBER

9. SPONSORING/MONITORING AGENCY NAME(S) AND ADDRESS(ES)

ONR, Arlington, VA

10. SPONSOR/MONITOR'S ACRONYM(S)

11. SPONSOR/MONITOR'S REPORT NUMBER(S)

12. DISTRIBUTION/AVAILABILITY STATEMENT

unlimited

13. SUPPLEMENTARY NOTES

14. ABSTRACT

In this work we aim developing a novel theoretical framework to evaluate the feasibility of attaining significant improvement of fuel cells performance and stability by increasing the transport processes in porous partially fluid filled cathode compartment through the application of acoustic and structural waves. We have developed a unified model of structural/acoustic wave propagation in the PEM cathode compartment and coupled it with mass transfer in the porous media. A novel generalized filtration law that accounts for dynamic loadings, varying saturation, and solid structure distortion describing mass transfer in this complex but generic system has been found. It has been demonstrated that vibration gives rise to net change of saturation inside porous medium. Based on the numerical and experimental results number of practical recommendations optimizing material selections and performance regime has been made. Developed methodology is useful for wide range of Fuel Cell problems as well as for wide range of other porous structures and could serve as an important design tool.

15. SUBJECT TERMS

Acoustics, partially saturated porous media, mass transfer; fuel cell, constitutive equations, homogenization technique, numerical methods

16. SECURITY CLASSIFICATION OF:			17. LIMITATION OF ABSTRACT	18. NUMBER OF PAGES	19a. NAME OF RESPONSIBLE PERSON
a. REPORT	b. ABSTRACT	c. THIS PAGE			19b. TELEPHONE NUMBER *(Include area code)*
unclassified	unclassified	unclassified		84	

This page is intentionally left blank

Summary

A fuel cell is an electrochemical energy conversion device that combines hydrogen and oxygen (from the air) to produce electricity. Currently, the Proton Exchange Membrane technology (PEM) is the most promising and is being developed by United Technologies Fuel Cells. One of the major obstacles in the commercialization of PEMFC technology is the performance loss at high current density due to liquid water accumulation in the porous components of the cathode compartment. This accumulation limits oxygen transport to the cathode and reduces PEMFC efficiency and performance stability.

In this work we aim developing a novel theoretical framework to evaluate the feasibility of attaining significant improvement of fuel cells performance and stability by increasing the transport processes in porous partially fluid filled cathode compartment through the application of acoustic and structural waves. The specific goal of the project is to develop a generic model of partially saturated multiphase flow in highly porous media (Fuel Cell cathode compartment) under structural waves.

We have developed a unified model of structural/acoustic wave propagation in the PEM cathode compartment and coupled it with mass transfer in the porous media. This is the first known to authors model of such kind fully coupling acoustics and filtration in porous medium. A new perturbation technique allows deriving the governing equations for multiphase flow under acoustic streaming. It has been demonstrated that the phase saturations have strong impact on wave dynamics in porous continuum. Explicit expressions for generalized multiphase Biot-type coefficients that explicitly depend on the phase saturations have been obtained. A novel generalized filtration law that accounts for dynamic loadings, varying saturation, and solid structure distortion describing mass transfer in this complex but generic system has been found. We also have been able to connect hysteretic phenomena to relaxation process due to filtration velocity gradient. The Lagrangian approach has been employed in order to develop consistent government equations. We have also conducted highly precise tests on flow measurements throughout porous media with and without applied acoustic signals.

The developed homogenization technique allows deducing effective body forces in mass transfer equations from acoustic terms and simple analytical evaluation of frequency and wave number dependencies of the effective mass driving body forces. It has been demonstrated using averaging principle that vibration gives rise to net change of saturation inside porous medium. This effect is analogous to the known phenomenon of acoustic streaming but has not been discovered before.

Numerical results demonstrate that applied structural vibration/acoustic loading *(i)* intensifies the process dynamics or in other words decreases time of transient process; (*ii*) might drain out up to 5-10% of distributed in porous media water if the mechanism preventing reverse acoustic-driven imbibitions is in place; (*iii*) The fast water removal from the surface is crucial for acoustic-driven drying. Based on the numerical and experimental results number of practical recommendations optimizing material selections and performance regime has been made. Developed methodology is useful for wide range of Fuel Cell problems as well as for wide range of other porous structures and could serve as an important design tool.

Table of Content

Program Overview

Technical Objectives

In this work our target is to develop a theoretical framework to evaluate the feasibility of attaining significant improvement of fuel cells performance and stability by increasing the transport processes in porous fluid filled cathode compartment through the application of acoustic and structural waves. The specific goal of the project is to develop a generic model of unsaturated multiphase flow in highly porous media (Fuel Cell cathode compartment) under structural waves.

In order to attain this goal the novel model predicting effects of structural acoustics on partially saturated mass transfer as well as effect of dynamic saturation on wave characteristics should be developed.

To the best of our knowledge, structural or acoustic excitation has never been applied to the fuel cells in particular and to the porous membranes in general. This project combines computational and experimental efforts including:

1) Developing of fully coupled physics-based model of structural and acoustic waves propagation in partially water- filled porous media and induced multiphase (gas/water) transport through the partially water- filled vibrating porous media;
2) Experimental calibration and verification of the models using company-developed rigs and fuel cells;
3) Numerical demonstration of transport process and fuel cell performance enhancement.

Technical Approach

We aim to improve the efficiency of a PEM fuel cell by intensifying the gas/water transport processes using either structural or acoustic waves. Structural excitation can be used for inducing waves that would propagate within the different layers of the fuel cell and perturb the trapped liquid water within pores, thereby enhancing the transport process. Introducing pulsations in the airflow past the cathode can also intensify the diffusion process; this is expected to set up pressure gradients in the fuel cell that would pull the trapped water cavities into the air stream.

The first step in this effort involves choosing of the modeling strategy. All possible approaches can be separated into two categories: 1. Continuum mechanics analysis including wave propagation and mass transfer analysis; and 2) Micro-structural / micro-mechanical considerations accounted for the local interactions. The second approach is good for the analysis of the role of material morphology but not suitable for waves and flux analysis. We chose the macroscopic (continuum mechanics) modeling approach, which is the best suitable for the analysis of wave propagations, multiphase fluxes (not one or even hundreds droplets) in real geometry and for coupling acoustic and mass transfer properties and time-scales The macroscopic modeling framework naturally (i) provides a unified system of governing equations describing the whole physical system; (ii) provides the solution of problems with real geometry,

layers, configuration, regimes, and boundary conditions; (iii) investigates effect combining both "elastic-wave" part and "viscous – mass transfer" part coupling transport and acoustic properties; (iv) the dynamic model provides a comprehensive description of multiphase flux, amount of trapped water and system behavior during drainage and imbibitions – hysteresis.

The second step, which will be reported, is the development of the novel governing equations accounted for multiphase unsaturated flow in vibrating porous media. The system should be developed in a consistent way to accommodate simultaneously all physical phenomena. Using the developed governing system (i) We study wave propagation and attenuation in partially saturated porous media. (ii) We calculate different waves in the structure and couple them with pressures and water/gas fluxes. (iii) We calculate inhomogeneous water saturation level with space and time – S(x,t) and relate it with oxygen transport. (iv) This approach needs to be matched with micromechanics in order to complete the governing system with constitutive laws.

This is followed by validation of the models in developed controlled laboratory experiments. We conduct highly precise tests on flow measurements throughout porous media with and without applied acoustic signals. Also, we conduct the full scale test on company developed Fuel Cell in order to compare power output with and without acoustic impact and under different acoustic regimes. These tests serve as model calibration and validation.

The validated models will then be used for predicting the level of structural/acoustic response needed for achieving the targeted improvements in fuel cell performance. The high-level actuation methodology will be chosen based on energy and efficiency considerations. The choice of actuation scheme will then be used to identify promising actuator design.

The major accomplishments are as follows:

(i) We have developed a unified model of structural/acoustic wave propagation in the PEM cathode compartment and coupled it with multiphase mass transfer in the partially saturated porous media. This is the first successful attempt to model coupling between acoustics and filtration in porous massive.
(ii) It has been demonstrated that the phase saturations have strong impact on wave dynamics in porous continuum. Explicit expressions for generalized multiphase Biot-type coefficients that explicitly depend on the phase saturations have been obtained. We also have been able to connect hysteretic phenomena to relaxation process due to filtration velocity gradient.
(iii) A novel generalized filtration law (generalized D'Arcy law) that accounts for dynamic loadings, varying saturation, and solid structure distortion describing mass transfer in this complex but generic system has been developed.
(iv) The new developed homogenization technique is crucial for numerical analysis of high frequency impacts. It allows circumventing the restriction on maximum allowed number of finite elements to resolve spatial frequency of the acoustic wave. Using asymptotic analysis we obtain simple analytical evaluations of frequency and wave number dependencies of the effective mass driving forces
(v). We conduct the extremely precise experimental procedure to measure bi-layer/substrate permeability under vibration. Test results for different substrates demonstrate *(i)* existence of the

effect, *(ii)* instability in highly hydrophobic structures under vibration and the need in wave generation.
(vi) Extensive numerical analysis of the vibration-induced mass transfer has been conducted and on the base of obtained numerical results (as well as experimental data) we have made the practical conclusions focused on (i) industrial (fuel cells) implementation and (ii) optimal material design rwequirements and operational conditions (iii) fundamental understanding of mass transfer in unsaturated porous media.

Developed methodology is useful for wide range of Fuel Cell problems as well as for wide range of other porous structures and could serve as an important design tool.

Technical Accomplishments

1. Technical Background and Problem Formulation

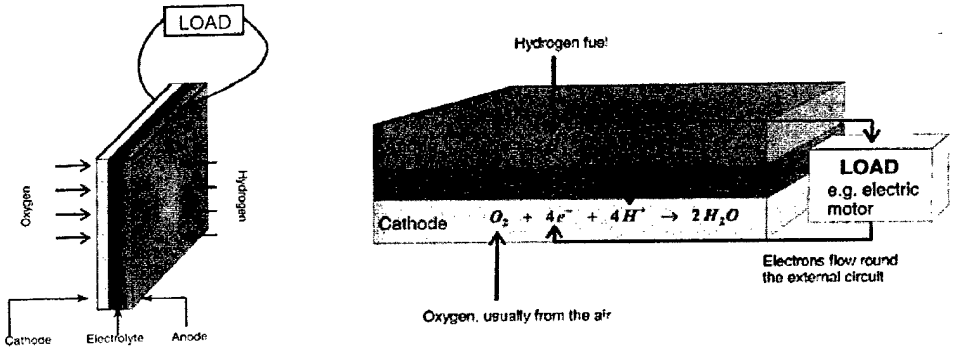

Figure 1. Basic Cathode-electrolyte-anode construction of Fuel Cell and electrode reactions [1]

The basic physical structure, or building block, of a fuel cell consists of an electrolyte layer in contact with a porous anode and cathode on either side as shown in Figure 1. The cells run on hydrogen, which reacts with oxygen from the air in such a way that a voltage is generated between two electrodes. The electrolyte in this Fuel Cell is the ion exchange membrane (Nafion or other similar polymers) and is an excellent proton (H^+) conductor. The electrons flow to the external circuit generating current.

Transport and reaction processes at the cathode limit PEMFC performance. Oxygen present in the air stream flowing through the channels in the so-called bipolar plate (BPP), is transferred to the platinum (Pt) catalytic particles that are dispersed in pores throughout the cathode, through a porous diffusion layer and a porous sub-layer (not shown in Figure 1). Water produced by the electrochemical reaction at the cathode is partially evacuated through the same porous medium to the air stream.

Limitations of PEM cell performance at useful current densities ($\geq$0.5 A/cm^2) are primarily dominated by mass transfer of water. The power density (i.e. W/cm^2) of PEM cells is typically highest at the current density at which performance starts to drop drastically due to reaching the

so-called "limiting current". In order to deploy PEM fuel cells in high power density applications (e.g. automobiles and ships), stable performance must be achieved at these high current densities. As the power density increases, the weight, volume, and cost of the fuel cell system all decrease, all of which are critical metrics for successful market penetration.

In order to obtain high current density, oxygen must be transported to and water removed from the electrochemically active catalyst sites. In a sense, the necessity for water removal comes from its role in inhibiting mass transfer of oxygen. Since the PEMFC operates at a low temperature, water hang up (known as cathode flooding) in a liquid state is unavoidable. This not only impacts PEMFC performance but also leads to performance instability [2]. Ideally, the water that has been produced at the cathode is driven to the air channel where the air would entrain excessive liquid water. At the same time this airflow would supply the necessary oxygen for the fuel cell. Thus, the directions of oxygen and water flows are opposite to each other.
In this work we analyze the feasibility of trapped water removing and increase of the material effective permeability by application of structural waves to the system. There have been a

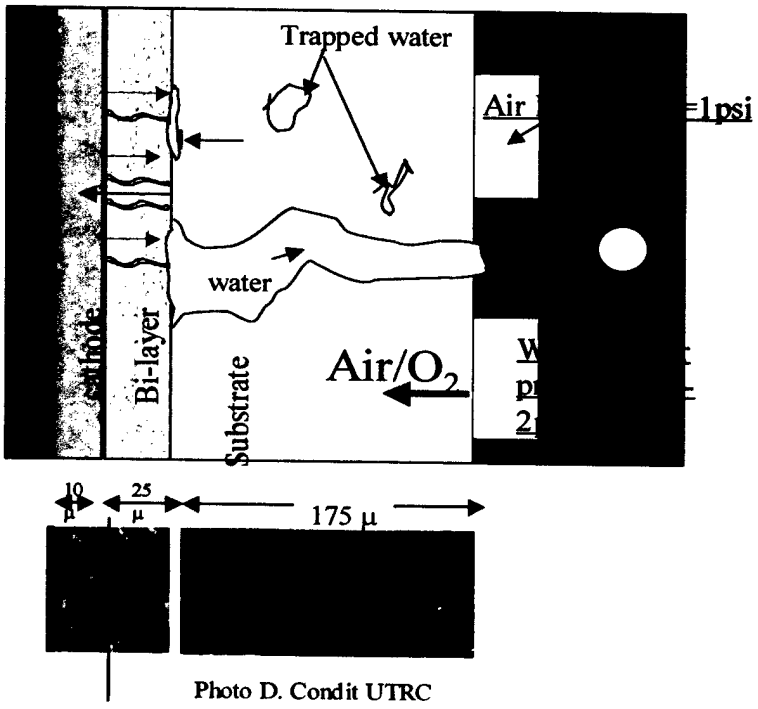

Figure 2. Structure of Fuel Cell Cathode compartment and directions of major mass flows.

number of works analyzing waves propagation in fully saturated porous media [3, 4] – so called Biot models. All known to us publications study the influence of properties of porous materials and fully saturated them fluids on waves characteristics. In contrast, we study wave propagation and attenuation in partially saturated porous media and extend Biot's approach for multiphase (solid, fluid, and gas) media. Also, we develop a novel approach combining both "elastic-wave"

part and "viscous – mass transfer" part coupling transport and acoustic properties. In other words we, first, develop a generic model allowing us to evaluate water and gas transfer induced by structural waves. We calculate characteristics of different waves in the structure and couple them with water/gas pressures and induced inhomogeneous in space and time water saturation level– S(x,t) and, also, relate it with oxygen transport answering the practical question – could the structural waves increase oxygen transport to catalytic sites. Generally, we develop the first model of acoustic streaming in unsaturated porous structures.

As shown in Figure 2, the cathode compartment is the layered structure of three porous materials with different morphology. The role of morphology in wave propagation is crucial and affects all model parameters, such as Biot parameters and Leverett-function, in other words, water transfer depends on morphology and is different in bi-layer and substrate. At low saturation flow is always channeled and water can be decomposed into connected water and trapped water. Trapped water does not "feel" external pressure and, subsequently does not move to WTP, blocking oxygen paths. Trapped water is the "trace" of water "lost from the mainstream." There are two competitive processes – imbibitions (from main stream) and drainage to the mainstream and structural or acoustic waves depending on their parameters might effectively "clean" or vise versa "spurge" the porous media changing the effective cross section of oxygen path as shown in Figure 3. Only structural vibrations might induce transport of such trapped water "mega-droplets". Parameters and characteristics of the most beneficial waves (for example, rotational or compression) need to be defined by numerical analysis for real-life geometry using the implemented model.

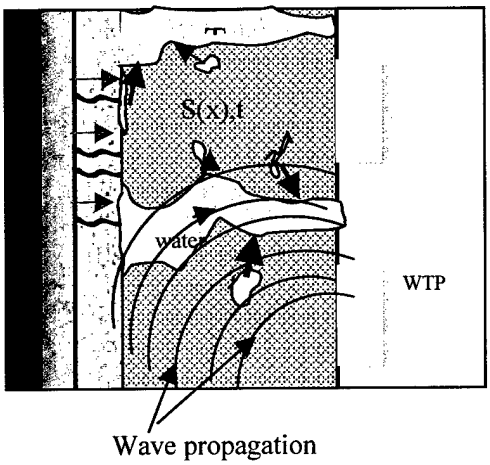

Figure 3. Schematic effect of waves on water transfer

In this first annual report we present our results on executing the contract according to the statement of work. The plan of this technical progress report is as follows: 1) Problem Formulation (above); timetables and budget. The report is continued with physics-based 2) Model Approach and Equations' derivation using the fact that characteristic time scale of structural waves/vibrations is much smaller than characteristic time of mass transfer and that wave amplitude is small. 3) New asymptotic technique has been developed and we report some obtained analytical solutions. 4) In order to calibrate the model and verify the model predictions we conduct two different sets of experiments. In this progress report we review the first Experimental Results and Technique for the permeability measurements with and without applied vibration. We close this progress report with some concluding remarks and the list of tasks that left to be executed during the work on the contract.

2. Scale for description of multiphase flow in vibrating porous medium.

For the description of the flow in the real macro structures one requires the scale of description l that is much less than the structure size but much larger than the size of a pore of the porous material - $\{l_{pore} << l << L_{device}\}$. This allows for continuum mechanics type of description of fluid

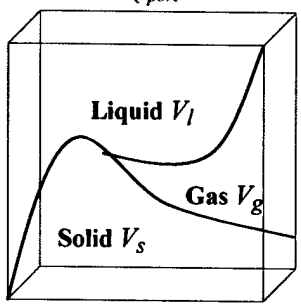

Fig.4. Mesoscopic volume $V = V_s + V_l + V_g$ for averaging procedure. It is small enough to consider all velocities constant and large enough to include many pores.

flow and vibration wave propagation, with the structure specific being taken care of by the geometry and boundary conditions of the domain and with porous medium specifics being incorporated into coefficients of the resulting system of equations. The later must be either measured experimentally or calculated with other methods that allow explicit description of the material morphology.

The chosen intermediate scale requires that the equations to be formulated through variables averaged or smoothed over l_{pore} scale. The usual procedure (see e.g. [5 and 6]) is to split the solution domain into sub-domains of the size l, Fig.4, and substitute all pertinent quantities like kinetic and elastic energies, mass flows, stresses and local pressures, with the quantities averaged of the volume of the sub-domain.

Multiphase materials deformations are always inhomogeneous at microscale, consisting of

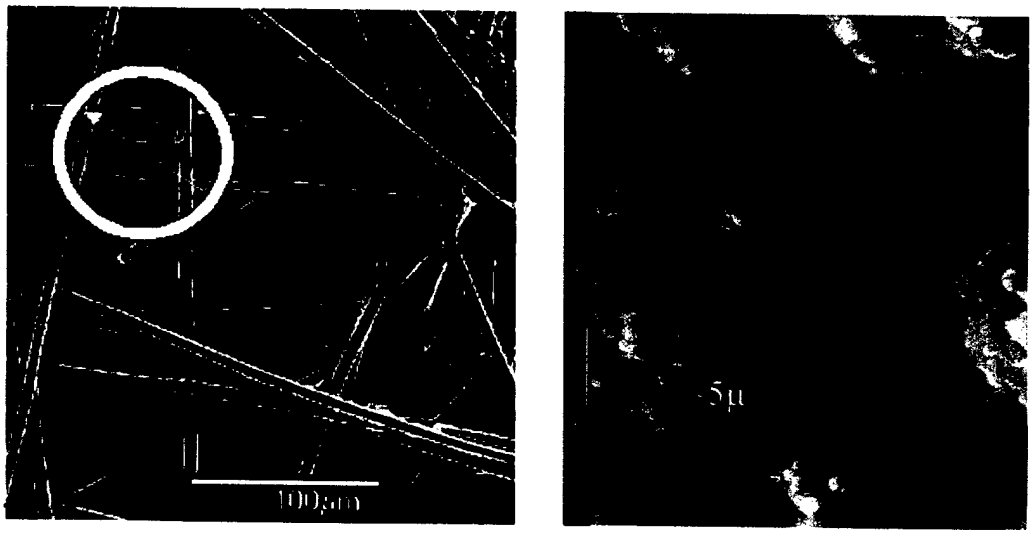

Figure 5. Microstructure of porous materials of FC cathode compartment

various constituents with different properties. Increasing the elementary volume of materials, we

homogenize the properties. A [minimal] statistically representative material volume is called Representative Volume Element (RVE) [6]. An RVE must include a large number of micro-elements to represent local continuum properties. Fuel Cells cathode compartment consists of three porous layers with different morphology, which predefines the characteristic size of the RVE. Thus, for Toray paper (sub-layer) with the typical pore-element size is about 20 μ in width and 3μ in depth, average size of RVE will be a block with the dimensions $l \times l \times b \sim 100\mu \times 100\mu \times 20\mu$. For the by-layer with the typical size of 3μ the average RVE size is 15 μ to ensure that at least a hundred microstructural objects are averaged in the RVE (as can be seen from the micrographs in Fig 5. Photo D. Condit, UTRC). In further consideration all sub-volumes are considered as points and all differential operations are understood in space of these points. The values of all physical quantities are equal to average values of the same quantities over the sub-volume. In this problem, we assign three characteristics (for solid, liquid, and gas) for each material point instead of one as used in single material analysis. The following notations are used in each material point:

$\{\mathbf{u}_s, \mathbf{u}_l, \mathbf{u}_g\}$ - displacement of solid, liquid and gas fractions;

$\{\mathbf{v}_s, \mathbf{v}_l, \mathbf{v}_g\}$ - velocities of solid, liquid and gas fractions;

$\{V_s, V_l, V_g\}$ - volumes of solid, liquid and gas phases;

$V_s + V_l + V_g = V$;

$\{\varepsilon_s, \varepsilon_l, \varepsilon_g\} = \left\{\frac{V_s}{V}, \frac{V_l}{V}, \frac{V_g}{V}\right\}$ - volume fractions of solid, liquid and gas phases;

$\varepsilon_s + \varepsilon_l + \varepsilon_g = 1$;

$\{\rho_s, \rho_l, \rho_g\}$ - densities of solid, liquid and gas fractions;

3. Lagrange formulation of the elastic vibration and inclusion of dissipation

The complete problem formulation of elastic waves propagation in porous medium filled with several fluids requires formulation of conservative part that results in vibration of all constitutive media and dissipative part that accounts for fluid viscosity and elastic energy dissipation in the solid matrix. For correct account of vibration impact on the flow dissipative and elastic terms must be mixed in visco-elastic constitutive relations of Maxwell-Voight type that involve both stress-strain and stress-strain rates pairs. Although for many materials parameters of visco-elastics constitutive relations have been measured and/or computed, the same for porous materials and especially for the recently invented porous membranes are absent. Here, we suggest simplified approach that is based on the fact that the time scales of vibration induced with the external source in kHz range and higher and filtration of fluids in the porous matrixes are very well separated. Additionally, computational implementation becomes much more simple as it allows natural computation of elastic part in Lagrangian coordinates and filtration part in the Eulerian ones.

The problem, therefore, is to split the formulation of Free Energy functional for the whole problem into Lagrange function for elastic vibration of all constituents, which has originally been formulated by Biot [3], and the part that is responsible for filtration due to slow varying gradients of hydrostatic pressures. Subsequently, various dissipation mechanisms are included to obtain generalization of the Darcy law and hysteresis phenomena.
Thus, the goal is to derive expressions for kinetic energy K, elastic energy U and dissipative function R in terms of averaged over representative volume physical quantities. Having in mind that generally all three functions depend on $\{\mathbf{u}, \mathbf{v}, \partial\mathbf{u}/\partial x\}$, the final equations have the following form:

$$\frac{\partial}{\partial x}\left(\frac{\partial L}{\partial(\partial\mathbf{u}/\partial x)}\right)+\frac{\partial}{\partial x}\left(\frac{\partial R}{\partial(\partial\mathbf{v}/\partial x)}\right)+\frac{\partial}{\partial t}\left(\frac{\partial L}{\partial\mathbf{v}}\right)-\frac{\partial L}{\partial\mathbf{u}}-\frac{\partial R}{\partial\mathbf{v}}=0 \qquad (1)$$

where $L = K - U$ and x is coordinate vector.

Theory of liquid flow through porous media uses equation of mass balance closed with the help of Darcy equation. It is the purpose of this work to show how vibration waves described by the system (1) influence filtration rate. The main philosophy of this approach is to add small elastic vibrations and mass transport induced by them "on top" of viscous flow. It is done in the further paragraphs.

3.1 Kinetic energy *K*.

Original Biot equations [3] have been derived for only one phase filling the porous medium. Two or more phases coexisting inside porous matrix require additional treatment and general guidelines on how to write correctly the mass tensor. The correct expressions for the mass tensor in fully saturated by single-phase porous media (Biot problem) have been recently obtained by an averaging procedure in [7]. We generalize this approach for the multiphase situation in order to obtain consistent expression for the kinetic energy and inertia force as functions of constituents.

We are looking for expression for kinetic energy $K=\frac{1}{2}\left(\rho_s\mathbf{v}_s^2+\rho_l\mathbf{v}_l^2+\rho_g\mathbf{v}_g^2\right)$ through averaged over some small volume of porous medium V values of $\{\langle\mathbf{v}_s\rangle,\langle\mathbf{v}_l\rangle,\langle\mathbf{v}_g\rangle\}$, where symbol $\langle\ldots\rangle=\frac{1}{V}\int_V dV\langle\ldots\rangle$ means averaging procedure over the RVE as shown on illustration Figure 5.

Each phase velocity $\{\mathbf{v}_s,\mathbf{v}_l,\mathbf{v}_g\}$ can be re- written as a sum of its average value and a deviation as follows: $\{\langle\mathbf{v}_s\rangle+\Delta\mathbf{v}_s,\langle\mathbf{v}_l\rangle+\Delta\mathbf{v}_l,\langle\mathbf{v}_g\rangle+\Delta\mathbf{v}_g\}$. Spatially averaged kinetic energy is a sum of terms with averaged squares of partial velocities, which can be expressed in the following form:

$$\langle K\rangle=\frac{1}{2}\left(\rho_s\left\langle \mathbf{v}_s^2\right\rangle+\rho_l\left\langle \mathbf{v}_l^2\right\rangle+\rho_g\left\langle \mathbf{v}_g^2\right\rangle\right)=$$

$$\frac{1}{2}\left(\rho_s\varepsilon_s\left\langle\left(\langle \mathbf{v}_s\rangle+\Delta\mathbf{v}_s\right)^2\right\rangle+\rho_l\varepsilon_l\left\langle\left(\langle \mathbf{v}_l\rangle+\Delta\mathbf{v}_l\right)^2\right\rangle+\rho_g\varepsilon_g\left\langle\left(\langle \mathbf{v}_g\rangle+\Delta\mathbf{v}_g\right)^2\right\rangle\right) \tag{2}$$

It is important to note that volume fractions $\{\varepsilon_s,\varepsilon_l,\varepsilon_g\}$ appears before averaging operation due to the fact that velocities $\{\mathbf{v}_s,\mathbf{v}_l,\mathbf{v}_g\}$ are non-zero only in their respective sub-domains $\{V_s,V_l,V_g\}$ within a RVE. Modifying (2) we get the expression for the averaged over RVE kinetic energy:

$$\langle K\rangle=\frac{1}{2}\left(\rho_s\varepsilon_s\langle \mathbf{v}_s\rangle^2+\rho_l\varepsilon_l\langle \mathbf{v}_l\rangle^2+\rho_g\varepsilon_g\langle \mathbf{v}_g\rangle^2+\rho_s\varepsilon_s\left\langle\left(\Delta\mathbf{v}_s\right)^2\right\rangle+\rho_l\varepsilon_l\left\langle\left(\Delta\mathbf{v}_l\right)^2\right\rangle+\rho_g\varepsilon_g\left\langle\left(\Delta\mathbf{v}_g\right)^2\right\rangle\right)$$

Due to solid matrix rigidity the term $\rho_s\varepsilon_s\left\langle\left(\Delta\mathbf{v}_s\right)^2\right\rangle$ is usually small and we neglect it from further consideration. To close system of equations of motion one has to assume relations between $\left\{\left\langle\left(\Delta\mathbf{v}_l\right)^2\right\rangle,\left\langle\left(\Delta\mathbf{v}_g\right)^2\right\rangle\right\}$ and $\left\{\langle \mathbf{v}_s\rangle,\langle \mathbf{v}_l\rangle,\langle \mathbf{v}_g\rangle\right\}$ as was pointed out in [7].

To obtain classical Biot kinetic energy terms for two phases flow, only $\left\{\left\langle\left(\Delta\mathbf{w}_l\right)^2\right\rangle,\left\langle\left(\Delta\mathbf{w}_g\right)^2\right\rangle\right\}$ should be expressed through mean velocities of constituents:

$$\begin{vmatrix}\left\langle\left(\Delta\mathbf{v}_l\right)^2\right\rangle\\ \left\langle\left(\Delta\mathbf{v}_g\right)^2\right\rangle\end{vmatrix}=\begin{vmatrix}\beta_l & \beta_{gl}\\ \beta_{gl} & \beta_g\end{vmatrix}\cdot\begin{vmatrix}\langle \mathbf{v}_l-\mathbf{v}_s\rangle^2\\ \langle \mathbf{v}_g-\mathbf{v}_s\rangle^2\end{vmatrix} \tag{3}$$

This parameterization is similar to the assumption of Poissonian statistics for velocities fluctuations. The final expression for the average kinetic energy in this case is as follows:

$$2\langle K\rangle=\rho_s\varepsilon_s\langle \mathbf{v}_s\rangle^2+\rho_l\varepsilon_l\langle \mathbf{v}_l\rangle^2+\rho_g\varepsilon_g\langle \mathbf{v}_g\rangle^2+\left(\rho_l\varepsilon_l\beta_l+\rho_g\varepsilon_g\beta_{gl}\right)\left(\langle \mathbf{v}_l\rangle-\langle \mathbf{v}_s\rangle\right)^2+$$
$$\left(\rho_l\varepsilon_l\beta_{gl}+\rho_g\varepsilon_g\beta_g\right)\left(\langle \mathbf{v}_g\rangle-\langle \mathbf{v}_s\rangle\right)^2 \tag{4}$$

One phase situation that has been treated by Biot corresponds to only one term -$\left\langle\left(\Delta\mathbf{v}_l\right)^2\right\rangle$ and $2\beta_l+1=a$- tortuosity in Biot's notation. In the two-fluid model β_{gl} describes correlation between relative motion of gas versus solid and correspondent motion liquid and vise versa.

The dynamic force acting on a system is the derivative of the kinetic energy with respect to velocity. Using (4) we can obtain the following form for (inertia) D'Alamber force:

$$\mathbf{F}^{\text{D'Alamber}} = \begin{pmatrix} \mathbf{F}_s^{\text{DAlamber}} \\ \mathbf{F}_l^{\text{DAlamber}} \\ \mathbf{F}_g^{\text{DAlamber}} \end{pmatrix} = \frac{\partial}{\partial t} \cdot \begin{pmatrix} \frac{\partial}{\partial \mathbf{v}_s}\langle K \rangle \\ \frac{\partial}{\partial \mathbf{v}_l}\langle K \rangle \\ \frac{\partial}{\partial \mathbf{v}_g}\langle K \rangle \end{pmatrix} = \frac{\partial}{\partial t} \cdot \left(\begin{array}{c|c|c} \rho_s \varepsilon_s + & & \\ \rho_l \varepsilon_l \beta_l + \rho_g \varepsilon_g \beta_{gl} + & -\rho_l \varepsilon_l \beta_l - \rho_g \varepsilon_g \beta_{gl} & -\rho_l \varepsilon_l \beta_{gl} - \rho_g \varepsilon_g \beta_g \\ \rho_l \varepsilon_l \beta_{gl} + \rho_g \varepsilon_g \beta_g & & \\ \hline -\rho_l \varepsilon_l \beta_l - \rho_g \varepsilon_g \beta_{gl} & \rho_l \varepsilon_l + & \\ & \rho_l \varepsilon_l \beta_l + \rho_g \varepsilon_g \beta_{gl} & 0 \\ \hline -\rho_l \varepsilon_l \beta_{gl} - \rho_g \varepsilon_g \beta_g & 0 & \rho_g \varepsilon_g + \\ & & \rho_l \varepsilon_l \beta_{gl} + \rho_g \varepsilon_g \beta_g \end{array} \right) \cdot \begin{pmatrix} \mathbf{v}_s \\ \mathbf{v}_l \\ \mathbf{v}_g \end{pmatrix} \quad (4a)$$

It is important that all elements of mass matrix explicitly depend on' volume fractions of constituents, that easy to relate with local fluid/gas saturations. This is the new result because classical Biot theory considers only fully saturated porous media and the solid body porosity is the primary characteristics of that. Now, the mass matrix depends on volume fractions and cross-correlations between relative phases motions that need to be approximated and/or experimentally measured. Usage of the averaging procedure allows explaining of non-diagonal form of the mass tensor in the Biot model [3]. It also provides connection between experimentally measured fluid densities and effective densities that is to be used in equation for wave propagation (1).

3.2 Elastic energy *U*

Usage of averaging procedure of the previous paragraph allows explaining non-diagonal form of the mass tensor in the Biot model [3]. It also provides connection between experimentally measured fluid densities and effective densities that is to be used in equation for wave propagation (1). One can also try to use the same averaging procedure as was used above, for the derivation of the averaged elastic energy U as a function of displacements averaged over RVE. This would be analogous to derivation of turbulent models, fluctuations being imposed by the randomness of the porous matrix rather than by the local flow instability. However, as numerous attempts to derive elastic constants show [4], those expressions strongly depend on material morphology. Here, we follow more pragmatic approach of Biot [3] and derive expressions[1] for elastic energy with parameters being measurable in specified set of experiments or calculated using direct microscale modeling. More important that for our purpose is sufficient to combine correctly equally phenomenological theories of liquid stagnation in porous media with the Biot-type vibration equations.

With standard notations of theory of elasticity small strain is

$e_{ij} = \frac{1}{2}\left(\frac{\partial u_i}{\partial x_j} + \frac{\partial u_j}{\partial x_i} \right)$ and $\theta = e_{11} + e_{22} + e_{33}$ - is dilatation. Because there are no stresses in the elastic body at zero strain, and stress is the derivative of elastic energy with respect to strain, there should be no linear terms in the energy expansion on strain. Terms with power higher then three would mean existence of several metastable states typical for phase transformations and

[1] Of course, we use phenomenological considerations here, so it is derivation in physical but pure mathematical sense.

not existing in elasticity. The expression for elastic energy can be written in the general form as follows:

$$U =$$

$$\frac{1}{2}\lambda\cdot\theta_s^2 + 2\mu\cdot\sum_{ij} e_{ij}\cdot e_{ij} + \qquad \text{self elastic energy of porous solid} \qquad (5)$$

$$\Im_l\left(\theta_s,\theta_l\right) + \Im_g\left(\theta_s,\theta_g\right) + \qquad \text{energy of liquid and gas dependent on solid distortion}$$

We assume there is no shear in gas phase. Additionally, taking into account that liquid flow rate in porous media is very low; we may neglect the shear component in liquid strain tensor. Therefore, the elastic energy for gas and liquid phases depends only on volume change or, in other words, strain dilatation. Stress tensor for solid matrix and pressures for liquid and gas can be obtained by taken correspondent derivatives:

$$\sigma_{ij}^s = \frac{\partial U}{\partial e_{ij}} = \lambda\cdot\theta_s\cdot\delta_{ij} + 2\cdot\mu\cdot e_{ij} + \frac{\partial\Im_l\left(\theta_s,\theta_l\right)}{\partial\theta_s} + \frac{\partial\Im_g\left(\theta_s,\theta_g\right)}{\partial\theta_s}$$

$$\sigma_{ij}^l = -\varepsilon_l\cdot p_l\cdot\delta_{ij} = \frac{\partial U}{\partial\theta_l} = \frac{\partial\Im_l\left(\theta_s,\theta_l\right)}{\partial\theta_l} \qquad (6)$$

$$\sigma_{ij}^g = -\varepsilon_g\cdot p_g\cdot\delta_{ij} = \frac{\partial U}{\partial\theta_g} = \frac{\partial\Im_g\left(\theta_s,\theta_g\right)}{\partial\theta_g}$$

Here δ_{ij} is Kronecker delta with components of unity matrix. Functions $\Im_{l,g}\left(\theta_s,\theta_{l,g}\right)$ account for the pressure change due to liquid and gas motion under solid deformation. The models for $\Im_{l,g}\left(\theta_s,\theta_{l,g}\right)$ are discussed in separate paragraph. Below we consider some special cases and the corresponding potential energy forms.

3.2.1 Small vibrations

In the absence of large motions and near equilibrium between all three phases, U can be expanded up to the second terms in $\left(\theta_s,\theta_{l,g}\right)$. As has been already discussed above, it means that at this internal state, reaction of all phases on applied deformation is reversible and elastic. We emphasize here that the theory we are constructing in this work is elastic correction to the "pre-existing" viscous flow. This assumption is fully justified for small vibrations, when signal magnitude does not exceed 5% of structural characteristic size. Naturally, bigger loads would lead to the structure fatigue failure.

Thus, in the absence of large motions and near equilibrium between all three phases, U can be expanded up to the second terms in $(\theta_s, \theta_{l,g})$, where $(\theta_{l,g})$ is defined as $(\Theta_g, \Theta_l) = ({}^{filtr}\Theta_g + \theta_g, {}^{filtr}\Theta_l + \theta_l)$:[2]

$U = U_s + U_{sl} + U_{sg} + U_l + U_g + U_{gl}$,

where

$U_s = \frac{1}{2}\lambda \cdot \theta_s^2 + 2 \cdot \mu \cdot \sum_{ij} e_{ij} \cdot e_{ij}$ - self-elastic energy of porous solid;

$U_{sl} = M_{ls} \cdot \theta_l \cdot \theta_s + M_{gs} \cdot \theta_g \cdot \theta_s$ - energy of interaction between liquid and solid and gas and solid;

$U_l = \frac{1}{2} M_l \cdot \theta_l^2; U_g = \frac{1}{2} M_g \cdot \theta_g^2$ -self-elastic energy of liquid and gas;

$M_{gl} \cdot \theta_l \cdot \theta_g$ -energy of interaction between liquid and gas;

$P_l \cdot \Theta_l + P_g \cdot \Theta_g$ -energy of interaction between liquid and gas and correspondent static pressures; and simple form for $\Im_{l,g}(\theta_s, \Theta_{l,g}) = P_{l,g} \cdot \varepsilon_{l,g} \cdot \Theta_{l,g}$ has been chosen.

Here, M_l and M_g are self influence bulk coefficients for liquid and gas correspondently, M_i, $(i = ls, gs, gl)$ are coefficients of mutual interaction. Constitutive relations relating stresses (pressures) and strains are obtained by differentiation of elastic energy with respect to strain tensor and take the form:

$$\sigma_{ij}^s = \frac{\partial U}{\partial e_{ij}} = \lambda \cdot \theta_s \cdot \delta_{ij} + 2 \cdot \mu \cdot e_{ij} + M_{ls} \cdot \theta_l + M_{gs} \cdot \theta_g$$

$$\sigma_{ij}^l = -\varepsilon_l \cdot p_l \cdot \delta_{ij} = \frac{\partial U}{\partial \theta_l} = M_l \cdot \theta_l + M_{ls} \cdot \theta_s + M_{gl} \cdot \theta_g \qquad (7)$$

$$\sigma_{ij}^g = -\varepsilon_g \cdot p_g \cdot \delta_{ij} = \frac{\partial U}{\partial \theta_g} = M_g \cdot \theta_g + M_{gs} \cdot \theta_s + M_{gl} \cdot \theta_l$$

3.2.2 Biot theory

In his original paper [3] Biot considered fully saturated porous media with only one liquid. He also disregards porous pressure P_l^{pore}. Under these simplifications, from relationship (7) setting

---

[2] (Here, $({}^{filtr}\Theta_g, {}^{filtr}\Theta_l)$ are quasi equilibrium values of liquid and gas dilations caused by static pressures, conditions of quasi equilibrium being $\frac{\partial \Im_{l,g}(\theta_s, {}^{filtr}\Theta_{l,g})}{\partial \theta_{l,g}} = 0$.)

all gas-related parameters as well as P_l^{pore} to zero we obtain the constitutive relations:

$$\sigma_{ij}^{s} = \frac{\partial U}{\partial e_{ij}} = \lambda \cdot \theta_s \cdot \delta_{ij} + 2 \cdot \mu \cdot e_{ij} + M_l \cdot \gamma_l \cdot \theta_l$$
$$\sigma_{ij}^{l} = -\phi \cdot p_l \cdot \delta_{ij} = \frac{\partial U}{\partial \theta_l} = M_l \cdot \theta_l + M_l \cdot \gamma_l \cdot \theta_s \qquad (8)$$

We substituted liquid volume fraction from (7) with material porosity, which, by definition, equals volume fraction of pores in the solid. Due to the fact that solid is fully saturated; liquid volume fraction is identically equal to the porosity. Thus, we deduced Biot's constitutive model from ours as a limiting case.

By this point we have considered Lagrangian and its constituents. In other words, we have derived all relations describing the *elastic* behavior of the system. In order to complete "elastic part" modeling and before we switch to dissipative effects, we would consider developing methodology for constitutive model coefficients (M_i and γ_i) determination.

4 Elastic-Biot-type coefficients

4.1 Effective Media

First, all Biot coefficients can be expressed directly from the effective bulk moduli of porous media, matrix, and a fluid [4]. The problem of estimating the effective properties is not trivial but might be performed by methods developed in the theory of mixtures [8]. Generally, the best we can do is to predict upper and low bounds of the effective parameters, because its precise value depends on geometrical details. It is important to note that all such estimates work well only for isotropic media. The extended review of methods is given in [8].

The best achievable bounds without specifying geometrical details are the Hashin-Shtrikman bounds [9]:

$$K^{HS\pm} = K_1 + \frac{\varepsilon_2}{(K_2 - K_1)^{-1} + \varepsilon_1 (K_1 + \frac{4}{3}\mu_1)^{-1}};$$
$$\mu^{HS\pm} = \mu_1 + \frac{\varepsilon_2}{(\mu_2 - \mu_1)^{-1} + \frac{2\varepsilon_1 (K_1 + 2\mu_1)}{5\mu_1 (K_1 + \frac{4}{3}\mu_1)}}. \qquad (9)$$

where K_i are bulk moduli of phases, μ_i are shear moduli of phases, and ε_i are volume fractions. These estimations for Toray paper (in-plane) are:

$1.2 \cdot 10^{-4} Gpa \equiv 17.4\ Psi \equiv K_{air} \le K \le K^{HS+} = 3.33\ Msi \equiv 23\ GPa$, where initial fibers compressibility has been taken equal $K_{fiber} = 20 Msi = 130 GPa$, $\mu_{fiber} = 25 msi = 160 GPa$

Bounds for shear modulus are $0 \equiv \mu_{air} \le \mu \le \mu^{HS+} = 4.5\ Msi \equiv 31\ GPa$. Difference in upper and low bounds are extremely large as expected, because there are significant differences in matrix and inclusion properties. Experimental data for in-plane elastic constants varies from 40 Ksi till

140 Ksi. We assume that $K_{test} = 60\ Ksi$[3]. We apply empirical approach of Marion [8, p. 177] and calculate the weight coefficient, which reduces the upper bounds to experimentally measured values: $w = \frac{M_{test} - M^-}{M^+ - M^-} \approx 0.018$. Thus we should expect in plane $\mu_{test} \approx 0.018 \cdot 31\ GPa = 558\ KPa = 80\ Ksi$. Measurements throughout the thickness gives extremely low number of $K_\perp \approx 1500\ psi$. This might be modeled using Hashin-Shtrikman bounds if we imagine that fibers contact only over small "point-like" area and effective porosity in this direction would be $\varepsilon_\perp \approx 0.9997$. Indeed, $\varepsilon \approx 1 - d^2_{contact} / D^2_{between} = 1 - 1/3600 = 0.9997$ and $K^{HS+} \approx 5000\ psi$[4].

There is also known test result that compression modulus of the composite of Toray paper and bi-layer together is 1699 psi. Assuming weights proportional to the thickness of each layer (25 μm and 175 μm) we might estimate $K_{bylayer} \approx 1.5 - 2.5\ Ksi$. Hashin-Shtikman estimates based on dual porosity give bounds $150\ psi = K^{HS-} \le K < K^{HS+} = 7\ Msi = 50\ GPa$. Such a big difference arose because we did not take into account the compactions of sintered powder. As noted by M. Kachanov, the stiffness of the media decreased when the pore shape is concave and we'd better use Mori-Tanaka approximation.

4.2 Estimation of Biot Coefficients for Solid-Liquid-Gas System

The "elastic" system that we consider now has the following general form:

$$\begin{aligned}
\sigma^s_{ij} &= \lambda \cdot \theta_s \cdot \delta_{ij} + 2 \cdot \mu \cdot e_{ij} + M_{ls} \cdot \theta_l + M_{gs} \cdot \theta_g \\
\sigma^l_{ij} &= -\varepsilon_l \cdot p_l \cdot \delta_{ij} = M_{ls} \cdot \theta_s + M_l \cdot \theta_l + M_{gl} \cdot \theta_g \\
\sigma^g_{ij} &= -\varepsilon_g \cdot p_g \cdot \delta_{ij} = M_{gs} \cdot \theta_s + M_{gl} \cdot \theta_l + M_g \cdot \theta_g
\end{aligned} \tag{10}$$

First, the dependence of the Biot coefficients on saturation is evaluated. It is clear that to satisfy the relations above near the limits $\varepsilon_l \to 0$ and $\varepsilon_g \to 0$, the elastic constants must have the following dependency on saturations:

$$\begin{aligned}
M_{ls} &= \varepsilon_l \cdot m_{ls}; M_{gl} = \varepsilon_l \cdot m_{gl}; M_l = \varepsilon_l \cdot m_l \\
M_{gs} &= \varepsilon_g \cdot m_{gs}; M_{gl} = \varepsilon_g \cdot m_{gl}; M_g = \varepsilon_g \cdot m_g
\end{aligned} \tag{11}$$

From this it follows

[3] We understand that there were attempts to measure Young modulus, so Bulk modulus should be about 3 times smaller for isotropic materials.

[4] Porosity here depends on the area of contacts and might vary a lot. We also can approximate the experiments if we use previously described Marion weight factors and $d \approx 5\ \mu m$, and subsequently, $\varepsilon = 1 - 25/3600 \approx 0.993$; $K \approx 0.018 \cdot \left(K^{HS} = 75\ Ksi\right) = 1350\ psi$.

$$M_{gl} = \varepsilon_l \cdot \varepsilon_g \cdot m_{gl}$$

Comparing Biot coefficients [3] for two-phase case:

$$M_{sf}^{Biot} = \frac{\left(1 - \varepsilon_s - \frac{K}{K_s}\right)\varepsilon_s K_s}{1 - \varepsilon_s - K/K_s + \varepsilon_s K_s/K_l}$$
$$M_f^{Biot} = \frac{(\varepsilon_s)^2 K_s}{1 - \varepsilon_s - K/K_s + \varepsilon_s K_s/K_l} \qquad (12)$$

where index f stands for "fluid" (gas or liquid), with the equations for $\{M_{l,g}, M_{ls}, M_{gs}, M_{gl}\}$ above one gets:

$$M_{ls} = \frac{\left(1 - \varepsilon_s - \frac{K}{K_s}\right)\varepsilon_l K_s}{1 - \varepsilon_s - K/K_s + \varepsilon_s K_s/K_l} = \varepsilon_l \cdot m_{ls} \qquad M_{gs} = \frac{\left(1 - \varepsilon_s - \frac{K}{K_s}\right)\varepsilon_g K_s}{1 - \varepsilon_s - K/K_s + \varepsilon_s K_s/K_g} = \varepsilon_g \cdot m_{gs}$$
$$M_l = \frac{\varepsilon_l \cdot \varepsilon_s \cdot K_s}{1 - \varepsilon_s - K/K_s + \varepsilon_s K_s/K_l} = \varepsilon_l \cdot m_l \qquad M_g = \frac{\varepsilon_g \cdot \varepsilon_s \cdot K_s}{1 - \varepsilon_s - K/K_s + \varepsilon_s K_s/K_g} = \varepsilon_g \cdot m_g \qquad (13)$$

And finally, defining moduli $K_s = \sigma/\theta_s$; $K_l = -p_l/\theta_l$; $K_g = -p_g/\theta_g$ one gets:

$$\begin{aligned}
&(K_b - K_s)\cdot\theta_s + M_{ls}\cdot\theta_l + M_{gs}\cdot\theta_g = 0 \\
&M_{ls}\cdot\theta_s + (M_l - \varepsilon_l p_l)\cdot\theta_l + M_{gl}\cdot\theta_g = 0 \\
&M_{gs}\cdot\theta_s + M_{gl}\cdot\theta_l + (M_g - \varepsilon_g p_g)\cdot\theta_g = 0
\end{aligned} \qquad (14)$$

This homogeneous linear system has a non-trivial solution only if its determinant equals to zero:

$$\begin{vmatrix} K_b - K_s & M_{ls} & M_{gs} \\ M_{ls} & M_l - \varepsilon_l p_l & M_{gl} \\ M_{gs} & M_{gl} & M_g - \varepsilon_g p_g \end{vmatrix} = 0 \qquad (15)$$

Solving this equation with plausible assumption that $K_g << K_l << K_s$, and substituting expressions for coefficients above, we obtain

$$M_{gl} = -2\frac{M_{ls}\cdot M_{gs}}{K_s - K_b} = \varepsilon_l \cdot \varepsilon_g \cdot m_{gl}\,.$$

4.3 Simplified Expressions for System Coefficients

Consider stiff matrix and assume that the equalities $K_g << K_l << K_s$ and $K << K_s$ are satisfied. In this case, coefficients have very simple form:

$M_{ls} = \frac{1-\varepsilon_s}{\varepsilon_s}\cdot\varepsilon_l \cdot K_l$; $M_l = \varepsilon_l K_l$; $M_{gs} = \frac{1-\varepsilon_s}{\varepsilon_s}\cdot\varepsilon_g \cdot K_g$; $M_g = \varepsilon_g K_g$; and finally,

$$M_{gl} \approx -2\frac{K_l K_g}{K_s}\left(1-\frac{K_b}{K_s}\right)\left(\frac{1-\varepsilon_s}{\varepsilon_s}\right)^2 \cdot \varepsilon_l \cdot \varepsilon_g\,. \qquad (16)$$

More accurate expression for the interaction coefficient is $M_{gl} \approx -2\frac{K_l K_g\left(1-\varepsilon_s-\frac{K_b}{K_s}\right)^2}{(K_s-K_b)}\cdot\frac{\varepsilon_l\cdot\varepsilon_g}{(\varepsilon_s)^2}$. It can be simplified to the form given above or neglecting the term $\frac{K_b}{K_s}$, to the simple expression $M_{gl} \approx -2\frac{K_l K_g}{K_s}\left(\frac{1-\varepsilon_s}{\varepsilon_s}\right)^2 \cdot \varepsilon_l \cdot \varepsilon_g\,.$

(17)

Thus, for Toray paper the full set of constants is $\lambda_{in-plane} = 70\ ksi$; $\mu_{in-plane} = 35\,ksi$; $\varepsilon_s = 0.75$; for through thickness we need to use $\lambda_\perp = 1.2\ ksi$; $\mu_\perp = 0.7\,ksi$ and the value of porosity in this direction is not clear at this time. Density of Toray paper is $\rho_{toray} = 450 - 1634\ \frac{kg}{m^3}$. For the bi-layer data are very few and far between. However, the first shot might be $\lambda_b = 1-2\ ksi$; $\mu_b = 1.5-3\ ksi$; $\phi \approx 0.25$; and density $\rho_b = 1634\frac{kg}{m^3}$. For further use one needs the following data:

$K_{water} = 2.2\ GPa$; $K_{air} = 1.2\cdot 10^{-4}\ GPa$. Viscosity of water is $\mu^{visc}_{water} = 10^{-3}\ Pa\cdot\sec$ and $\mu^{visc}_{air} = 10^{-4}\ Pa\cdot\sec$.

Closing this section we emphasize that here we report novel results revealing dependence of the constitutive model coefficients from the species volume fractions or saturation. We recognized and derived exact expressions showing that dynamic stress – strain relationship strongly depend on local saturation of porous media. Thus, the pressure distribution under acoustic signal is naturally inhomogeneous in an inhomogeneously saturated media.

We have completed the analysis of the "elastic" deformation. Next, we focus on "viscous-dissipation" part, and, then; couple them in a unified model. Inelastic effects are added to the

model by addition of appropriate dissipative function. This function will describe flow phenomena and solid stress attenuation.

5. Dissipative function *R*

Dissipative function determines amount of energy that mechanical system losses per unit time [10]. Dissipative processes are always irreversible, so the dissipative function should not change sign and, consequently, to the first approximation should be positive definite quadratic form. We assume there are three major dissipative processes in the porous partially saturated continuum. First, it is energy losses associated with the friction due to liquid/gas phase relative flow with respect to the solid matrix. We would call this D'Arcy term $R^{D'Arcy}$, emphasizing the mass-transfer role in this process. The second, energy is lost due to waves damping/attenuation in the solid matrix, or in other words, R^{solid} terms responsible for viscous friction in dry solid matrix. The third term $\Re_{gl}$ is the energy dissipation rate due to spatial gradients of relative solid-liquid and solid-gas motion. This term, in particularly, describes hysteretic effects.

$$R = R^{D'Arcy} + R^{Solid} + \Re_{gl} =$$

$$\frac{\mu_l}{2\cdot K_0}\langle \mathbf{w}_l\rangle^T \mathbf{K}_l^{-1}\langle \mathbf{w}_l\rangle + \frac{\mu_g}{2\cdot K_0}\langle \mathbf{w}_g\rangle^T \mathbf{K}_g^{-1}\langle \mathbf{w}_g\rangle + \frac{\sqrt{\mu_l\cdot\mu_g}}{K_0}\langle \mathbf{w}_g\rangle^T \mathbf{K}_{gl}^{-1}\langle \mathbf{w}_l\rangle + \tag{18}$$

$$\frac{1}{2}\varsigma\cdot\langle \vartheta_s\rangle^2 + 2\cdot\eta\cdot\sum_{ij} v_{ij}^s v_{ij}^s + \Re_{gl}\left(\omega_l,\omega_g,\vartheta_s\right)$$

Here we denote throughout vectors $\mathbf{w}_{l,g} = \varepsilon_{l,g}\cdot\left(\mathbf{v}_{l,g} - \mathbf{v}_s\right)$ filtration velocities of liquid and gas. We also introduce symmetric part of velocity gradient tensor v_{ij}^s for solid matrix – strain rate tensor and solid strain dilatation rate - ϑ_s as well as filtration dilatation rate for liquid and gas as follows:

$$v_{ij}^s = \frac{1}{2}\left(\frac{\partial v_i^s}{\partial x_j} + \frac{\partial v_j^s}{\partial x_i}\right),\quad \vartheta_s = v_{11}^s + v_{22}^s + v_{33}^s,\quad \omega_{l,g} = \frac{\partial w_1^{l,g}}{\partial x_1} + \frac{\partial w_2^{l,g}}{\partial x_2} + \frac{\partial w_3^{l,g}}{\partial x_3}$$

In fluid mechanics equations velocity ($v = \dot{u}$) plays the same role as displacement (u) in solid mechanics.

Dissipation function R^{Solid} describes inner friction and should be zero if there is no internal motion [10], particularly in case of rigid motion. It means that this term should depend on velocities gradients. For isotropic body two viscosities (bulk and shear) should be introduced as it shown in (18).

In special case of weak liquid-gas interaction $\Re_{gl}\left(\omega_l,\omega_g,\vartheta_s\right)$ can be simplified to just a sum $\Re_l\left(\omega_l\right) + \Re_g\left(\omega_g\right)$. Functions $\Re_{l,g}\left(\omega_{l,g}\right)$ and $\Re_{gl}\left(\omega_l,\omega_g,\vartheta_s\right)$ are discussed in special paragraph below. Under assumption of small oscillations near equilibrium, $\Re_{gl}\left(\omega_l,\omega_g,\vartheta_s\right)$ has a general quadratic form [11]:

$$\Re_{gl}(\omega_l,\omega_g,\vartheta_s)=\frac{1}{2}R_l\cdot\omega_l^2+\frac{1}{2}R_g\cdot\omega_g^2+R_{gl}\cdot\omega_l\cdot\omega_g+R_{ls}\cdot\omega_l\cdot\vartheta_s+R_{gs}\cdot\omega_g\cdot\vartheta_s$$

In this case, the corresponding friction forces are linear with filtration dilatations rates and equal to zero at zero dilatation rates. To include hysteresis into this formalism, non-quadratic form of $\Re_{l,g}(\omega_{l,g})$ must be preserved.

According to the basic equation (1) the corresponding dissipative forces can be obtained from the dissipative function by derivation with respect to appropriate velocities and velocities gradients. We start with forces caused by filtration. The first three terms in the right hand site of (18) give the general expression for Darcy type forces:

$$\mathbf{F}_s^{D'Arcy}=\frac{\partial R}{\partial \mathbf{v}_s}=-\frac{\partial R}{\partial \mathbf{v}_l}-\frac{\partial R}{\partial \mathbf{v}_g}$$

$$\mathbf{F}_l^{D'Arcy}=\frac{\partial R}{\partial \mathbf{v}_l}=\varepsilon_l\frac{\mu_l}{K_0}\mathbf{K}_l^{-1}\mathbf{w}_l+\varepsilon_l\frac{\sqrt{\mu_l\cdot\mu_g}}{K_0}\mathbf{K}_{gl}^{-1}\mathbf{w}_g \qquad (19a)$$

$$\mathbf{F}_g^{D'Arcy}=\frac{\partial R}{\partial \mathbf{v}_g}=\varepsilon_g\frac{\mu_g}{K_0}\mathbf{K}_g^{-1}\mathbf{w}_g+\varepsilon_g\frac{\sqrt{\mu_l\cdot\mu_g}}{K_0}\mathbf{K}_{gl}^{-1}\mathbf{w}_l$$

As everywhere in this report, subscripts (s, l, and g) correspond to solid, liquid, and gas phases accordingly. $\mathbf{K}_l$, $\mathbf{K}_g$, and $\mathbf{K}_{gl}$ are tensors for liquid permeability, gas permeability and cross liquid-gas permeability. Last term characterizes the flux of one of species when pressure is applied to another. All permeability tensors components are functions of liquid saturation $S=\varepsilon_l/\phi$ or ε_l and ε_g accordingly.

The velocities gradients dependent terms contribute to internal stresses and need to be added to expressions (7) for completion of constitutive relations:

$$\sigma_{ij}^{s\,diss}=\frac{\partial R^{Solid}}{\partial v_{ij}}+\frac{\partial \Re_{gl}}{\partial v_{ij}}=\varsigma\cdot\vartheta_s\cdot\delta_{ij}+2\cdot\eta\cdot v_{ij}-\varepsilon_l\frac{\partial \Re_l(\omega_l)}{\partial\omega_l}\delta_{ij}-\varepsilon_g\frac{\partial \Re_g(\omega_g)}{\partial\omega_g}\delta_{ij}$$

$$\sigma_{ij}^{l\,diss}=-\varepsilon_l\cdot p_l^{\,diss}\cdot\delta_{ij}=\frac{\partial \Re_l}{\partial \mathbf{v}_l}=\varepsilon_l\frac{\partial \Re_l(\omega_l)}{\partial\omega_l}\delta_{ij} \qquad (20)$$

$$\sigma_{ij}^{g\,diss}=-\varepsilon_g\cdot p_g^{\,diss}\cdot\delta_{ij}=\frac{\partial \Re_g}{\partial \mathbf{v}_g}=\varepsilon_g\frac{\partial \Re_g(\omega_g)}{\partial\omega_g}\delta_{ij}$$

For filtration part, an assumption is that $\mu_{l,g},\mathbf{K}_{l,g}$ are the same as those for acoustic part. In other words, frequency dependence of $\mu_{l,g},\mathbf{K}_{l,g}$ is neglected. Thus, relaxation forces for filtration of gas and liquid are:

$$ {}^{filtr}\mathbf{F}_l^{D'Arcy} = \frac{\partial R}{\partial \mathbf{V}_l} = (\varepsilon_l)^2 \frac{\mu_l}{K_0}\mathbf{K}_l^{-1}\mathbf{V}_l + (\varepsilon_l)^2 \frac{\sqrt{\mu_l \cdot \mu_g}}{K_0}\mathbf{K}_{gl}^{-1}\mathbf{V}_g $$

$$ {}^{filtr}\mathbf{F}_g^{D'Arcy} = \frac{\partial R}{\partial \mathbf{V}_g} = (\varepsilon_g)^2 \frac{\mu_g}{K_0}\mathbf{K}_g^{-1}\mathbf{V}_g + (\varepsilon_g)^2 \frac{\sqrt{\mu_l \cdot \mu_g}}{K_0}\mathbf{K}_{gl}^{-1}\mathbf{V}_l \qquad (19b) $$

Here, absolute velocities of liquid and gas $\mathbf{V}_{l,g}$ stand instead of relative velocities $\mathbf{w}_{l,g} = \varepsilon_{l,g} \cdot (\mathbf{v}_{l,g} - \mathbf{v}_s)$ as filtration velocity of solid is zero - non-consolidating porous material.

6 J-Leverett function, dissipative functions and hysteresis.

To provide a model of two non-mixing fluids that includes effect of residual saturation we have to account for strong dependence of material properties on saturation and wettability. Liquid saturation is defined as $S = \frac{\varepsilon_l}{\phi} = \frac{\varepsilon_l}{1-\varepsilon_s}$.

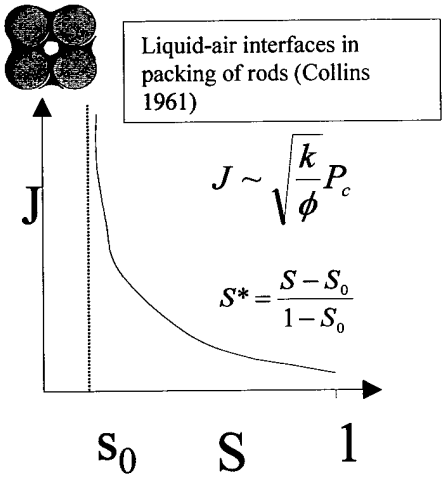

Figure 6. Schematic explanation of J-Leverett function

Capillary pressure P_c is usually defined as the pressure difference between two (wetting and non-wetting) phases as a function of the saturation

Therefore, we define the capillary pressure as: $P_c(S) = P_l - P_g$. For modeling and correlation purposes the capillary pressure can be described by a dimensionless Leverett-J function: $J = \frac{\Delta P(S)}{\sigma}\sqrt{\frac{K}{\phi}}$, where σ is interfacial tension between the two phases and ϕ the porosity of the solid matrix. Definitely, we can write down the same kind of functions for each phase and their difference would determine the capillary pressure. In our modeling we would call $J_{l,g}(\varepsilon_{l,g})$ Leverett function for liquid and gas separately. In principle they depend on θ_s as well, but the dependency is unknown and requires additional measurement and/or microscale simulations. One

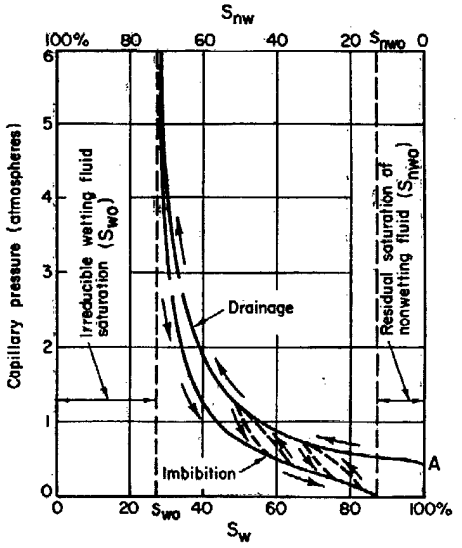

Figure 7. Hysteresis in drainage-imbibitions process (From Bear [15])

can identify $J_{l,g}(\varepsilon_{l,g})$ with $P_{l,g}^{pore}$. Leverett function correlates data over several orders of magnitude change in permeability as stated in [15]. Capillary pressure is a measure of the curvature of the interface separating phases, therefore Leverett J-function is a strong function of morphology. During a subsequent water-drive and turns off some amount of water eventually remains capillary trapped, floating as disconnected blobs in the pores. The residual water saturation S_0 is determined by the pore space morphology and the structure wettability. S_0 is called the "irreducible saturation", which correlates with the amount of trapped water and for wetting phase appears to be around 0.08 [16].

It is important to note that J-Leverett function describes quasi - equilibrium state and small deviations from the equilibrium, which corresponds to slow species flow through the porous media. As has been already mentioned, this slow flow does not appear in Biot-type dynamic (wave) equations. Only combined "slow" and "fast" motions describe mass transfer phenomenon. General expression of the appropriate (Leverett) term of the Lagrangian or free energy is the function of the saturation and material properties[5]. Dropping all details, for the sake of clarity, we can say that in the first approximation $R^{Leverett} = R^{static}(S) + R^{fast}(\dot{S})$. This form leads to the expression for capillary pressure $P_c(S) = P_l - P_g = \frac{\partial R^{static}}{\partial S} + \frac{\partial R^{fast}}{\partial \dot{S}} \triangleq \underbrace{J(s)}_{slow} + \underbrace{F(\dot{S})}_{fast}$.

Dependency of constitutive relations on $\dot{S} = \frac{\partial \varepsilon_l}{\partial t}$ leads to the hysteresis [12]. The rate dependent part might be specified in Lagrangian by $\Re_{l,g}(\omega_{l,g}) = \int_0^{\omega_{l,g}} F_{l,g}(\varsigma)\, d\varsigma$. In general, it is multi-valued function with even power of terms to insure it positive definiteness. Piecewise-linear approximations have been suggested [12].

As shown on illustration in Figure 7 for wettable materials to drain fluid from the porous material the higher pressure should be applied then to imbibe to the same saturation. It means that when we have pressure oscillation in a hydrophilic material the residual water should stay in the porous media and vise versa for hydrophobic materials. The first conclusion from this qualitative picture we can do is that one need to use hydrophobic substrates in fuel cells to appreciate cleaning effect of pressure oscillations.

7. Equations of filtration for two non-mixing fluids and generalized D'Arcy law.

Fluid filtration in porous media is traditionally described by equations based on mass conservation [5, 12, 13, and 15] rather than on Biot type equation [3]:

$$\begin{aligned} &\frac{\partial}{\partial t}\left(\varepsilon_l \rho_l\right) + \nabla \cdot \left(\rho_l \left(\mathbf{V}_l + \mathbf{w}_l\right)\right) = 0 \\ &\qquad\qquad \text{and } \mathbf{w}_{l,g} = \varepsilon_{l,g} \cdot (\mathbf{v}_{l,g} - \mathbf{v}_s) \\ &\frac{\partial}{\partial t}\left(\varepsilon_g \rho_g\right) + \nabla \cdot \left(\rho_g \left(\mathbf{V}_g + \mathbf{w}_g\right)\right) = 0 \end{aligned} \qquad (21)$$

[5]Recent advances in thermodynamics of multiphase flow in porous media [for example, 5,11,12] provide a theoretical framework for a proper and consistent definition of Leverett function in acoustic field.

In the case of *saturated incompressible fluids* those equations are simply direct consequences of the definition of the dilatation: $\theta_l \equiv \nabla\cdot(\mathbf{u}_l - \mathbf{u}_s)$. In the two-fluid case when saturations ε_l and ε_g change both in time and space, situation becomes more complicated especially taking in mind that Leverett functions and $\Re_{l,g}(\omega_s, \omega_{l,g})$ are measured as functions of ε_l and ε_g rather than $\theta_{l,g}$ - $\Im_{l,g}(\theta_s, \varepsilon_{l,g})$. One can consider, therefore, the two continuity equations as equations for additional variable $\varepsilon_{l,g}$ and solve them together with Biot equations for vibration. Note that because the continuity equations are conservation laws and expressed as full time derivatives, their contribution to Lagrange equations taken with the Lagrange multipliers don't change equations of motion.

Note that when liquid and gas can be considered incompressible, densities can be cancelled in (21) and rate hysteresis function from the Leverett expression, which in general depends on flux dilatation, can be simplified to the form mentioned in the previous section as follows:

$$F_{l,g}\left(\nabla\cdot\left[\varepsilon_{l,g}\frac{\partial}{\partial t}(\mathbf{u}_{l,g} - \mathbf{u}_s)\right]\right) = F_{l,g}\left(\frac{\partial\varepsilon_{l,g}}{\partial t}\right). \tag{22}$$

Equilibrium condition requires that the resultant of all applied forces be compensated by internal stresses. For the liquid the total pressure gradient should be equal to the sum of D'Alamber and D'Arcy forces (see equations 7 and 10).

$$\nabla(-\varepsilon_l p_l) = \mathbf{F}_l^{\text{DAlamber}} + \mathbf{F}_l^{D'Arcy} \tag{23}$$

Next, without loss of generality, we neglect all "gas terms" and obtain the simple form of the generalized D"Arcy law for unsaturated porous media under acoustic loading.[6] Expressions for liquid components of these forces are given in the derived expressions (4a) and (19) accordingly. Note, that, as everywhere in this work, hydrostatic pressure has the sign minus in accord with continuum mechanics sign agreement. Thus, equation (23) can be re-written in the following form:

$$\nabla(-\varepsilon_l p_l) = \frac{\partial}{\partial t}\left(\beta\rho_l\varepsilon_l(\mathbf{v}_l - \mathbf{v}_s)\right) + \frac{\partial}{\partial t}(\rho_l\varepsilon_l\mathbf{v}_l) + \frac{\varepsilon_l\mu_l}{K_0}\mathbf{K}^{-1}\mathbf{w}_l; \qquad \mathbf{w}_l = \varepsilon_l(\mathbf{v}_l - \mathbf{v}_s).$$

The D'Alamber term depends on both relative ($\mathbf{v}_l$-$\mathbf{v}_s$) and absolute liquid velocities. Resolving this equality with respect to the flux $\mathbf{q} \triangleq \mathbf{w}$, and also taking into account that $p_l = P^{static} - M\theta_l - M\gamma\theta_s$, we immediately obtain:

$$\mathbf{q} = -\frac{K_0\mathbf{K}}{\mu_l}\left(\frac{\nabla(\varepsilon_l P)}{\varepsilon_l} - \frac{M}{\varepsilon_l}\left(\nabla(\varepsilon_l\theta_l) + \gamma\nabla(\varepsilon_l\theta_s)\right) + \frac{\beta\rho_l}{\varepsilon_l}\frac{\partial}{\partial t}\left(\varepsilon_l\frac{\partial(\mathbf{u}_l - \mathbf{u}_s)}{\partial t}\right) + \frac{\rho_l}{\varepsilon_l}\frac{\partial}{\partial t}\left(\varepsilon_l\frac{\partial\mathbf{u}_l}{\partial t}\right)\right) \tag{24}$$

Here the flux tensor depends on all components gradient of pressure, dilatations and kinematical terms. This is *the novel generalization of the D'Arcy Law for the acoustically loaded unsaturated porous media.* The first term represents generalization of "traditional" pressure gradient corrected for the variable saturation. Very important, that saturation gradient

[6] In all further derivations and calculations we use the full system and simplified expression here only for illustrative purposes.

$P\frac{\nabla\varepsilon}{\varepsilon} = P\nabla \ln \varepsilon$ is also strong driving force specific only for unsaturated inhomogeneously filled porous structure. This term plays an important role but only if either external pressure or "external" dilatation has been applied. The second term explains the role of solid and liquid deformation as a driving force for the flux. Due to dilatation, fluid is squeezed out of the compressed pores due to induced increased fluid pressure in the "extended" area with reduced liquid pressure. The two last terms show the role of dynamics (acoustics) on the liquid flux.

Using the new formulation (24) and assuming everywhere that saturation does not change significantly, we might estimate orders of magnitude for the required parameters of structural acoustics impact to achieve the comparable effect with static pressure. D'Arcy term for the fuel cell cathode compartment is generated by application of the pressure of 1 *psi* over the distance of 200 m. Thus, the "static" pressure gradient is of the order of $\nabla p \approx \frac{1psi}{200\ \mu m} = 34E6\ \frac{Pa}{m}$. Letting magnitude be 1% of the thickness, we immediately obtain that a dynamic term has the order of magnitude $\rho_l \frac{\partial^2 u}{\partial t^2} \cong \rho A\omega^2 \approx 1.E-3\ \omega^2$ and, subsequently, equating these two pressures, we obtain that the required frequency is about 30 KHz.

8. Constitutive relations and complete system of governing equations

By this point we have described all forces acting in the system and the system possible reactions. We introduced elastic and dissipative models. Combination of "elastic" and "viscous" equations completes physics-based system and allows us to predict the influence of vibration on mass transfer and dynamics of saturation on vibration parameters. Using these derived partial models one can get the following constitutive relations:

$$\sigma_{ij}^{s} + \sigma_{ij}^{s\,diss} = \frac{\partial U}{\partial e_{ij}} + \frac{\partial R}{\partial v_{ij}} = \lambda \cdot \theta_s \cdot \delta_{ij} + 2 \cdot \mu \cdot e_{ij} + \varsigma \cdot \vartheta_s \cdot \delta_{ij} + 2 \cdot \eta \cdot v_{ij} + M_{ls} \cdot \theta_l + M_{gs} \cdot \theta_g$$
$$- \varepsilon_l \cdot F_l(\omega_l) \cdot \delta_{ij} - \varepsilon_g \cdot F_g(\omega_g) \cdot \delta_{ij}$$

$$\sigma_{ij}^{l} + \sigma_{ij}^{l\,diss} = \frac{\partial U}{\partial \theta_l} + \frac{\partial \Re}{\partial \omega_l} = -\varepsilon_l \cdot \left(p_l + p_l^{\,diss}\right) \cdot \delta_{ij} = M_l \cdot \theta_l + M_{ls}\theta_s + M_{gl} \cdot \theta_g + \varepsilon_l \cdot F_l(\omega_l) \qquad (25)$$

$$\sigma_{ij}^{g} + \sigma_{ij}^{g\,diss} = \frac{\partial U}{\partial \theta_g} + \frac{\partial \Re}{\partial \omega_g} = -\varepsilon_g \cdot \left(p_g + p_g^{\,diss}\right) \cdot \delta_{ij} = M_g \cdot \theta_g + M_{gs} \cdot \theta_s + M_{gl} \cdot \theta_l + \varepsilon_g \cdot F_g(\omega_g)$$

Here, each of the matrix equations corresponds to solid, liquid, and gas phases accordingly. As was mentioned already J is a static part of Leverett function for each component (liquid and gas) and F is a "hysteresis" part. These constitutive relations should be supplemented by the definition of the Leverett function, simplified form of which is:

$$T(\varepsilon_l)\cdot\frac{\partial\varepsilon_l}{\partial t}-P_g+P_l=J(\varepsilon_l) \tag{26}$$

Some particular expressions for $T(\varepsilon)$ and $J(\varepsilon)$ can be found in [12]. However, physics-based derivation of these coefficients is ongoing task closely related with numerical analysis and will be presented in the final report. The last equation for $P_{l,g}$ has been derived in [11] using consideration of Coleman and Noll on positiveness of entropy production

Complete system of governing equations needs to be added to the constitutive relations. Combination of "elastic" and "viscous" momentum (or in other words Newton's) equations for each species has the following general form:

$$\begin{aligned}
&\frac{\partial\sigma_{ij}^{s}}{\partial x_j}+\frac{\partial\sigma_{ij}^{s\,diss}}{\partial x_j}=\mathbf{F}_s^{\mathrm{DAlamber}}+\mathbf{F}_s^{D'Arcy}\\
&\nabla\left(-\varepsilon_l\left(p_l+p_l^{diss}\right)\right)=\mathbf{F}_l^{\mathrm{DAlamber}}+\mathbf{F}_l^{D'Arcy}\\
&\nabla\left(-\varepsilon_g\left(p_g+p_g^{diss}\right)\right)=\mathbf{F}_g^{\mathrm{DAlamber}}+\mathbf{F}_g^{D'Arcy}\\
&\nabla\left(-\varepsilon_l P_l\right)={}^{filtr}\mathbf{F}_l^{D'Arcy}\\
&\nabla\left(-\varepsilon_g P_g\right)={}^{filtr}\mathbf{F}_g^{D'Arcy}
\end{aligned} \tag{27}$$

The second of these equations we have already used deriving novel generalization of D'Arcy law for unsaturated porous media under impact of dynamic loading. Thus, we have described stress-strain relationship, forces causing these stresses, and constituents displacements and velocities resulting from these stresses. To complete this system description one needs to add the mass transfer equations (filtration).

$$\begin{aligned}
&\frac{\partial}{\partial t}\left(\varepsilon_l\rho_l\right)+\nabla\cdot\left(\rho_l\left(\mathbf{V}_l+\mathbf{w}_l\right)\right)=0\\
&\frac{\partial}{\partial t}\left(\varepsilon_g\rho_g\right)+\nabla\cdot\left(\rho_g\left(\mathbf{V}_g+\mathbf{w}_g\right)\right)=0
\end{aligned} \tag{28}$$

Finally we have the system of governing equations describing multiphase flow in porous media with acoustic streaming. The transmission of sound through unsaturated porous media can be predicted only in the context of the extended Biot model we have developed here. The water and air move simultaneously with solid matrix. The completed fully coupled model predicting waves propagations in multiphase porous media and acoustic streaming is given below:

$$M_{ls}\cdot\nabla\left(\nabla\cdot\mathbf{u}_l\right)+M_{gs}\cdot\nabla\left(\nabla\cdot\mathbf{u}_g\right)-$$
$$-\nabla\left(\varepsilon_l\cdot F_l\left(\nabla\cdot\left[\varepsilon_l\frac{\partial}{\partial t}\left(\mathbf{u}_l-\mathbf{u}_s\right)\right]\right)\right)-\nabla\left(\varepsilon_g\cdot F_g\left(\nabla\cdot\left[\varepsilon_g\frac{\partial}{\partial t}\left(\mathbf{u}_g-\mathbf{u}_s\right)\right]\right)\right)=$$
$$-\left(\varepsilon_l\right)^2\frac{\mu_l}{K_0}\mathbf{K}_l^{-1}\frac{\partial}{\partial t}\left(\mathbf{u}_l-\mathbf{u}_s\right)-\left(\varepsilon_g\right)^2\frac{\mu_g}{K_0}\mathbf{K}_g^{-1}\frac{\partial}{\partial t}\left(\mathbf{u}_g-\mathbf{u}_s\right)-\frac{\sqrt{\mu_l\cdot\mu_g}}{K_0}\varepsilon_l\cdot\varepsilon_g\cdot\mathbf{K}_{gl}^{-1}\left(\frac{\partial}{\partial t}\left(\mathbf{u}_l-\mathbf{u}_s\right)+\frac{\partial}{\partial t}\left(\mathbf{u}_g-\mathbf{u}_s\right)\right)+$$
$$\frac{\partial}{\partial t}\left(\left(\rho_s\varepsilon_s+\rho_l\varepsilon_l\beta_l+\left(\rho_g\varepsilon_g+\rho_l\varepsilon_l\right)\beta_{gl}+\rho_g\varepsilon_g\beta_g\right)\frac{\partial}{\partial t}\mathbf{u}_s\right)-$$
$$-\frac{\partial}{\partial t}\left(\left(\rho_l\varepsilon_l\beta_l+\rho_g\varepsilon_g\beta_{gl}\right)\frac{\partial}{\partial t}\mathbf{u}_l\right)-\frac{\partial}{\partial t}\left(\left(\rho_g\varepsilon_g\beta_g+\rho_l\varepsilon_l\beta_{gl}\right)\frac{\partial}{\partial t}\mathbf{u}_g\right)$$

The next two vector equations describe induced waves and acoustic streaming in liquid and gas phases.

$$M_{ls}\cdot\nabla\left(\nabla\cdot\mathbf{u}_s\right)+M_l\cdot\nabla\left(\nabla\cdot\mathbf{u}_l\right)+M_{gl}\cdot\nabla\left(\nabla\cdot\mathbf{u}_g\right)+\nabla\left(\varepsilon_l\cdot F_l\left(\nabla\cdot\left[\varepsilon_l\frac{\partial}{\partial t}\left(\mathbf{u}_l-\mathbf{u}_s\right)\right]\right)\right)=$$
$$\left(\varepsilon_l\right)^2\frac{\mu_l}{K_0}\mathbf{K}_l^{-1}\frac{\partial}{\partial t}\left(\mathbf{u}_l-\mathbf{u}_s\right)+\frac{\sqrt{\mu_l\cdot\mu_g}}{K_0}\varepsilon_l\cdot\varepsilon_g\cdot\mathbf{K}_{gl}^{-1}\cdot\frac{\partial}{\partial t}\left(\mathbf{u}_g-\mathbf{u}_s\right)-$$
$$-\frac{\partial}{\partial t}\left(\left(\rho_l\varepsilon_l\beta_l+\rho_g\varepsilon_g\beta_{gl}\right)\frac{\partial}{\partial t}\mathbf{u}_s\right)+\frac{\partial}{\partial t}\left(\left(\rho_l\varepsilon_l+\rho_l\varepsilon_l\beta_l+\rho_g\varepsilon_g\beta_{gl}\right)\frac{\partial}{\partial t}\mathbf{u}_l\right)$$

$$M_{gs}\cdot\nabla\left(\nabla\cdot\mathbf{u}_s\right)+M_{gl}\cdot\nabla\left(\nabla\cdot\mathbf{u}_l\right)+M_g\cdot\nabla\left(\nabla\cdot\mathbf{u}_g\right)+\nabla\left(\varepsilon_g\cdot F_g\left(\nabla\cdot\varepsilon_g\frac{\partial}{\partial t}\left(\mathbf{u}_g-\mathbf{u}_s\right)\right)\right)=$$
$$\left(\varepsilon_g\right)^2\frac{\mu_g}{K_0}\mathbf{K}_g^{-1}\frac{\partial}{\partial t}\left(\mathbf{u}_g-\mathbf{u}_s\right)+\frac{\sqrt{\mu_l\cdot\mu_g}}{K_0}\cdot\varepsilon_l\cdot\varepsilon_g\cdot\mathbf{K}_{gl}^{-1}\cdot\frac{\partial}{\partial t}\left(\mathbf{u}_l-\mathbf{u}_s\right)-$$
$$-\frac{\partial}{\partial t}\left(\left(\rho_g\varepsilon_g\beta_g+\rho_l\varepsilon_l\beta_{gl}\right)\frac{\partial}{\partial t}\mathbf{u}_s\right)+\frac{\partial}{\partial t}\left(\left(\rho_g\varepsilon_g+\rho_g\varepsilon_g\beta_g+\rho_l\varepsilon_l\beta_{gl}\right)\frac{\partial}{\partial t}\mathbf{u}_g\right)$$

Close with (filtration) mass transfer equations:

$$\frac{\partial}{\partial t}\left(\varepsilon_l\rho_l\right)+\nabla\cdot\left(\rho_l\varepsilon_l\frac{\partial}{\partial t}\left(\mathbf{V}_l+\mathbf{u}_l-\mathbf{u}_s\right)\right)=0$$
$$\frac{\partial}{\partial t}\left(\varepsilon_g\rho_g\right)+\nabla\cdot\left(\rho_g\varepsilon_g\frac{\partial}{\partial t}\left(\mathbf{V}_g+\mathbf{u}_g-\mathbf{u}_s\right)\right)=0$$

Note that when liquid and gas can be considered incompressible

$$F_{l,g}\left(\nabla\cdot\left[\varepsilon_{l,g}\frac{\partial}{\partial t}\left(\mathbf{u}_{l,g}-\mathbf{u}_s\right)\right]\right)=F_{l,g}\left(\frac{\partial\varepsilon_{l,g}}{\partial t}\right).$$

As was already mentioned in the section 7 in accord with results in hysteresis in [12].

There are solid-matrix attenuation terms, which have exactly the same general form as elastic part but displacements are substituted with appropriate velocities. As in case of elastic solid, the wave equations describe dilatational and rotational waves. For the case of strong coupling between phases there exist two compression waves – fast and slow. It is important to note that characteristic time scales for wave propagation and for D'Arcy mass transfer are very different, which makes direct numerical analysis difficult if impossible but at the same time allows asymptotic analytical solution. What is more, asymptotical transformations can prepare the system for numerical analysis.

Flow under static pressures is expressed through "filtration - viscous" velocities as follows:

$$\nabla\left(-\varepsilon_l P_l\right)=\left(\varepsilon_l\right)^2\frac{\mu_l}{K_0}\mathbf{K}_l^{-1}\mathbf{V}_l+\left(\varepsilon_l\right)^2\frac{\sqrt{\mu_l\cdot\mu_g}}{K_0}\mathbf{K}_{gl}^{-1}\mathbf{V}_g$$

$$\nabla\left(-\varepsilon_g P_g\right)=\left(\varepsilon_g\right)^2\frac{\mu_g}{K_0}\mathbf{K}_g^{-1}\mathbf{V}_g+\left(\varepsilon_g\right)^2\frac{\sqrt{\mu_l\cdot\mu_g}}{K_0}\mathbf{K}_{gl}^{-1}\mathbf{V}_l$$

With the constitutive relations for static pressures (here, as everywhere in this report, saturation $S=\varepsilon_l/\phi$):

$$P_g-P_l=J(S)+T\cdot\frac{\partial}{\partial t}S$$

The general feature of the developed model that we account for material morphology and performance regime (start up, shut down, long steady working regime, etc.) in order to predict fuel cell performance and degradation caused by increased water residual content.

9. Model summary.

9.1 Physical phenomena included in the model.

The model separates elastic and plastic properties of three immiscible phases involved in mass and momentum transfer on the basis of difference in time scale for vibration (elastic part) and filtration (plastic part). The plasticity of the solid porous phase is neglected as well as all temperature effects.

The vibration part is represented as three interconnected elastic bodies, only solid having non-zero share module. Two types of dissipative mechanisms have been included: damping of the vibration proportional to velocity gradients and momentum transfer due to phase-to-phase interaction.

The filtration part is modeled as the motion in slowly varying static pressure fields, dissipation mechanism being of D'Arcy type i.e. proportional to relative velocities of liquid and gas.

The above-mentioned two types of motion interact through dependency of saturation field at every point. It means that elastic parameters and slowly varying static pressures are functions of saturation. Two mass transfer equations for liquid and gas phases contain contributions from both vibration and filtration parts.

A special equation that closes the system is a constitutive relation for two static pressures and the rate of saturation change. This equation determines the stationary state and, therefore, remaining liquid after all transient process dies out.

Of special interest are non-classical boundary conditions that result in the net desaturation of the porous sample. They should account for dependency on the flux direction and on the rate of the water removal from the boundary for the net effect to exist.

9.2 Physical phenomena not included in the model.

Ideally, there should be only one system for momentum transfer that is not divided into vibration and filtration parts. This could be important in all cases when time scales between fluids flow due to external pressures and caused by vibration are close to each other. Such model would require using mixed elasto-plastic constitutive relations of Maxwell-Voight type.
Another potentially important gap to fill in this model is to evaluate dependency of parameters in Leveret function on vibrations. That would require deep analysis of droplet instabilities trapped inside porous structure. The results unavoidably are morphology dependent.

10 Analytical approach and Scale Separation

The primary goal of this work is to show that a periodic perturbation of the solid matrix or pulsation of the gas phase causes non-periodic flow of the liquid component. Although the complete solution of the full system of equations requires numerical simulations (results of which will be reported in the final document), it is possible to observe the effect using the fact that all filtration processes are substantially slower than the vibration/pulsation period. Under such circumstances one can split the complete system into vibration (Biot) part and filtration part and solve them iteratively. In the first step all saturations $\{\varepsilon_s, \varepsilon_l, \varepsilon_g\}$ or in other notation $\left\{S = \frac{\varepsilon_l}{1-\varepsilon_s},\ 1-S = \frac{\varepsilon_g}{1-\varepsilon_s}\right\}$ and $\{p_l, p_g\}$ that makes the whole system nonlinear are considered constant. The periodic solution of the resulting linear system for $\{\mathbf{u}_s, \mathbf{u}_l, \mathbf{u}_g\}$ can be found. At the next step, these periodic perturbations are imbedded into filtration equations as a source term.

$$\frac{\partial}{\partial t}(\varepsilon_l \rho_l) + \nabla \cdot \left(\rho_l \varepsilon_l \frac{\partial}{\partial t}(\mathbf{u}_l - \mathbf{u}_s) \right) = 0$$

$$\frac{\partial}{\partial t}(\varepsilon_g \rho_g) + \nabla \cdot \left(\rho_g \varepsilon_g \frac{\partial}{\partial t}(\mathbf{u}_g - \mathbf{u}_s) \right) = 0$$

We assume that the periodic signals are in certain sense small in order to resolve the problem analytically. Having a small parameter at hand one can use asymptotic expansion based on averaging principle [17] to obtain an averaged filtration equations that describe the slow non-periodic flow caused by periodic perturbation.

One more important motivation for the asymptotic analysis of the derived equations comes from the fact that the accuracy of the numerical analysis of the wave processes is spatially limited by the size of the finite element (or the step in the finite-difference scheme). Therefore, even theoretically, it is practically impossible to develop a direct computational approach for the analysis of high frequency waves interactions with mass flow process. The only feasible approach is to homogenize the mass transfer equations over high frequency acoustic vibrations treated as effective body forces.

For the sake of simplicity and without loss of generality we assume that solid matrix is rigid ($\varepsilon_s = const$), both liquid and gas are uncompressible at the applied pressures. Also, D'Arcy flows for both components are uncorrelated. Crucial assumption for analytical evaluation, is that displacements $\{\mathbf{u}_s, \mathbf{u}_l, \mathbf{u}_g\}$ are caused by an actuator attached to the porous matrix in such a way that, when it is turned off, $\{\mathbf{u}_s, \mathbf{u}_l, \mathbf{u}_g\} = 0$. So, the case of small vibrations, magnitude of the displacements is proportional to small parameter $\{\mathbf{u}_s, \mathbf{u}_l, \mathbf{u}_g\} \sim \lambda$. Non-destructive acoustic excitation is applied with λ is a small amplitude of external source.

Using equations (21) and derived generalization of the D'Arcy law we can write filtration equations with periodic terms down as follows:

$$\frac{\partial}{\partial t}\begin{pmatrix}\varepsilon_l \rho_l \\ \varepsilon_g \rho_g\end{pmatrix} = K_0 \cdot \nabla \cdot \left[\mathbf{K} \cdot \begin{pmatrix} \rho_l \varepsilon_l^{-1} \mu_l^{-1} \left(\nabla\left(\varepsilon_l \left[P_l - F_l^P\right]\right) - \frac{\partial}{\partial t}\varepsilon_l \mathbf{F}_\mathbf{l}^\mathbf{K} \right) \\ \rho_g \varepsilon_g^{-1} \mu_g^{-1} \left(\nabla\left(\varepsilon_g \left[P_g - F_g^P\right]\right) - \frac{\partial}{\partial t}\varepsilon_g \mathbf{F}_\mathbf{g}^\mathbf{K} \right) \end{pmatrix} \right] \tag{30}$$

where

$$\mathbf{K} = \begin{pmatrix} \mathbf{K}_l^{-1} & \sqrt{\frac{\mu_g}{\mu_l}} \cdot \varepsilon_g \cdot \mathbf{K}_{gl}^{-1} \\ \sqrt{\frac{\mu_l}{\mu_g}} \cdot \varepsilon_l \cdot \mathbf{K}_{gl}^{-1} & \mathbf{K}_g^{-1} \end{pmatrix}^{-1}$$

$$\begin{pmatrix} F_l^P \\ F_g^P \end{pmatrix} = \begin{pmatrix} m_{ls} \cdot \nabla \cdot \mathbf{u}_s + m_l \cdot \nabla \cdot \mathbf{u}_l + m_{gl} \cdot \varepsilon_g \cdot \nabla \cdot \mathbf{u}_g \\ m_{gs} \cdot \nabla \cdot \mathbf{u}_s + m_{gl} \cdot \varepsilon_l \cdot \nabla \cdot \mathbf{u}_l + m_g \cdot \nabla \cdot \mathbf{u}_g \end{pmatrix}$$

$$\begin{pmatrix}\mathbf{F}_l^{\mathbf{K}}\\ \mathbf{F}_g^{\mathbf{K}}\end{pmatrix}=\begin{pmatrix}\rho_l\frac{\partial}{\partial t}\mathbf{u}_l+\left(\rho_l\beta_l+\rho_g\frac{\varepsilon_g}{\varepsilon_l}\beta_{gl}\right)\frac{\partial}{\partial t}\left(\mathbf{u}_l-\mathbf{u}_s\right)\\ \rho_g\frac{\partial}{\partial t}\mathbf{u}_g+\left(\rho_g\beta_g+\rho_l\frac{\varepsilon_l}{\varepsilon_g}\beta_{gl}\right)\frac{\partial}{\partial t}\left(\mathbf{u}_g-\mathbf{u}_s\right)\end{pmatrix}$$

and constitutive relations for $\{P_l,P_g\}$:

$$P_g-P_l=J\left(\varepsilon_l,\varepsilon_g\right)+F\left(\frac{\partial}{\partial t}\varepsilon_l,\frac{\partial}{\partial t}\varepsilon_g\right)$$

and $\{\varepsilon_s,\varepsilon_l,\varepsilon_g\}$

$$\varepsilon_s+\varepsilon_l+\varepsilon_g=1$$

The following simplifications make the system more tractable analytically:

- $\{\rho_l,\rho_g\}=const$ - both liquid and gas are uncompressible;
- $\mathbf{K}_{gl}^{-1}$ - Darcy flows for both components are uncorrelated;
- $\varepsilon_s=const$ - solid matrix is rigid;

Re-writing these relations through unique variable – water saturation S, we immediately have:

$$\frac{\partial}{\partial t}\begin{pmatrix}S\\ -S\end{pmatrix}=\frac{K_0}{\varepsilon}\cdot\begin{pmatrix}\mu_l^{-1}\cdot\nabla\cdot\mathbf{K}_l S^{-1}\left(\nabla S\left[P_l-\lambda\cdot F_l^P\right]-\lambda\cdot\frac{\partial}{\partial t}S\cdot\mathbf{F}_l^{\mathbf{K}}\right)\\ \mu_g^{-1}\cdot\nabla\cdot\mathbf{K}_g\left(1-S\right)^{-1}\left(\nabla\left(1-S\right)\left[P_g-\lambda\cdot F_g^P\right]-\lambda\cdot\frac{\partial}{\partial t}\left(1-S\right)\cdot\mathbf{F}_g^{\mathbf{K}}\right)\end{pmatrix}$$

where

$\varepsilon=1-\varepsilon_s$ - porosity;

$$\begin{pmatrix}F_l^P\\ F_g^P\end{pmatrix}=\begin{pmatrix}m_{ls}\cdot\nabla\cdot\mathbf{u}_s+m_l\cdot\nabla\cdot\mathbf{u}_l+\varepsilon\cdot m_{gl}\cdot S\cdot\nabla\cdot\mathbf{u}_g\\ m_{gs}\cdot\nabla\cdot\mathbf{u}_s+\varepsilon\cdot m_{gl}\cdot\left(1-S\right)\cdot\nabla\cdot\mathbf{u}_l+m_g\cdot\nabla\cdot\mathbf{u}_g\end{pmatrix}$$

$$\begin{pmatrix}\mathbf{F}_l^{\mathbf{K}}\\ \mathbf{F}_g^{\mathbf{K}}\end{pmatrix}=\begin{pmatrix}\rho_l\cdot\frac{\partial}{\partial t}\mathbf{u}_l+\left(\rho_l\cdot\beta_l+\rho_g\cdot\left(S^{-1}-1\right)\cdot\beta_{gl}\right)\frac{\partial}{\partial t}\left(\mathbf{u}_l-\mathbf{u}_s\right)\\ \rho_g\cdot\frac{\partial}{\partial t}\mathbf{u}_g+\left(\rho_g\cdot\beta_g+\rho_l\cdot\left(\left(1-S\right)^{-1}-1\right)\cdot\beta_{gl}\right)\frac{\partial}{\partial t}\left(\mathbf{u}_g-\mathbf{u}_s\right)\end{pmatrix}$$

Here equation $P_g-P_l=J\left(\varepsilon_l,\varepsilon_g\right)+F\left(\frac{\partial\varepsilon_l}{\partial t},\frac{\partial\varepsilon_g}{\partial t}\right)$ has been resolved versus $\frac{\partial S}{\partial t}$ due to the simplifications above, with two branches correspondent to drainage and imbibitions respectively.

$$P_g - P_l = \begin{cases} J^{dr}(S) + T \cdot \dfrac{\partial S}{\partial t} & \text{for drainage } \left(\dfrac{\partial S}{\partial t} < 0\right) \\ J^{imb}(S) + T \cdot \dfrac{\partial S}{\partial t} & \text{for imbibition } \left(\dfrac{\partial S}{\partial t} > 0\right) \end{cases}$$

As it can be seen from (30), two forces $\mathbf{F}_{l,g}^{K}$ and $F_{l,g}^{p}$ stemmed from a source of vibration affect fluid flow in porous material. As they are linear combinations of $\{\mathbf{u}_s, \mathbf{u}_l, \mathbf{u}_g\}$ and their time and spatial derivative, one can conclude that in general the spectral composition of the forces includes both natural frequencies of porous medium (Biot waves) and frequencies that correspond to the particular porous layer structure. The whole picture, therefore, is both geometry and material dependent and requires numerical analysis for any specific geometry. One can show, however, in very general terms, that periodic forces $\mathbf{F}_{l,g}^{K}$ and $F_{l,g}^{p}$ cause non-periodic mass transport. Similar results have been obtained in [18] in different setting. An approached adopted here is that one originally proposed in [17] and more generally in the theory of normal forms (see for example, [19]). We are looking for a substitution of original variables such that in the new (slow) variables the mass flow equation does not contain vibration terms, both the substitution and the new mass equation being sought as an asymptotic expansion in the small parameter λ.

$$\begin{aligned} S(\mathbf{x},t) &= \overline{S}(\mathbf{x},t) + \lambda \cdot s_1\left(\overline{S},\overline{P_l},\overline{P_g},\mathbf{x},t\right) + \lambda^2 \cdot s_2\left(\overline{S},\overline{P_l},\overline{P_g},\mathbf{x},t\right) + \ldots \\ P_l(\mathbf{x},t) &= \overline{P_l}(\mathbf{x},t) + \lambda \cdot p_1^l\left(\overline{S},\overline{P_l},\overline{P_g},\mathbf{x},t\right) + \lambda^2 \cdot p_2^l\left(\overline{S},\overline{P_l},\overline{P_g},\mathbf{x},t\right) + \ldots \\ P_g(\mathbf{x},t) &= \overline{P_g}(\mathbf{x},t) + \lambda \cdot p_1^g\left(\overline{S},\overline{P_l},\overline{P_g},\mathbf{x},t\right) + \lambda^2 \cdot p_2^g\left(\overline{S},\overline{P_l},\overline{P_g},\mathbf{x},t\right) + \ldots \end{aligned} \qquad (31)$$

All fast (vibration terms) parameters affect the solution through the cross-correlations averaged over the time period. Substituting expansions (31) into flow equations (30) and equating terms at the same powers of small parameter we obtain the sequence of recurrent differential equations, from which all unknown functions of the substitution could be defined. In other words, we find a solution for s_1 as a functional of slow variables $\{\overline{S}, \overline{P_l}, \overline{P_g}\}$. This term, being purely vibrational, gives zero contribution into equation for the slow variables $\{\overline{S}, \overline{P_l}, \overline{P_g}\}$. The first non-zero contribution comes from s_2, that could be found as a functional of $\{\overline{S}, \overline{P_l}, \overline{P_g}\}$ in the same way as s_1 .All details of calculations are shown in the **Appendix 1**. Finally, the slow non-periodic flow is expressed through all of these components that play role of body forces. The most important results are as follows: (*i*) the principal term of the asymptotic solution $(\overline{S}, \overline{P_l}, \overline{P_g})$ represents slow multiphase flow under static external pressure (D'Arcy flow) without acoustic impact. (*ii*) First correction (at λ^1) is identically equal to zero, so there is no first order effect of periodic vibration on mass flow. In the second - quadratic term the effect is noticeably pronounced. All vibration terms are coupled and their self and cross-correlations cause additional driving forces similar (in some sense) to the effect of gravitation on the reservoir flow. The final expression for slow non-periodic flow is the following:

$$\frac{\partial \bar{S}}{\partial t} = \frac{K_0}{\varepsilon \mu_l} \cdot$$

$$\Big[\underbrace{\left(\frac{\mathbf{K}_l}{\bar{S}} \nabla \left(\overline{S P_l} \right) \right)}_{\text{Static unsaturated flow}} + \underbrace{\left(\frac{1}{2} \frac{\partial^2 \mathbf{K}_l(\bar{S})}{\partial \bar{S}^2} \bar{S} + \frac{\mathbf{K}_l(\bar{S})}{\bar{S}} \right) \overline{\left(\frac{s_1}{\bar{S}} \right)^2} \nabla \left(\bar{S} \cdot \bar{P}_l \right)}_{\text{Vibration induced flux enhancement due to pressure gradient}} + \underbrace{\left(\frac{\partial \mathbf{K}_l(\bar{S})}{\partial \bar{S}} - \frac{\mathbf{K}_l(\bar{S})}{\bar{S}} \right) \overline{\left(\frac{s_1}{\bar{S}} \cdot p_1^l \right)} \nabla \bar{S}}_{\text{Vibration induced flux enhancement due to saturation gradient}} +$$

$$\underbrace{\frac{\partial \mathbf{K}_l(\bar{S})}{\partial \bar{S}} \overline{s_1 \nabla p_1^l} + \frac{\mathbf{K}_l(\bar{S})}{\bar{S}} \overline{p_1^l \nabla s_1}}_{\text{Influence of vibration induced pressure and saturation gradients. (Non-zero only for structural deformations}} \Big]$$

One can see from the expression above that total non-periodic flux is a sum of the static unsaturated flow, vibration induced flux enhancement due to pressure gradient, saturation gradient and their cross correlations. It is worth to note that without external pressure gradient the vibration does not cause any non-periodic effect. The third term has always-positive coefficient (permeability assumed to be a power function of saturation [15]) and increases with inhomogeneity of saturation, i.e. the bigger droplets the stronger effect. All terms include local pressure gradients, caused by deformation gradients, so the local waves- induced dilatation gradients are crucial.

To obtain simple formulas for vibration-induced contribution to the mass flow we use method of harmonic balance. In the simplest case of harmonic acoustic excitation, we can express all parameters as mono-harmonic wave functions[7]:

$$\mathbf{u}_i = {}^c\mathbf{u}_i \cdot \cos(\omega \cdot t + \mathbf{k} \cdot \mathbf{x}) + {}^s\mathbf{u}_i \cdot \sin(\omega \cdot t + \mathbf{k} \cdot \mathbf{x}); \quad i = s, l, g;$$

and calculate additional pressure and permeability that this simple vibration induces in porous material. First, a response to this driving force needs to be calculated in the following form:

$$\begin{Bmatrix} s_1 \\ p_1^l \\ p_1^g \end{Bmatrix} = \begin{Bmatrix} {}^c s_1 \\ {}^c p_1^l \\ {}^c p_1^g \end{Bmatrix} \cdot \cos(\omega \cdot t + \mathbf{k} \cdot \mathbf{x}) + \begin{Bmatrix} {}^s s_1 \\ {}^s p_1^l \\ {}^s p_1^g \end{Bmatrix} \cdot \sin(\omega \cdot t + \mathbf{k} \cdot \mathbf{x})$$

Substituting this into differential equations obtained for λ^1 and relating variables $\{s_1(\mathbf{x},t), p_1^l(\mathbf{x},t), p_1^g(\mathbf{x},t)\}$, one finds the linear system for amplitudes $\{{}^c s_1, {}^s s_1, {}^c p_1^l, {}^s p_1^l, {}^c p_1^g, {}^s p_1^g\}$ (see Appendix 2), from which explicit expressions for self and cross-correlations are to be found. As have been shown by the method of harmonic balance the self-correlation of the first asymptotic term is $\overline{s_1}^2 = \left\| F^l - F^g \right\|^2 \sim \omega^4$. All derived formulae are given at the end of the Appendix 2 and the work on the analysis is still in progress. However, it is clear that the acoustic streaming driving force is proportional to the ratio of the fluxes induced by

[7] It can be easily generalized using Fourier series

dilatation and by the saturation gradient $F \sim \rho\omega^2 \cdot \frac{\mathbf{k}\cdot\mathbf{K}_l\hat{\mathbf{u}}}{\mathbf{k}\cdot\mathbf{K}_l\mathbf{k}} + \alpha\mathbf{k}\cdot\hat{\mathbf{u}}$. General relation between acoustic streaming driving force and frequency depends on dependency between wave vector and the frequency and, therefore, varies with geometry. For the general case of the plates dispersion relation is $k \sim \omega^{\chi}$ and, subsequently, $\overline{s_1}^2 = \left\|F^l - F^g\right\|^2 \sim \omega^{4-2\chi} + \omega^{2\chi}$, where parameter χ is controlled by geometry. Below we show a limiting case where an analytical analysis allows for qualitatively important results. Shaking of the structure, as a rigid body is a particular case we investigated during our permeability test program. For this case driving force is proportional to the square of the frequency, to the magnitude of the vibration, and to the some power of the saturation level: $F \sim \rho\omega^2 \cdot Amp \cdot \overline{S}^{\lambda}$, allowing estimation of the frequency role on induced water transport.

We close this section with some concluding remarks. Based on the first results of the asymptotic analysis one may see that *(i)* Acoustic streaming effect in the porous unsaturated media does exist; *(ii)* Result depends both on global geometry as well as on local effects. The power of the source depends on geometrical parameters. *(iii)* Important [and now possible] to study wave excitation for different options: air pulsation, structural waves, surface waves, etc.

11 Experimental Study

We have conducted tests intended to measure liquid water permeability of the cathode layers under vibration, static pressure and their combination. Under operating conditions, water is wicked away by the pressure difference between catalytic layer (where water is generated) and water transport plate (WTP) with negative pressure (sink). In the development of the experimental methodology we have used and modified original approach of UTC Fuel Cell [20].

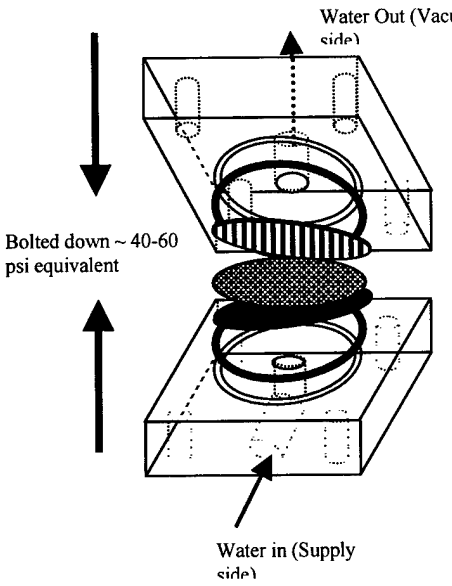

Figure 8. Specimen Setup

A scheme of the setup is shown in Figure 8 and the picture of the stand is given in Figure 9. A sample (porous layer from fuel cell cathode) of two-inch diameter is placed between two bi-polar plates. The two bi-polar plates (WTP) are then housed between two Plexiglas plates. O-rings are inserted between the Plexiglas and plates contact to provide a good seal. One of the plates is connected to a water reservoir. The second plate is channeled and the vacuum pump provides a vacuum (negative pressure). The water flow rate is measured by the high precesion balance with the accuracy of 0.1 microgramm. We apply vibration using shaker on top of external constant pressure gradient to the sample. We compare the flux (permeability) under different conditions.

The principal difficulty of this test is the necessity of comparison between very small fluxes of the order of microgramms/sec. Another principal limitation of the developed setup originated from small size of the specimens (thickness of the porous carbon paper is about 200 μ). Using such a test setup is impossible to generate a dilatational wave within this porous structure. Taking all these circumstances into account we have applied vibration (shaking) of the whole setup as a rigid structure. It means that during this type of the tests we were able to investigate only the role of inertial forces but dilatation. Analysis of the role of the dilatational waves is now ongoing task and bigger setup and results will be discussed later. However, current results demonstrate the non-zero effect of the zero-mean vibrations on the permeability.

We have tested two types of the porous substrate materials with different degrees of hydrophobicity. The first set of tests have been conducted on 10-wt% PTFE (10% of Teflon), 90-wt% carbon sublayer. This material manifests low hydrophobicity. We apply two different pressure gradients. The first is water pressure driving water into the porous membrane; the

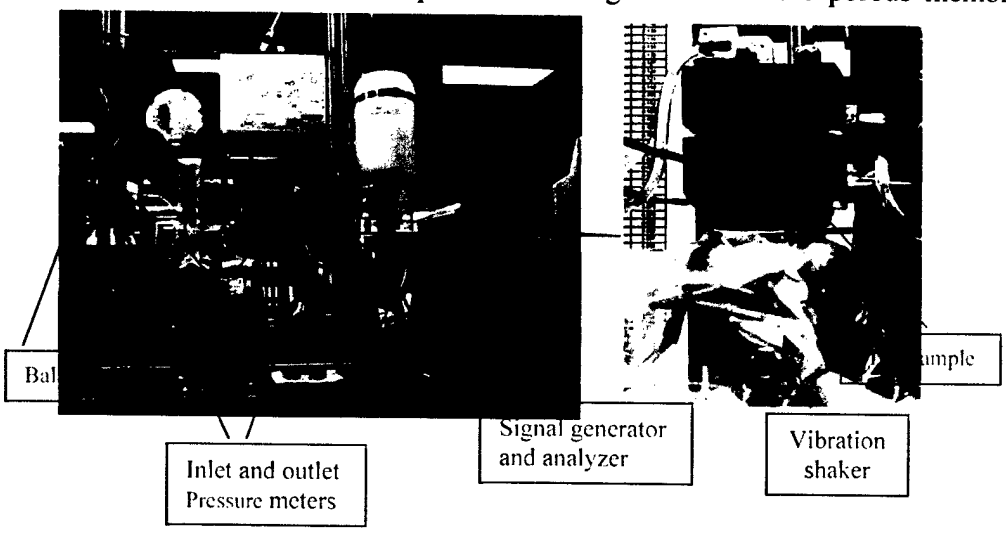

Figure 9 Permeability measurement test setup

second one is the so-called vacuum pressure, driving water out of the porous plate. The porous plate is not completely sealed in the sense that gas pressure is assumed to be equal to atmospheric. Typical test results are shown in Figure 10 when water pressure was 20 Kpa and vacuum pressure was 10 Kpa. During both reported tests, the flow rate was steady and approximately equal to 0.205 ± 0.005 milligrams per minute. The shaker were started at the point of time=4 (red line on the plot). Power of the signal was 500 μV/ms with broadband frequency excitation level.

As one can see from the Figure 10 the increase of the flux has been observed. If we integrate the area under the experimental curves, we obtain the total flux. Thus, the total flux increase due to specimens shaking equals to 0.1 milligrams. Total amount of additional released water is about 15% of usual connected water flow. Estimations of the amount of trapped (disconnected) water based on Leverett function show that 15% is close to the upper bound of the possible trapped

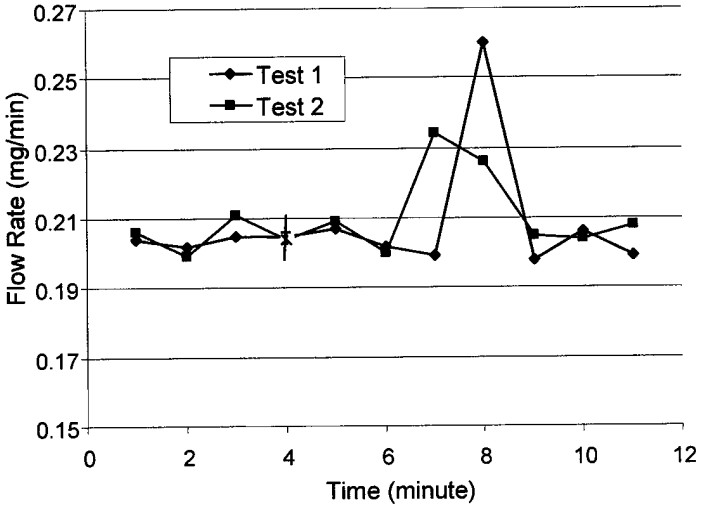

Figure 10. Permeability Measurement with water pressure=20 kPa; vacuum pressure=10 kPa

water amount. Thus, during vibration, almost all trapped water has been removed. In both tests the the amount of the released water was the same. The increase in water flux starts after 2-3 minutes after turning the shaker on. Electronic balance reading takes place every minute, so the difference is related to the time-reading rounding.

The second set of test have been performed on highly hydrophobic materials, where 50% of teflon is added to the carbon matrix. The flux has been unstable under water pressure of 3 psi and vacuum pressure of 1.5 psi. It requires some time to accumulate water on the specimen surface prior it penetrates into specimen. Because of high hydrophobicity, water practically does

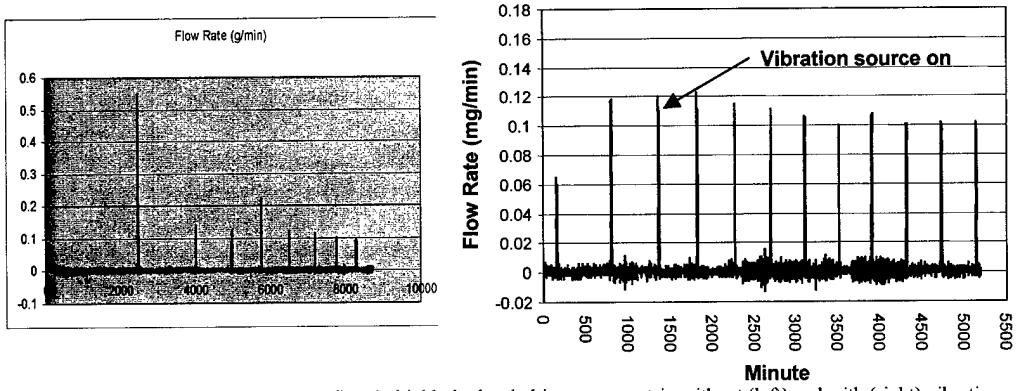

Figure 11. Comparison of water flow in highly hydrophobic porous matrix without (left) and with (right) vibration source.

not stop inside the specimen. As a result one can observe discrete droplets coming out the

hydrophobic specimen on the graph in Figure 11(a). Initially the time interval between droplets was 2000 minutes, and slowly decreases with each successive dropllet cycle. It might be explained by the increased of residual saturation in the porous media and subsequent decrease of the Leverett function. In other words, with the increase of the residual saturation, the hydrophobic resistance to new water imbibition getting smaller and the droplets frequency increases. When we turning the excitation source on, the time interval practically immediately decreases and stabilizes at 400 minute. It demonstrates the strong vibration effect on the residual water distribution and on the amount of residual water saturation in highly hydrophobic structures.

As a conclusion to this section, we note that extremely precise experimental procedure has been developed and conducted. Test results demonstrate a) existence of the effect of zero-mean vibration on directional unsatutrated water flow in the porous structure (fuel cell cathode compartment), b) instability in the water flow in highly hydrophobic structures under vibration and the need in wave generation.

12. Numerical Implementation and Results.

12.1 Computational Tool

At this part of the final report we focus mostly on the Task 3 developing a comprehensive numerical model. We implement the derived constitutive equations into the finite element software FEMLAB and conduct numerical analysis with different boundary and initial conditions. FEMLAB has been chosen because of its ability to combine physical/mathematical problems arisen from different fields in one generalized system. Combination of the different types equations into one template is the major advance of the FEMLAB. In our problem, we combine hyperbolic system (waves equations) for dynamics response with mass transfer equations. In our system equations (26)-(28) can be modified to the system of two elliptic equations and the first order (transport) equation for water saturation S. We use the advantage of multiphysical coupling of (1) acoustics and (2) porous media multiphase flow. FEMLAB allows running uncoupled problems (pure dynamics) and (static mass-transfer) automatically without any reformulation.

The underlying structure of FEMLAB is a system of PDE, which might be represented in one of the following forms: coefficient form (better suitable for almost linear problems), general form ($div\Gamma = \mathbf{f}$) where matrix Γ and forces-vector $\mathbf{f}$ are explicitly specified by user; and weak form that is very convenient for coupled problems. It is important to note that in finite element method, all equations eventually should be expressed in weak form anyway. Thus, we implement all our equations as a user formulated routines in FEMLAB template.

FEMLAB integrates seamlessly with MATLAB that provides the computational platform. FEMLAB models run in MATLAB structures environment and we can use all MATLAB programs and procedures. As our numerical experimentation has demonstrated, the major disadvantage of the FEMLAB is underdeveloped meshing procedure and impossibility to modify the solver routine. It limits the applicability of this tool (in it current version) to relatively simple geometries with not large number of elements.

12.2 Formulation and Normalization of the Governing Equations.

First, we consider the filtration part of the equations as it follows from Eq. (21)

$$\frac{\partial S}{\partial t} + \nabla \cdot (\mathbf{w}_l) = 0; \quad \text{and} \quad \mathbf{w}_l = S \cdot (\mathbf{v}_l - \mathbf{v}_s)$$

This is expression for water content, similar equation can be easily written for gas phase.

For the successful numerical analysis we have to determine material constants and extract J-Leverett functions from the available experimental and theoretical evaluation. We conduct combined theoretical-experimental study on formulating and calibrating models parameters. The

particular form of J-Leverett function and its relation with acoustic loading is the subject of the thermodynamic analysis.

Now, have to emphasize the very important point of the "elastic-plastic" decomposition. This has been already described in the "theoretical" part of the report but we repeat it again in numerical part of the report. Motion of the fluid is to be decomposed into two parts: elastic or dynamically induced inertial motion and the motion induced by pressure/saturation and controlled by modified D'Arcy law. In other words, we decompose the total motion into "elastic" wave-related motion and "plastic" filtration flow[8]:

$$v = v_{dynamical} + v_{filtration}$$

The D'Arcy part of the flux is described by gradients and as shown in Chapter 7 can be expressed as

$$\mathbf{w}_{D'Arcy} = -k\frac{\nabla(SP)}{S}; \qquad k = \frac{K_0\mathbf{K}}{\mu_l}$$

if we neglect effects of solid finite dilatation. Finally, the conservation law can be re-written as follows:

$$\frac{\partial S}{\partial t} = \nabla\cdot\left(k(S)\frac{\nabla(PS)}{S}\right) + \nabla\cdot(S\cdot(\mathbf{v}_l - \mathbf{v}_s))$$

The similar equation can be derived for the gas phase. Equation for the dynamic equilibrium .has the following general form

$$T(S)\cdot\frac{\partial S}{\partial t} - P^g + P^l = J(S)$$

These constitutive relations are supplemented by the definition of the Leverett function, simplified form of which is: $J(S) = -\dfrac{C_0(S - S_{middle})}{(S - S_{left})(1-S)}$, where S_{left} is the left saturation asymptote and S_{in} is the dynamic saturation equilibrium specific for the pair porous media-fluid. In our current calculations T(S) has been taken as a constant. In limiting case of equilibrium ($\dfrac{\partial S}{\partial t} = 0$) this equation is equivalent to well-known Laplace –Leverett equilibrium condition.

Combining together both transport equations for liquid and gas and the equilibrium condition and eliminating time derivatives from the first two equations, we obtain the following system of two elliptic and one first-order equation

$$\begin{cases} -T(S)\cdot K_1\cdot\nabla\cdot\left[S^2\cdot\nabla P_1 + S\cdot\nabla S\cdot P_1\right] + \nabla\cdot S(v_l - v_s) + P_1 - P_2 = -J(S) \\ -T(S)\cdot K_2\cdot\nabla\cdot\left[(1-S)^2\cdot\nabla P_2 - (1-S)\cdot\nabla S\cdot P_2\right] + \nabla\cdot(1-S)(v_g - v_s) + P_2 - P_1 = J(S) \\ P_1 - P_2 + J(S) = T(S)\cdot\dfrac{\partial S}{\partial t}; \qquad J(S) = -\dfrac{C_0(S - S_{middle})}{(S - S_{left})(1-S)} \end{cases}$$

[8] This decomposition is also correct for finite deformation and similar to the velocity gradient decomposition in deformation plasticity.

This system describes only "viscous" part of the system, or, in other words, only filtration part. It is coupled with dynamic part mostly through species velocities but also through the pressure distribution.

12.3 Normalization and Calibration of the Parameters

During this project we analyze harmonic signals, so the natural choice for time scaling is $\tau = \omega t$. For the stability of numerical procedure, it is desirable to get the coefficient in front of highest derivative of the order of unity. This dictates the choice of special scaling: $\tilde{\mathbf{x}} = \frac{\mathbf{x}}{\sqrt{KT}} = \frac{\mathbf{x}}{\sqrt{T\frac{k}{\mu\phi}}}$.

This set of substitutions leads to introducing of new normalized parameters/variables: $C = \frac{C_0}{\omega T}$ and $\tilde{P} = \frac{P}{\omega T}$. It is easy to see from these groups that the role of applied "static" pressure gradient decreases with the increase of the applied acoustic frequency[9].

There are two limited cases of the problem of acoustic enhancement of mass transfer in porous media. The first reflects the case when small vibration perturbs filtration process. The principal term in the equation here is $\nabla \cdot \left(k(S)\frac{\nabla(P\,S)}{S} \right)$. This corresponds to the numerical situation when coefficient of filtration K is relatively large. Asymptotical analysis of this situation has been reported in the section above. The other limiting case corresponds to small permeability (say, k~1e-15) and the problem becomes close to singular perturbation ($\varepsilon\ddot{x} + \dot{x} + \omega^2 x = f$). The numerical finite element software developed in this program covers wide range of the parameters variation.

In order to calibrate and verify the developed model we need evaluate material parameters and fit model parameters against experimental data.
For isotropic Toray paper the following material parameters are accepted:
$\lambda = \frac{\lambda_{\|} + \lambda_{\perp}}{2} \approx 30\ Ksi$; $\mu = \frac{\mu_{\|} + \mu_{\perp}}{2} \approx 20\,Ksi$; $\rho \approx 1000\,kg/m^3$ and porosity $\phi \approx 0.75$.
Material properties for Toray-paper bulk compressibility is $K_b \approx 30\,Ksi$ and for structural fibers is $K_{fiber} \approx 20\,Msi$, also $\mu_{fiber} \approx 25\,Msi \approx 160\,GPa$. Viscous properties and acoustic waves decay for this material has been accepted from literature review and based on averaging for test results for different woven carbon materials:

---

[9] Other normalizations are possible, however we stopped on the described above. We have checked several different substitutions of which the most numerically-convenient lead to the normalization of the coefficient in front of D'Arcy term in the dynamic system. For example, $\tau = \frac{(\lambda + 2\mu)}{l^2}\frac{k_l}{\mu_l |\phi S|^2}t$; $\tilde{x} = \frac{x}{l}$, where l is the characteristic size

$A = A_0 e^{-\gamma x}$; $\gamma \sim \frac{\omega^2}{2\rho c^3}(\frac{4}{3}\eta + \zeta)$ (Ref. Landau and Lifshits Hydrodynamics). Calculating plane wave decay (γ) based on Delany and Bazley laws we were able to estimate $\eta \approx 0.05 \div 0.5\ Mpa \cdot s$ and $\zeta \approx 0.02 \div 0.2\ MPa \cdot s$. Elastic generalized Biot coefficients have been evaluated based on elastic properties as follows:
$q = 690\,MPa \cdot \phi$; $t = 0.04\,MPa \cdot \phi$; $r = 220\,MPa \cdot \phi$; $s = 0.12\,MPa \cdot \phi$; where modified Biot's coefficients has been expressed:
$Q = q\varepsilon_l = q\phi S$; $R = r\varepsilon_l = r\phi S$; $T = t\varepsilon_g = t\phi(1-S)$; $S^{Biot} = s\varepsilon_g = s\phi(1-S)$. It is important that we assumed that *q, t, r,* and *s* are constants and do not depend on saturation.
Next, we estimated transport properties, which requires fitting of model parameters.
Viscosity of water is assumed to be equal
$\mu_{water} = 0.5cp = 5e-4\,{}^{kg}/_{m \cdot s}$; $\mu_{gas} = 0.022cp = 2e-5\,{}^{kg}/_{m \cdot s}$. We need to evaluate permeability of water in the porous. Using Klinkenberg effect we approximate $k_{air} \sim 1.4 \cdot k_{liquid}$.
Testing of water permeation through substrate at different pressure gradients have been conducted at UTRC and UTC Fuel Cell. We fitted the flux vs. pressure finite element calculations against experimental data as shown in Figure 12 below.

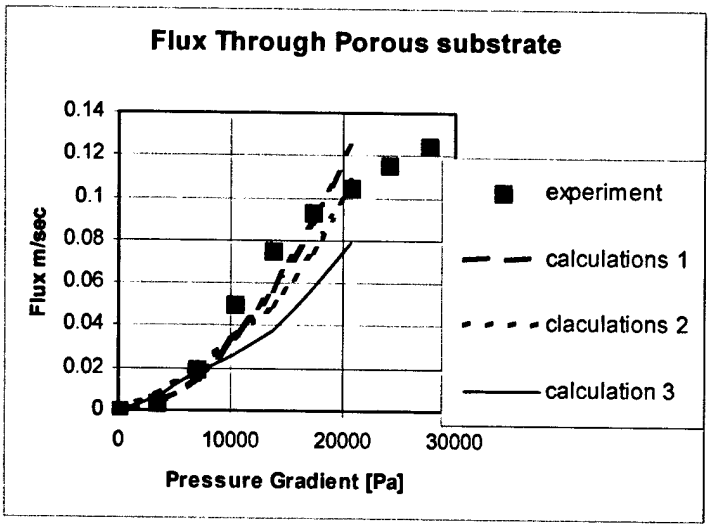

Figure 12. Fitting transport parameters against experimental

We varied several major parameters of the system aiming to obtain the closest fit. Leaving the question of the uniqueness open, we are able to find the set of parameters providing good fit. With decrease of viscosity T, the flux increases; Coefficient C_0 –magnitude of Leverett function defines the rate of stabilization and with the increase of C_0 the flux decreases.

Calculated fitting parameters are shown in **Table 1.**

	Calculations 1	Calculations 2	Calculations 3
K	3E-15	3E-15	3E-15
T	0.6E5	0.6E5	1.E5
C_0	0.8E4	1.E4	1.E4

More exact fitting, especially for big pressure gradients can be obtained by the use of Forchheimer model[10]. We have done some numerical experiments in that direction but this work is out of scope of the reported project.

12.4 Boundary conditions.

The system derived above belongs to mixed hyperbolic-parabolic type, vibration part being hyperbolic and filtration parabolic wit ordinary differential equation for static pressures.

For **vibration part** zero normal forces are defined **on free** boundaries:

$$n_j \cdot \sigma_{ij}^s = \left(\lambda \cdot \theta_s + M_{ls} \cdot \theta_l + M_{gs} \cdot \theta_g\right) \cdot n_j \cdot \delta_{ij} + 2 \cdot \mu \cdot n_j \cdot e_{ij} = 0$$

$$n_j \cdot \sigma_{ij}^l = -p_l \cdot n_j \cdot \delta_{ij} = n_j \cdot \delta_{ij} \cdot \left(M_l \cdot \theta_l + M_{ls} \cdot \theta_s + M_{gl} \cdot \theta_g\right) = 0$$

$$n_j \cdot \sigma_{ij}^g = -p_g \cdot n_j \cdot \delta_{ij} = n_j \cdot \delta_{ij} \cdot \left(M_g \cdot \theta_g + M_{gs} \cdot \theta_s + M_{gl} \cdot \theta_l\right) = 0$$

on **fixed** boundaries zero displacements are defined for all phases:

$$\mathbf{u}_s = 0; \mathbf{u}_l = 0; \mathbf{u}_g = 0.$$

Boundary with **excitation**:

$$\left(\mathbf{n} \cdot \mathbf{u}_s\right)\mathbf{n} = \mathbf{f}(t); \mathbf{u}_s - \left(\mathbf{n} \cdot \mathbf{u}_s\right)\mathbf{n} = 0; \mathbf{u}_l = 0; \mathbf{u}_g = 0$$

where $\mathbf{f}(t)$ is a given motion of the excitation boundary. It can be pulse-like or periodic.
To be consistent it requires appropriate definition of velocities:

$$\left(\mathbf{n} \cdot \mathbf{v}_s\right)\mathbf{n} = \partial \mathbf{f}(t)/\partial t; \mathbf{v}_s - \left(\mathbf{n} \cdot \mathbf{v}_s\right)\mathbf{n} = 0; \mathbf{v}_l = 0; \mathbf{v}_g = 0.$$

For **filtration part** the boundary conditions should reflect the physical conditions of water removal from the boundary. As one can see from the **Constitutive relations for static pressures** above, the sign of derivative $\partial S/\partial t$ on the boundary depends on the relation between boundary values of static pressures $\{P_g, P_l\}$, which means that varying due to vibration saturation S might change this condition from imbibitions to drainage and vice versa. To obtain net drying effect a boundary condition that prevents liquid flow from the outside must be imposed when $\partial S/\partial t > 0$. It also means that to achieve overall drying effect caused by vibration, a physical mechanism preventing reverse flow back into sample must be found. In other words, a boundary that is open for liquid exchange must favor liquid flow in one direction. That can be due to fast removal of

---

[10] The transport law for such a model has the following form:

$\left(\alpha_l \cdot \left|S \cdot \mathbf{q}_l\right|^{\beta_l} + 1\right) \cdot S \cdot \mathbf{q}_l = -\left(\frac{k_l(S)}{S}\right) \cdot \nabla\left(S \cdot P_l\right)$ and predicts the convex shape of the flux vs. pressure curve.

water from the boundary with the rate higher than the frequency of vibration or applying special hydrophobic boundary layer. Therefore, the boundary conditions on the boundaries opened for liquid flow is:

$$P_g =_{boundary} P_g; P_l =_{boundary} P_l \; if \; \frac{\partial}{\partial t} S < 0$$

$$Flux_g =_{boundary} J_g; Flux_l =_{boundary} J_l; if \; \frac{\partial}{\partial t} S \geq 0$$

$_{boundary} J_g = 0; _{boundary} J_l = 0$ means the best case condition for acoustic water removal.

$$\begin{pmatrix} Flux_l \\ Flux_g \end{pmatrix} = K_0 \cdot \mathbf{K} \cdot \begin{pmatrix} \rho_l \varepsilon_l^{-1} \mu_l^{-1} \left(\nabla \left(\varepsilon_l P \right) + \mathbf{w}_l \right) \\ \rho_g \varepsilon_g^{-1} \mu_g^{-1} \left(\nabla \left(\varepsilon_g P_g \right) + \mathbf{w}_g \right) \end{pmatrix}$$

where

$$\mathbf{K} = \begin{pmatrix} \mathbf{K}_l^{-1} & \sqrt{\frac{\mu_g}{\mu_l}} \cdot \varepsilon_g \cdot \mathbf{K}_{gl}^{-1} \\ \sqrt{\frac{\mu_l}{\mu_g}} \cdot \varepsilon_l \cdot \mathbf{K}_{gl}^{-1} & \mathbf{K}_g^{-1} \end{pmatrix}^{-1}$$

12.5 Results of Numerical Calculations for Different Boundary Conditions

First we considered the problem in the rectangular with pressure defined as boundary conditions as shown in the scheme. Vibration is applied to the upper boundary as follows: $u_y = A\sin(\omega t - kx)$, and $v_y = \frac{\partial u_y}{\partial t}$. There are two limiting cases depending on material

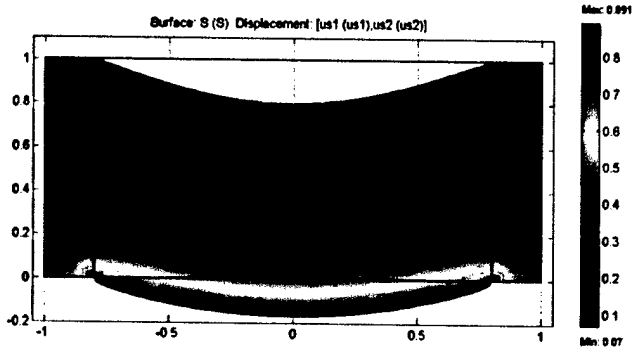

Figure 13. Deformed shape of the plate . Contours of Saturation are shown.

parameters and BC. The first, when vibration [acoustic pressure] is small with respect to applied

to boundaries "static" pressure gradient. The second case corresponds to the situation when acoustic pressure is large in comparison with static pressure gradient. We have considered both situations. The Figure below illustrated the simplest deformed shape of the structure.

The results of calculations corresponding to the first situation are shown in Figures 13-16. Saturation distributions under both static and small vibration conditions are similar to each other and show steep saturation gradient near to sink. Figure 14 illustrates formation of steady distribution.

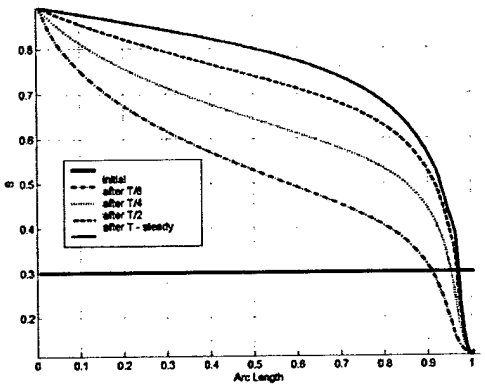

Figure 14. Saturation Distribution in the layer after different time till reaching the steady regime. No vibration applied.

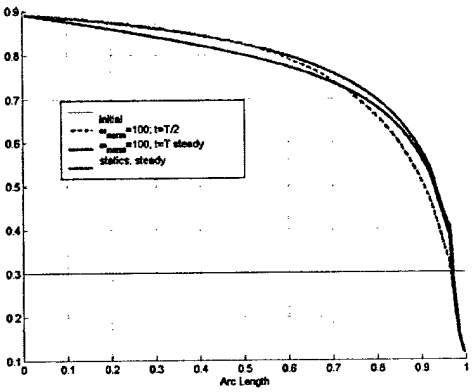

Figure 15. Distribution of Steady Saturation with and without vibration

The total effect of small vibrations on total water content is small and illustrated by graphs in Figure 15. These direct finite element calculations are in good agreement with analytical (asymptotical) analysis (part 9), which in turn predicts second order effect of small vibration on water content in the porous unsaturated media. It is important that in this calculation the water transport is primary controlled by filtration process.

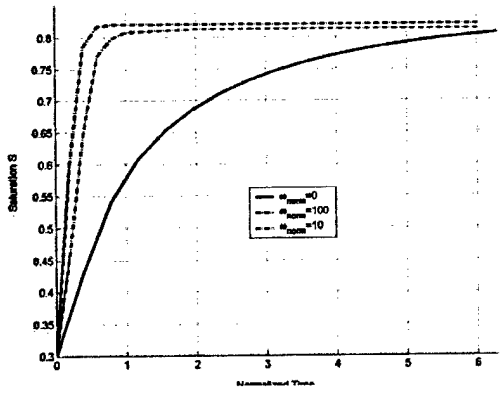

Figure16. Decrease of transient time with frequency of applied vibration

The most pronounced effect of vibrations on transport process is substantial acceleration of water transport. Under vibration impact, transient period is insignificant in comparison to pure D'Arcy filtration (static) case. Thus, under pressure boundary conditions and dominating filtration term the water just follows the motion of the solid phase. This leads to fast process stabilization and to small integral effect in flux evaluation as shown in Fig. 16. The homogenization of water distribution is significantly faster under vibration impact. Increase of the effect relates with the increase of the term $\nabla\cdot(S(v_{water}-v_{solid}))$. Therefore, this product after averaging should be not only significant but noticeably changes with space to guarantee existence of not small derivative (div).

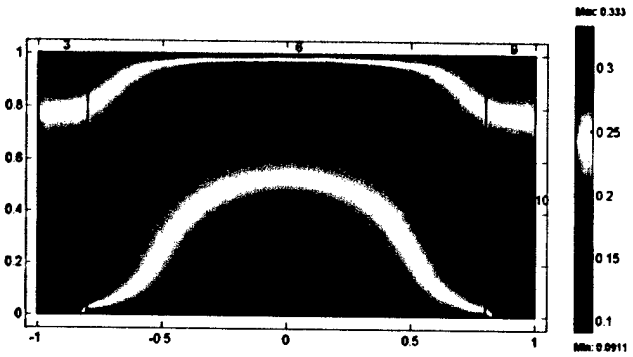

Figure 17. Formation of the boundary layer on the top boundary under acoustic impact.

During each half-cycle water efficiently drains from the bottom boundary and imbibes back during another half cycle. The same situation is observed on upper boundary. Only with the development of the mechanism preventing back imbibing from the surface or in other words the way of fast removing water from the surface would lead to effective acoustic drying.

Another qualitative situation appears when filtration coefficient is small (as typical for Toray paper and bi-layer) and, therefore, coefficient in front of highest derivative is a small parameter. This and pressure boundary conditions leads to creation of a boundary layer. The characteristic size of such boundary layer can be evaluated by equating orders of both terms in transport equation above: $l \sim KT \sim \frac{k_{water}}{\mu_{water}} T \sim 1 \div 5\,\mu m$. The thickness of the boundary layer is about several percents of the cathode porous layer. All changes consisting the boundary conditions with the bulk solution take place in this boundary layer and saturation in the internal part of the porous plate practically does not change with vibrations. As can be seen from the Figure 17, the region with decreased water content occurs inside the porous plate and. the saturation is higher at surface regions, therefore water flux is directed inside the porous plate. In other words, during vibration, plate starts imbibe water, if pressure is defined on the boundary. This is very important situation for PEM FC materials because calculations fit range of material constants. This leads to the conclusion that the most important process of acoustic drying is effective water removal from the surface. Assuming it is technically possible to realize, we analyze water transfer under this semi-permeable boundary conditions. The modeling results provide us with upper bound estimations of the amount of acoustically induced water flux. Acoustically induced flux is naturally more pronounced if applied static pressure gradient is small. We have numerically analyzed in details the situation when the in-bound water flux at the sink boundary is semi-sealed. As was described in the previous section, we implemented such a semi-permeable physical model by constraining the boundary conditions as $\int_{boundary} \Gamma \vec{n} dA \geq 0$.

The set of cross-section snapshots of water saturation (S) reflecting dynamics of saturation with normalized time under influence of structural waves. "Low" bottom is semi-sealed: if

$\int_{boundary} \frac{\partial S}{\partial y} dA > 0$, then flux is zero, otherwise is not constrained. Pressure on the "upper" boundary has been set constant P=0. The detailed (in time) set of snapshots is shown in the Appendix III. Below we show only the most important pictures.

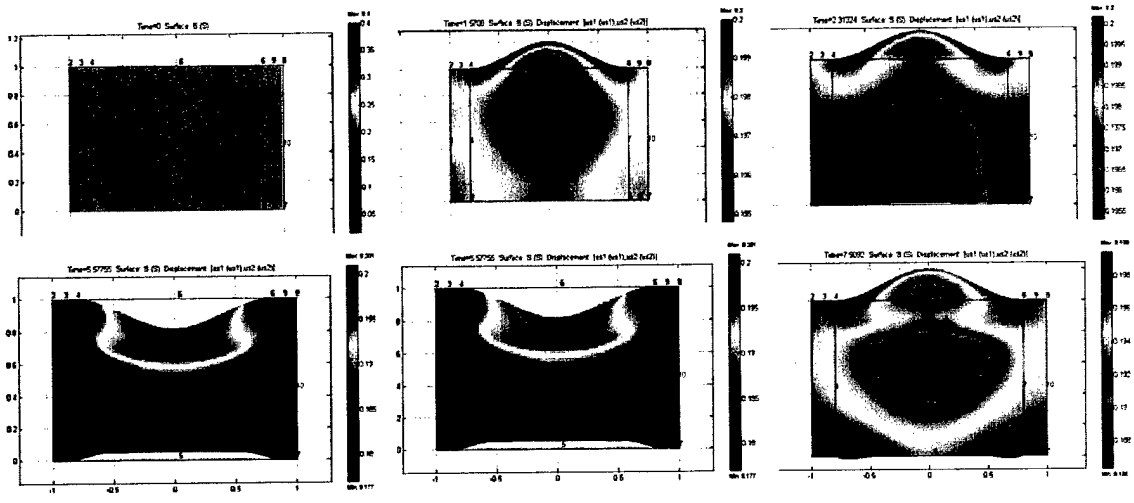

Figure 18. Series of snapshots of water saturation distributions under the impact of structural vibrations. Development of thin "boundary layer on the top boundaries observed under "tension" mode of vibration.

As can be seen from the Figures 18 reflecting the acoustically driven mass transfer, the boundary layer is developed on the boundary where the pressure has been defined. Also, the integrated amount of water in the plate gradually decreases on approximately 5% and stabilizes there. Process starts with relatively fast drainage, then after first half of vibration period the internal pressure gradient is developed in such a way that water would be imbibed from the upper boundary. Up to time ~ 4.8 semi-permeable boundary conditions lead to invariable amount of water content in the porous media (see Fig 19). Then, during another period of vibrations, pressure conditions change again and drainage takes place. After this the process is almost stabilized and further drainage has not been numerically observed. The most important conclusion from these calculations can be summarized as follows:

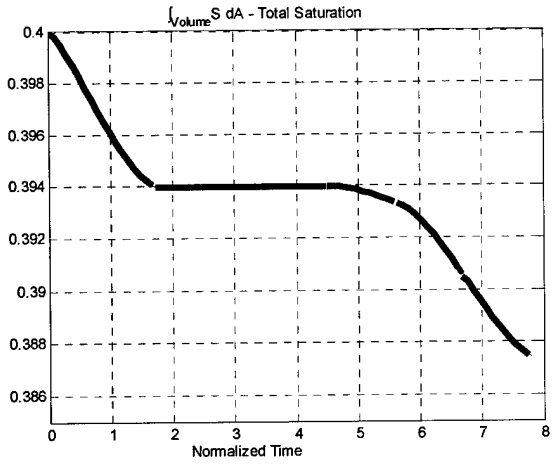

Figure 19. Dynamics of acoustically driven water drainage through semi-permeable boundary

(i) The acoustically driven water removal from the porous plate is numerically observed;

(ii) Acoustic drying is possible if and only if water removal from the surface mechanism does exist. Otherwise, water is imbibed back immediately.

(iii) The acoustic drying/drainage is very fast process, which requires only several vibration periods to reach saturation;

(iv) Total amount of the removed water under given parameters is not exceed 5%[11].

From the series of snap-shots showing changes in liquid and gas pressure with structural (solid) vibrations demonstrate the structure of acoustic waves in the liquid and gas phases of partially saturated porous media. Model calculations shown in Figures 20 (Detailed series of snap shots are given in Appendix III) clearly show that liquid and gas motions follow the solid structure vibrations. This effect takes place solely due to the "effective viscosity" generated by D'Arcy term in the constitutive equations.

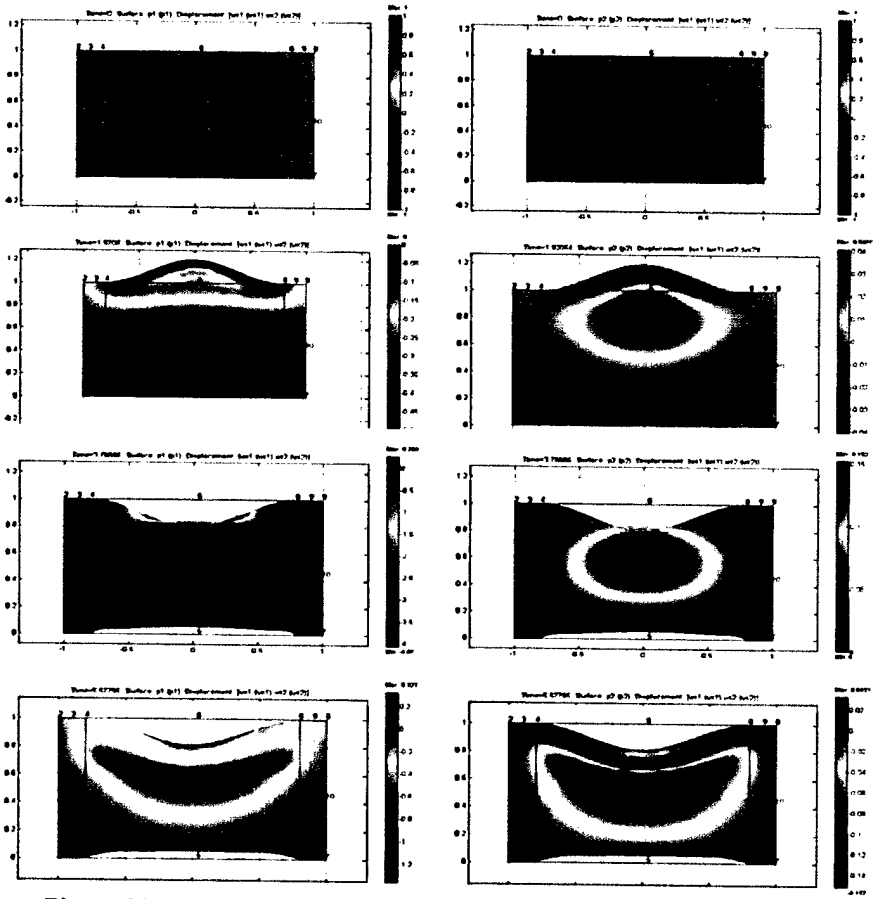

Figure 20. Series of snap-shots demonstrating changes in liquid and gas pressure with structural (solid) vibrations

Figure 21 illustrates in-phase vibration of liquid and solid phases in both structural vibration modes: longitude and shear waves. Therefore, the dynamics of saturation (liquid and gas) within

[11]Parameters variations might lead to increase of the removed water, but it would not exceed 10%.

the porous structure is a strong function of structural waves. Very important result that can be deduced from this numerical modeling is that under structural vibrations/waves applied to the

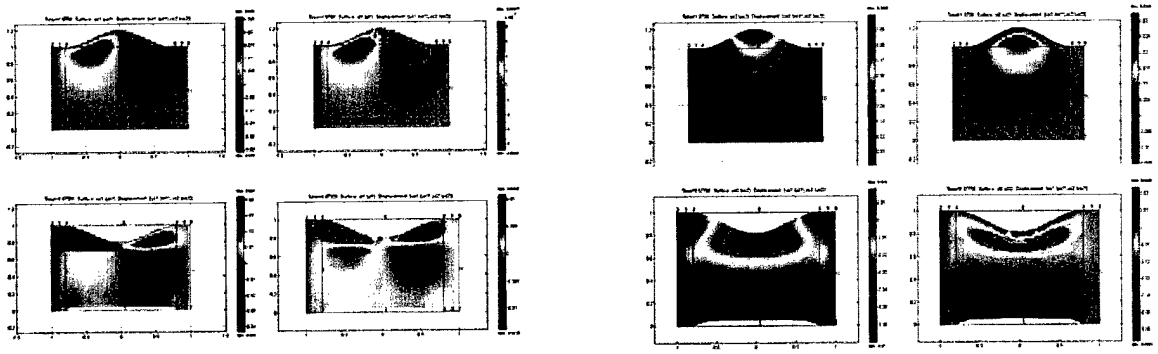

Figure 21. Displacement along (a-left four figures) x-direction (u_1) of solid (left) and liquid (right) phases and (b- right four figures) y-direction (u_2) of solid (left) and liquid (right) phases

partially saturated porous body, the liquid and gas pressures have a non-trivial form and shape within the body. The pressure strongly affects the diffusion coefficients and, therefore, affects transport of species. The gas (oxygen in our case) transport would be determined by not a diffusion as previously been accepted but by convection-diffusion mechanism.

13. Concluding Remarks

We have developed a unified model of structural/acoustic wave propagation in the PEM cathode compartment and coupled it with mass transfer in the porous media. This is the first known to the authors model of such kind coupling acoustics and filtration in porous media. A set of consistent constitutive relations and governing equations for multiphase partially saturated porous dynamic media have been developed using Lagrangian approach with subsequent inclusion of various dissipative mechanisms. Developed unified methodology is useful for the wide range of Fuel Cell problems as well as for the wide range of other porous structures and could serve as an important design tool.

It has been demonstrated that the phase saturations have strong impact on wave dynamics in porous continuum. Explicit expressions for generalized multiphase Biot-type coefficients that explicitly depend on the phase saturations have been obtained.

We have succeeded to generalize filtration (D'Arcy) law on dynamic system with water saturation varying with space and time. It has been shown that the viration-induced flux is a strong function of solid matrix distortion, saturation gradient and inertial forces. We also were able to connect hysteretic phenomena to relaxation process due to gradients of filtration rate.

The developed homogenization technique is crucial for numerical analysis of high frequency impacts. It allows circumventing restrictions on maximum allowed number of finite elements to resolve spatial frequency of the acoustic/structural wave. Using asymptotic analysis we

demonstrated the crucial role of cathode geometry on the water-transport enhancement effect. We also obtained analytical results evaluating the role of acoustic loading on the flow and frequency and wave number dependencies of the effective mass driving forces. It has been demonstrated using averaging principle that vibration gives rise to net change of saturation inside porous medium. This effect is analogous to the known phenomenon of acoustic streaming [18, 21] but has not been discovered before.

We conduct the extremely precise experimental procedure to measure bi-layer/substrate permeability under vibration. Test results for different materials demonstrate *(i)* existence of the effect, *(ii)* instability in highly hydrophobic structures under vibration and the strong correlation between induced mass-transport and spatial inhomogeneity generated by structural waves.

The most useful application of the equations derived for time-averaged fluxes is when the leading zero-order approximation is vanished. In the opposite case, vibration-induced fluxes are small and the transport is determined by static pressure gradients. This also specifies potential application of the vibration-induced saturation dynamics. It is most useful when for some reason pressure-induced transport is either impossible or undesirable. Numerical results demonstrate that applied structural vibration/acoustic loading *(i)* intensifies the process dynamics or in other words decreases time of transient process; (*ii*) might drain out up to 5-10% of distributed in porous media water if the mechanism preventing reverse acoustic-driven imbibitions is in place; (*iii*) The fast water removal from the surface is crucial for acoustic-driven drying; (*iv*) In a working Fuel Cell, vibrations cause increase of the water flux from the porous cathode in both directions out to WTP and back to the catalytic layer, which in turn makes the Fuel Cell performance worse; (*v*) Acoustic/Structural vibrations accelerates the stabilization of the system (porous media-liquid-gas) at some level predefined by material properties in general and by Leverett function in particular. Therefore, for over-saturated porous media, vibrations lead to fast drying up to stable level and, subsequently, for FC performance improvement. If the initial saturation is smaller then the steady-stable level, the porous layer would be immediately imbibed up to the stable level and, subsequently, performance would deteriorates. Both types of phenomena have been observed (see also, [22]) in practical nature.

On the base of the results mentioned above, we make the following practical conclusions focused on results industrial (fuel cells) implementation: (i) Acoustic/structural vibration drying can be used when other mass-transfer driven processes are small. It means that the best operational moment for the application of the acoustics is the shutdown drying preventing from possible frosting of the PEM fuel cell cathode compartment. Another optimum performance regime is fuel cell dry start up, when vibrations would significantly cut the start-up stabilization (warming) time. (ii) Fast and efficient water removal from the surfaces and interfaces is crucial for the acoustic drying. Much work needs to be done to develop such a material/technology design. This work shows the direction for the optimal material selection. (iii) Based on numerical results, one can conclude that the acoustically driven material drying (water drainage) is the fast process, therefore, the application of vibration field should be performed as a short impulse series, preferably while source or sink of water is sealed (start-up and shutdown). (iv) Project results show that cathode compartment acoustic cleaning would be beneficial if the cell is turned-off at the moment of cleaning. Therefore subsequent short-time (~1 min) disconnections of one or several cells from the stack for a cleaning would provide positive performance effect.

14 Reference:

[1] J. Larminie and A. Dicks, *Fuel Cell Systems Explained.* J. Wiley & Sons 2000, 308 p.

[2] K. Kordesch, G. Simader, *Fuel Cells and their applications.* VCH, 1996, 374 p

[3] M. A. Biot, Theory of Propagation of Elastic Waves in a Fluid Saturated Porous Solid. I. Low Frequency Range. II. Higher Frequency Range. *The Journal of the Acoustical Society of America* **28** (2) 168-191, 1956

[4] J. Allard. Propagation of Sound in Porous Media. Elsever Applied Science, 1993

[5] W. Gray and S. Hassanizadeh. Macroscale continuum mechanics for multiphase porous-media flow including phases, interfaces, common lines and common points. *Advances in Water Resources*, **21**, pp.261-281, 1998.

[6] S. Nemat_Nasser and M Hori. Micromechanics: overall properties of heterogeneous materials. Elsevier 1999

[7] L.Molotkov. On tortuosity coefficients in effective Biot model. *Notes of scientific seminars of POMI*, **257**, 1999, pp. 157-163. (In Russian).

[8] G. Mavko, T. Mukerji, and J. Dvorkin The Rock Physics Handbook. Tools for Seismic Analysis in Porous Media, Cambridge University Press, 1999

[9] Z. Hashin and S. Shtrikman, A variational approach to the elastic behavior of multiphase materials. JMPS, **11**, pp.127-140, 1963

[10] L. Landau and E. Lifshitz. Theory of Elasticity. 1987.

[11] S.M. Hassanizadeh and W.G. Gray. Mechanics and thermodynamics of multiphase flow in porous media including interphase boundaries. *Advanced Water Resources*, **13**, pp169-186.

[12] A. Beliaev and S.M. Hassanizadeh. A Theoretical Model of Hysteresis and Dynamic Effects in the Capillary Relation for Two-phase Flow in Porous Media. *Transport in Porous Media,* **43**, pp.487-510, 2001.

[13] G.I. Barenblatt. Filtration of Two Non-mixing Fluids in a Homogeneous Porous Medium. *Mechanics of Gas and Fluids*, **5**, pp.857-864, 1971.

[14] O. Coussy, Mechanics of Porous Continua, J. Wiley & Sons, 1995, 455p.

[15] J. Bear. Dynamics of Fluids in Porous Media. Dover Publications, INC. 1988.

[16] Z. I. Khatib, G. J. Hirasaki, and A. H. Falls, "Effects of Capillary Pressure on Coalescence and Phase Mobilities in Foams Flowing Through Porous Media", *SPE RE* (Aug. 1988), 919-926.

[17] N.N.Bogolubov and Y.A.Mitropolsky. Asymptotic Methods in the Theory of Non-linear Oscillations. Hindustan Publishing Corpn. 1961.

[18] A.M.Maksimov, E.V.Radkevich and I.Ja.Edelman. The Mechanism of Nonperiodic Motion in Porous Media as a Result of the Accumulating Effect of Nonlinear Waves. Journal of Engineering Physics and Thermophysics, **70**, pp.1-8, 1997.

[19] A. D.Bruno. Local method of nonlinear analysis of differential equations. Springer-Verlag, 1979.

[20] A. Lubag and J. Yi Studies on Water Permeation through the Sub-layer. UTCFC report, 2002.

[21] W.L.Nyborg. Acoustic streaming. In: *Mason W.P., ed., Physical acoustics, IIB,* New York: Academic Press; pp.265-331, 1965.

[22] Carlstrom Jr., Maynard, W., Fuel Cell with Selective Pressure Variation and Dynamic Inflection, US6093502

Appendix I

Introducing the new variable $S = \varepsilon_l / (1 - \varepsilon_s)$ the system takes the form:

$$\frac{\partial}{\partial t}\begin{pmatrix} S \\ -S \end{pmatrix} = \frac{K_0}{\varepsilon} \cdot \begin{pmatrix} \mu_l^{-1} \cdot \nabla \cdot \mathbf{K}_l S^{-1} \left(\nabla S \left[P_l - \lambda \cdot F_l^P \right] + \lambda \cdot \frac{\partial}{\partial t} S \cdot \mathbf{F}_\mathbf{l}^\mathbf{K} \right) \\ \mu_g^{-1} \cdot \nabla \cdot \mathbf{K}_g (1-S)^{-1} \left(\nabla (1-S) \left[P_g - \lambda \cdot F_g^P \right] + \lambda \cdot \frac{\partial}{\partial t} (1-S) \cdot \mathbf{F}_\mathbf{g}^\mathbf{K} \right) \end{pmatrix}$$

where

$\varepsilon = 1 - \varepsilon_s$ - porosity;

$$\begin{pmatrix} F_l^P \\ F_g^P \end{pmatrix} = \begin{pmatrix} q \cdot \nabla \cdot \mathbf{u}_s + r \cdot \nabla \cdot \mathbf{u}_l + \varepsilon \cdot b \cdot S \cdot \nabla \cdot \mathbf{u}_g \\ t \cdot \nabla \cdot \mathbf{u}_s + \varepsilon \cdot b \cdot (1-S) \cdot \nabla \cdot \mathbf{u}_l + s \cdot \nabla \cdot \mathbf{u}_g \end{pmatrix}$$

$$\begin{pmatrix} \mathbf{F}_\mathbf{l}^\mathbf{K} \\ \mathbf{F}_\mathbf{g}^\mathbf{K} \end{pmatrix} = \begin{pmatrix} \rho_l \cdot \frac{\partial}{\partial t} \mathbf{u}_l + \left(\rho_l \cdot \beta_l + \rho_g \cdot \left(S^{-1} - 1 \right) \cdot \beta_{gl} \right) \frac{\partial}{\partial t} (\mathbf{u}_l - \mathbf{u}_s) \\ \rho_g \cdot \frac{\partial}{\partial t} \mathbf{u}_g + \left(\rho_g \cdot \beta_g + \rho_l \cdot \left((1-S)^{-1} - 1 \right) \cdot \beta_{gl} \right) \frac{\partial}{\partial t} (\mathbf{u}_g - \mathbf{u}_s) \end{pmatrix}$$

and constitutive relations for $\{P_l, P_g\}$:

$$P_g - P_l = J^{dr}(S) + T \cdot \frac{\partial}{\partial t} S \text{ for drainage } \left(\frac{\partial}{\partial t} S < 0 \right)$$

and

$$P_g - P_l = J^{imb}(S) + T \cdot \frac{\partial}{\partial t} S \text{ for imbibition } \left(\frac{\partial}{\partial t} S > 0 \right)$$

Here equation $P_g - P_l = J(\varepsilon_l, \varepsilon_g) + F\left(\frac{\partial}{\partial t} \varepsilon_l, \frac{\partial}{\partial t} \varepsilon_g \right)$ has been resolved versus $\frac{\partial}{\partial t} S$ due to the simplifications above, with two branches correspondent to drainage and imbibitions respectively.

Additional, substantial for analytical evaluation assumption, is that the vibrations $\{\mathbf{u}_s, \mathbf{u}_l, \mathbf{u}_\mathbf{g}\}$ are caused by a vibrator attached to the porous matrix such that, when it is turned off, $\{\mathbf{u}_s, \mathbf{u}_l, \mathbf{u}_\mathbf{g}\} = 0$. So, the case of small vibrations $\{\mathbf{u}_s, \mathbf{u}_l, \mathbf{u}_\mathbf{g}\} \sim \lambda$ is considered where λ is small amplitude of external source.

Asymptotic analysis.

As it can be seen from the above, two forces $F_{l,g}^{K,P}$ stemmed from a source of vibration affect fluid flow in porous material. As they are linear combinations of $\{\mathbf{u}_s, \mathbf{u}_l, \mathbf{u}_g\}$ and their time and spatial derivative, one can conclude that in general the spectral composition of the forces includes both natural frequencies of porous medium (Biot waves) and frequencies that correspond to the particular porous layer structure. The whole picture, therefore, is both geometry and material dependent and requires numerical analysis for any specific geometry. One can show, however, in very general terms that periodic forces $F_{l,g}^{K,P}$ cause non-periodic mass transport.

A change of variables:

$$S(\mathbf{x},t) = \overline{S}(\mathbf{x},t) + \lambda \cdot s_1\left(\overline{S},\overline{P_l},\overline{P_g},\mathbf{x},t\right) + \lambda^2 \cdot s_2\left(\overline{S},\overline{P_l},\overline{P_g},\mathbf{x},t\right) + \ldots$$

$$P_l(\mathbf{x},t) = \overline{P_l}(\mathbf{x},t) + \lambda \cdot p_1^l\left(\overline{S},\overline{P_l},\overline{P_g},\mathbf{x},t\right) + \lambda^2 \cdot p_2^l\left(\overline{S},\overline{P_l},\overline{P_g},\mathbf{x},t\right) + \ldots$$

$$P_g(\mathbf{x},t) = \overline{P_g}(\mathbf{x},t) + \lambda \cdot p_1^g\left(\overline{S},\overline{P_l},\overline{P_g},\mathbf{x},t\right) + \lambda^2 \cdot p_2^g\left(\overline{S},\overline{P_l},\overline{P_g},\mathbf{x},t\right) + \ldots$$

is sought in form of asymptotic expansion in λ such that

$$\overline{\begin{Bmatrix} s_i\left(\overline{S},\overline{P_l},\overline{P_g},\mathbf{x},t\right) \\ p_i^l\left(\overline{S},\overline{P_l},\overline{P_g},\mathbf{x},t\right) \\ p_i^g\left(\overline{S},\overline{P_l},\overline{P_g},\mathbf{x},t\right) \end{Bmatrix}} = \lim_{T,L\to\infty} \frac{1}{T\cdot L^3} \int_0^{T,L} dt\mathbf{dx} \begin{Bmatrix} s_i\left(\overline{S},\overline{P_l},\overline{P_g},\mathbf{x},t\right) \\ p_i^l\left(\overline{S},\overline{P_l},\overline{P_g},\mathbf{x},t\right) \\ p_i^g\left(\overline{S},\overline{P_l},\overline{P_g},\mathbf{x},t\right) \end{Bmatrix} = 0$$

and $\left\{\overline{S}(\mathbf{x},t), \overline{P_l}(\mathbf{x},t), \overline{P_g}(\mathbf{x},t)\right\}$ satisfy filtration equation without vibration terms:

$$\frac{\partial}{\partial t}\begin{pmatrix} \overline{S} \\ -\overline{S} \end{pmatrix} = \frac{K_0}{\varepsilon} \cdot$$

$$\begin{pmatrix} \mu_l^{-1}\cdot\nabla\cdot\left(\begin{bmatrix}\left[\mathbf{K}_0^l\left(\overline{S},\overline{P_l},\overline{P_g}\right) + \lambda\cdot\mathbf{K}_1^l\left(\overline{S},\overline{P_l},\overline{P_g}\right) + \lambda^2\cdot\mathbf{K}_2^l\left(\overline{S},\overline{P_l},\overline{P_g}\right)\ldots\right]\cdot \\ \overline{S}^{-1}\left(\nabla\cdot\overline{S}\left[\overline{P}_0^l\left(\overline{S},\overline{P_l},\overline{P_g}\right) + \lambda\cdot P_1^l\left(\overline{S},\overline{P_l},\overline{P_g}\right) + \lambda^2\cdot P_2^l\left(\overline{S},\overline{P_l},\overline{P_g}\right)\ldots\right]\right)\end{bmatrix}\right) \\ \mu_g^{-1}\cdot\nabla\cdot\left(\begin{bmatrix}\left[\mathbf{K}_0^g\left(\overline{S},\overline{P_l},\overline{P_g}\right) + \lambda\cdot\mathbf{K}_1^g\left(\overline{S},\overline{P_l},\overline{P_g}\right) + \lambda^2\cdot\mathbf{K}_2^g\left(\overline{S},\overline{P_l},\overline{P_g}\right)\ldots\right]\cdot \\ \left(1-\overline{S}\right)^{-1}\left(\nabla\cdot\left(1-\overline{S}\right)\left[\overline{P}_0^g\left(\overline{S},\overline{P_l},\overline{P_g}\right) + \lambda\cdot P_1^g\left(\overline{S},\overline{P_l},\overline{P_g}\right) + \lambda^2\cdot P_2^g\left(\overline{S},\overline{P_l},\overline{P_g}\right)\ldots\right]\right)\end{bmatrix}\right) \end{pmatrix}$$

$$\overline{P}_g - \overline{P}_l = J_0^{dr}\left(\overline{S},\overline{P_l},\overline{P_g}\right) + \lambda\cdot J_1^{dr}\left(\overline{S},\overline{P_l},\overline{P_g}\right) + \lambda^2\cdot J_2^{dr}\left(\overline{S},\overline{P_l},\overline{P_g}\right) + T\cdot\frac{\partial}{\partial t}\overline{S} \text{ for drainage } \left(\frac{\partial}{\partial t}\overline{S} < 0\right)$$

and

$$\overline{P}_g - \overline{P}_l = J_0^{imb}\left(\overline{S},\overline{P_l},\overline{P_g}\right) + \lambda\cdot J_1^{imb}\left(\overline{S},\overline{P_l},\overline{P_g}\right) + \lambda^2\cdot J_2^{imb}\left(\overline{S},\overline{P_l},\overline{P_g}\right) + T\cdot\frac{\partial}{\partial t}\overline{S} \text{ for imbibition } \left(\frac{\partial}{\partial t}\overline{S} > 0\right)$$

The resulted equation for non-periodic variables $\left\{\overline{S}(\mathbf{x},t),\overline{P_l}(\mathbf{x},t),\overline{P_g}(\mathbf{x},t)\right\}$ has the same type and shape as the equation when vibration is absent $(\lambda=0)$. It is therefore, possible to interpret $\mathbf{K}_i^{l,g}\left(\overline{S},\overline{P_l},\overline{P_g}\right)$ as an effective increase in permeability and $P_i^{l,g}\left(\overline{S},\overline{P_l},\overline{P_g}\right)$ as an effective increase in hydrostatic pressure due to applied vibration.

Functions $\mathbf{K}_i^{l,g}$ and $P_i^{l,g}$ can be determined by substituting $\left\{S(\mathbf{x},t),P_l(\mathbf{x},t),P_g(\mathbf{x},t)\right\}$ with their asymptotic expressions through $\left\{\overline{S}(\mathbf{x},t),\overline{P_l}(\mathbf{x},t),\overline{P_g}(\mathbf{x},t)\right\}$ and $\left\{s_i(\mathbf{x},t),p_i^l(\mathbf{x},t),p_i^g(\mathbf{x},t)\right\}$ and applying conditions that the time and space averages of $\left\{s_i(\mathbf{x},t),p_i^l(\mathbf{x},t),p_i^g(\mathbf{x},t)\right\}$ are equal zero:

$$\frac{\partial}{\partial t}\begin{pmatrix} \overline{S}+\lambda\cdot s_1\left(\overline{S},\overline{P_l},\overline{P_g},\mathbf{x},t\right)+\lambda^2\cdot s_2\left(\overline{S},\overline{P_l},\overline{P_g},\mathbf{x},t\right)+\ldots \\ -\overline{S}-\lambda\cdot s_1\left(\overline{S},\overline{P_l},\overline{P_g},\mathbf{x},t\right)-\lambda^2\cdot s_2\left(\overline{S},\overline{P_l},\overline{P_g},\mathbf{x},t\right)-\ldots \end{pmatrix}=\frac{K_0}{\varepsilon}\cdot$$

$$\begin{pmatrix} \mu_l^{-1}\cdot\nabla\cdot\begin{pmatrix} \left[\mathbf{K}_0^l\left(\overline{S},\overline{P_l},\overline{P_g}\right)+\lambda\cdot\mathbf{K}_1^l\left(\overline{S},\overline{P_l},\overline{P_g}\right)+\lambda^2\cdot\mathbf{K}_2^l\left(\overline{S},\overline{P_l},\overline{P_g}\right)\ldots\right]\cdot \\ \overline{S}^{-1}\left(\nabla\cdot\overline{S}\left[\overline{P}_0^l\left(\overline{S},\overline{P_l},\overline{P_g}\right)+\lambda\cdot P_1^l\left(\overline{S},\overline{P_l},\overline{P_g}\right)+\lambda^2\cdot P_2^l\left(\overline{S},\overline{P_l},\overline{P_g}\right)\ldots\right]\right) \end{pmatrix} \\ \mu_g^{-1}\cdot\nabla\cdot\begin{pmatrix} \left[\mathbf{K}_0^g\left(\overline{S},\overline{P_l},\overline{P_g}\right)+\lambda\cdot\mathbf{K}_1^g\left(\overline{S},\overline{P_l},\overline{P_g}\right)+\lambda^2\cdot\mathbf{K}_2^g\left(\overline{S},\overline{P_l},\overline{P_g}\right)\ldots\right]\cdot \\ \left(1-\overline{S}\right)^{-1}\left(\nabla\cdot\left(1-\overline{S}\right)\left[\overline{P}_0^g\left(\overline{S},\overline{P_l},\overline{P_g}\right)+\lambda\cdot P_1^g\left(\overline{S},\overline{P_l},\overline{P_g}\right)+\lambda^2\cdot P_2^g\left(\overline{S},\overline{P_l},\overline{P_g}\right)\ldots\right]\right) \end{pmatrix} \end{pmatrix}+$$

$$\frac{\partial}{\partial t}\begin{pmatrix} \lambda\cdot s_1\left(\overline{S},\overline{P_l},\overline{P_g},\mathbf{x},t\right)+\lambda^2\cdot s_2\left(\overline{S},\overline{P_l},\overline{P_g},\mathbf{x},t\right)+\ldots \\ -\lambda\cdot s_1\left(\overline{S},\overline{P_l},\overline{P_g},\mathbf{x},t\right)-\lambda^2\cdot s_2\left(\overline{S},\overline{P_l},\overline{P_g},\mathbf{x},t\right)-\ldots \end{pmatrix}=\frac{K_0}{\varepsilon}\cdot$$

$$\begin{pmatrix} \mu_l^{-1}\cdot\nabla\cdot\begin{pmatrix} \left[\mathbf{K}_l\left(\overline{S}+\lambda\cdot s_1+\lambda^2\cdot s_2\ldots\right)\right]\cdot \\ \left(\overline{S}+\lambda\cdot s_1+\lambda^2\cdot s_2\ldots\right)^{-1}\begin{pmatrix} \nabla\cdot\left(\overline{S}+\lambda\cdot s_1+\lambda^2\cdot s_2\ldots\right)\left[\overline{P}_l+\lambda\cdot p_1^l+\lambda^2\cdot p_2^l\ldots-\lambda\cdot\left(F_l^P+\lambda\cdot{}^1F_l^P\right)\right] \\ -\lambda\cdot\frac{\partial}{\partial t}\left(\overline{S}+\lambda\cdot s_1\ldots\right)\left(\mathbf{F}_\mathbf{l}^\mathbf{K}+\lambda\cdot{}^1\mathbf{F}_\mathbf{l}^\mathbf{K}\right) \end{pmatrix} \end{pmatrix} \\ \mu_g^{-1}\cdot\nabla\cdot\begin{pmatrix} \left[\mathbf{K}_g\left(1-\overline{S}-\lambda\cdot s_1-\lambda^2\cdot s_2\ldots\right)\right]\cdot \\ \left(1-\overline{S}-\lambda\cdot s_1-\lambda^2\cdot s_2\ldots\right)^{-1}\begin{pmatrix} \nabla\cdot\left(1-\overline{S}-\lambda\cdot s_1-\lambda^2\cdot s_2\ldots\right)\begin{bmatrix} \overline{P}_g+\lambda\cdot p_1^g+\lambda^2\cdot p_2^g\ldots \\ -\lambda\cdot\left(F_g^P+\lambda\cdot{}^1F_g^P\right) \end{bmatrix} \\ -\lambda\cdot\frac{\partial}{\partial t}\left(1-\overline{S}-\lambda\cdot s_1\ldots\right)\left(\mathbf{F}_\mathbf{g}^\mathbf{K}+\lambda\cdot{}^1\mathbf{F}_\mathbf{g}^\mathbf{K}\right) \end{pmatrix} \end{pmatrix} \end{pmatrix}$$

where

$$\begin{pmatrix} F_l^P \\ F_g^P \end{pmatrix}=\begin{pmatrix} q\cdot\nabla\cdot\mathbf{u}_s+r\cdot\nabla\cdot\mathbf{u}_l+\varepsilon\cdot b\cdot\overline{S}\cdot\nabla\cdot\mathbf{u}_g \\ t\cdot\nabla\cdot\mathbf{u}_s+\varepsilon\cdot b\cdot\left(1-\overline{S}\right)\cdot\nabla\cdot\mathbf{u}_l+s\cdot\nabla\cdot\mathbf{u}_g \end{pmatrix};\quad \begin{pmatrix} \mathbf{F}_\mathbf{l}^\mathbf{K} \\ \mathbf{F}_\mathbf{g}^\mathbf{K} \end{pmatrix}=\begin{pmatrix} \rho_l\cdot\frac{\partial\mathbf{u}_l}{\partial t}+\left(\rho_l\cdot\beta_l+\rho_g\cdot\left(\overline{S}^{-1}-1\right)\cdot\beta_{gl}\right)\frac{\partial\left(\mathbf{u}_l-\mathbf{u}_s\right)}{\partial t} \\ \rho_g\cdot\frac{\partial\mathbf{u}_g}{\partial t}+\left(\rho_g\cdot\beta_g+\rho_l\cdot\left(\left(1-\overline{S}\right)^{-1}-1\right)\cdot\beta_{gl}\right)\frac{\partial\left(\mathbf{u}_g-\mathbf{u}_s\right)}{\partial t} \end{pmatrix}$$

and

$$\begin{pmatrix} {}^1F_l^P \\ {}^1F_g^P \end{pmatrix} = \begin{pmatrix} +\varepsilon\cdot b\cdot s_1\cdot\nabla\cdot\mathbf{u}_g \\ -\varepsilon\cdot b\cdot s_1\cdot\nabla\cdot\mathbf{u}_l \end{pmatrix} + \begin{pmatrix} q\cdot\nabla\cdot{}^1\mathbf{u}_s + r\cdot\nabla\cdot{}^1\mathbf{u}_l + \varepsilon\cdot b\cdot\overline{S}\cdot\nabla\cdot{}^1\mathbf{u}_g \\ t\cdot\nabla\cdot{}^1\mathbf{u}_s + \varepsilon\cdot b\cdot\left(1-\overline{S}\right)\cdot\nabla\cdot{}^1\mathbf{u}_l + s\cdot\nabla\cdot{}^1\mathbf{u}_g \end{pmatrix}$$

$$\begin{pmatrix} {}^1\mathbf{F}_\mathbf{l}^\mathbf{K} \\ {}^1\mathbf{F}_\mathbf{g}^\mathbf{K} \end{pmatrix} = \begin{pmatrix} -\rho_g\beta_{gl}\dfrac{s_1}{S^2}\dfrac{\partial}{\partial t}\left(\mathbf{u}_l-\mathbf{u}_s\right) \\ +\rho_l\beta_{gl}\dfrac{s_1}{\left(1-S\right)^2}\dfrac{\partial}{\partial t}\left(\mathbf{u}_g-\mathbf{u}_s\right) \end{pmatrix} + \begin{pmatrix} \rho_l\cdot\dfrac{\partial}{\partial t}{}^1\mathbf{u}_l + \left(\rho_l\cdot\beta_l+\rho_g\cdot\left(S^{-1}-1\right)\cdot\beta_{gl}\right)\dfrac{\partial}{\partial t}\left({}^1\mathbf{u}_l-{}^1\mathbf{u}_s\right) \\ \rho_g\cdot\dfrac{\partial}{\partial t}{}^1\mathbf{u}_g + \left(\rho_g\cdot\beta_g+\rho_l\cdot\left(\left(1-S\right)^{-1}-1\right)\cdot\beta_{gl}\right)\dfrac{\partial}{\partial t}\left({}^1\mathbf{u}_g-{}^1\mathbf{u}_s\right) \end{pmatrix}$$

(Here $\left\{{}^1\mathbf{u}_s, {}^1\mathbf{u}_l, {}^1\mathbf{u}_\mathbf{g}\right\}$ are the second order terms in λ to be calculated from the vibration part of the full equation set with $\left\{\varepsilon_s,\varepsilon_l\right\}$ substituted with $\left\{\varepsilon_l+\varepsilon\cdot s_1, \varepsilon_g-\varepsilon\cdot s_1\right\}$ - not needed in equations for slow variable in the second order in λ).

$$\overline{P}_g-\overline{P}_l+\lambda\cdot\left(p_1^g-p_1^l\right)+\lambda^2\cdot\left(p_2^g-p_2^l\right)=$$

$$J^{dr}\left(\overline{S}\right)+\lambda\cdot\frac{\partial J^{dr}\left(\overline{S}\right)}{\partial\overline{S}}s_1+\lambda^2\cdot\left[\frac{\partial^2 J^{dr}\left(\overline{S}\right)}{\partial\overline{S}^2}\frac{\left(s_1\right)^2}{2}+\frac{\partial J^{dr}\left(\overline{S}\right)}{\partial\overline{S}}s_2\right]+T\cdot\frac{\partial}{\partial t}\left(\overline{S}+\lambda\cdot s_1+\lambda^2\cdot s_2\right)=$$

$$J_0^{dr}\left(\overline{S}\right)+\lambda\cdot J_1^{dr}\left(\overline{S},\overline{P}_l,\overline{P}_g\right)+\lambda\cdot J_2^{dr}\left(\overline{S},\overline{P}_l,\overline{P}_g\right)+T\cdot\frac{\partial}{\partial t}\left(\overline{S}+\lambda\cdot s_1+\lambda^2\cdot s_2\right)\ \text{for drainage}\left(\frac{\partial}{\partial t}\overline{S}<0\right)$$

and

$$\overline{P}_g-\overline{P}_l+\lambda\cdot\left(p_1^g-p_1^l\right)+\lambda^2\cdot\left(p_2^g-p_2^l\right)=$$

$$J^{imb}\left(\overline{S}\right)+\lambda\cdot\frac{\partial J^{imb}\left(\overline{S}\right)}{\partial\overline{S}}s_1+\lambda^2\cdot\left[\frac{\partial^2 J^{imb}\left(\overline{S}\right)}{\partial\overline{S}^2}\frac{\left(s_1\right)^2}{2}+\frac{\partial J^{imb}\left(\overline{S}\right)}{\partial\overline{S}}s_2\right]+T\cdot\frac{\partial}{\partial t}\left(\overline{S}+\lambda\cdot s_1+\lambda^2\cdot s_2\right)=$$

$$J_0^{imb}\left(\overline{S}\right)+\lambda\cdot J_1^{imb}\left(\overline{S},\overline{P}_l,\overline{P}_g\right)+\lambda\cdot J_2^{imb}\left(\overline{S},\overline{P}_l,\overline{P}_g\right)+T\cdot\frac{\partial}{\partial t}\left(\overline{S}+\lambda\cdot s_1+\lambda^2\cdot s_2\right)\ \text{for imbibition}\left(\frac{\partial}{\partial t}\overline{S}>0\right)$$

Now, collecting terms with the same power of λ^n, one gets

for λ^0

$$\nabla\cdot\left(\mathbf{K}_0^l\left(\overline{S},\overline{P}_l,\overline{P}_g\right)\cdot\overline{S}^{-1}\left(\nabla\cdot\overline{S}\cdot\overline{P}_0^l\left(\overline{S},\overline{P}_l,\overline{P}_g\right)\right)\right)=\nabla\cdot\left(\mathbf{K}_l\left(\overline{S}\right)\cdot\overline{S}^{-1}\left(\nabla\cdot\overline{S}\cdot\overline{P}_l\right)\right)$$

$$\nabla\cdot\left(\mathbf{K}_0^g\left(\overline{S},\overline{P}_l,\overline{P}_g\right)\cdot\left(1-\overline{S}\right)^{-1}\left(\nabla\cdot\left(1-\overline{S}\right)\cdot\overline{P}_0^g\left(\overline{S},\overline{P}_l,\overline{P}_g\right)\right)\right)=\nabla\cdot\left(\mathbf{K}_g\left(1-\overline{S}\right)\cdot\left(1-\overline{S}\right)^{-1}\left(\nabla\cdot\left(1-\overline{S}\right)\cdot\overline{P}_g\right)\right)$$

$$\overline{P}_g-\overline{P}_l=J_0^{dr}\left(\overline{S},\overline{P}_l,\overline{P}_g\right)+T\cdot\frac{\partial}{\partial t}\overline{S}\ \text{ for drainage }\left(\frac{\partial}{\partial t}\overline{S}<0\right)$$

$$\overline{P}_g-\overline{P}_l=J_0^{imb}\left(\overline{S},\overline{P}_l,\overline{P}_g\right)+T\cdot\frac{\partial}{\partial t}\overline{S}\ \text{ for imbibition }\left(\frac{\partial}{\partial t}\overline{S}>0\right)$$

from which one can conclude:

$$\mathbf{K}_0^l\left(\overline{S},\overline{P}_l,\overline{P}_g\right)=\mathbf{K}_l\left(\overline{S}\right);\quad \mathbf{K}_0^g\left(\overline{S},\overline{P}_l,\overline{P}_g\right)=\mathbf{K}_g\left(1-\overline{S}\right)$$

$$\overline{P}_0^l\left(\overline{S},\overline{P}_l,\overline{P}_g\right)=\overline{P}_l;\quad \overline{P}_0^g\left(\overline{S},\overline{P}_l,\overline{P}_g\right)=\overline{P}_g$$

$$J_0^{imb}\left(\overline{S}\right)=J^{imb}\left(\overline{S}\right);\quad J_0^{dr}\left(\overline{S}\right)=J^{dr}\left(\overline{S}\right)$$

and for λ^1

$$\frac{\partial}{\partial t}\begin{pmatrix}s_1\left(\overline{S},\overline{P}_l,\overline{P}_g,\mathbf{x},t\right)\\-s_1\left(\overline{S},\overline{P}_l,\overline{P}_g,\mathbf{x},t\right)\end{pmatrix}+\frac{K_0}{\varepsilon}\cdot$$

$$\begin{pmatrix}\mu_l^{-1}\cdot\nabla\cdot\left(\mathbf{K}_1^l\left(\overline{S},\overline{P}_l,\overline{P}_g\right)\cdot\overline{S}^{-1}\left(\nabla\cdot\overline{S}\overline{P}_0^l\left(\overline{S},\overline{P}_l,\overline{P}_g\right)\right)+\mathbf{K}_0^l\left(\overline{S},\overline{P}_l,\overline{P}_g\right)\cdot\overline{S}^{-1}\left(\nabla\cdot\overline{S}\cdot P_1^l\left(\overline{S},\overline{P}_l,\overline{P}_g\right)\right)\right)\\ \mu_g^{-1}\cdot\nabla\cdot\left(\mathbf{K}_1^g\left(\overline{S},\overline{P}_l,\overline{P}_g\right)\cdot\left(1-\overline{S}\right)^{-1}\left(\nabla\cdot\left(1-\overline{S}\right)\overline{P}_0^g\left(\overline{S},\overline{P}_l,\overline{P}_g\right)\right)+\mathbf{K}_0^g\left(\overline{S},\overline{P}_l,\overline{P}_g\right)\cdot\left(1-\overline{S}\right)^{-1}\left(\nabla\cdot\left(1-\overline{S}\right)\cdot P_1^g\left(\overline{S},\overline{P}_l,\overline{P}_g\right)\right)\right)\end{pmatrix}=$$

$$\frac{K_0}{\varepsilon}\cdot\begin{pmatrix}\mu_l^{-1}\cdot\nabla\cdot\left(\dfrac{\partial\mathbf{K}_l\left(\overline{S}\right)}{\partial\overline{S}}s_1\cdot\left(\overline{S}\right)^{-1}\left(\nabla\cdot\overline{S}\cdot\overline{P}_l\right)+\mathbf{K}_l\left(\overline{S}\right)\cdot\left(\nabla\cdot\dfrac{s_1}{\overline{S}}\right)\overline{P}_l+\mathbf{K}_l\left(\overline{S}\right)\cdot\left(\overline{S}\right)^{-1}\nabla\cdot\left(\overline{S}\cdot p_1^l\right)\right)\\ \mu_g^{-1}\cdot\nabla\cdot\left(\dfrac{\partial\mathbf{K}_g\left(1-\overline{S}\right)}{\partial\overline{S}}s_1\cdot\left(1-\overline{S}\right)^{-1}\left(\nabla\cdot\left(1-\overline{S}\right)\cdot\overline{P}_g\right)-\mathbf{K}_g\left(1-\overline{S}\right)\cdot\left(\nabla\cdot\dfrac{s_1}{1-\overline{S}}\right)\overline{P}_g+\mathbf{K}_g\left(1-\overline{S}\right)\cdot\left(1-\overline{S}\right)^{-1}\nabla\cdot\left(\left(1-\overline{S}\right)\cdot p_1^g\right)\right)\end{pmatrix}+$$

$$-\frac{K_0}{\varepsilon}\cdot\begin{pmatrix}\mu_l^{-1}\cdot\nabla\cdot\left(\mathbf{K}_l\left(\overline{S}\right)\cdot\left(\overline{S}\right)^{-1}\left(\nabla\cdot\left(\overline{S}\cdot F_l^P\right)+\dfrac{\partial}{\partial t}\left(\overline{S}\cdot\mathbf{F}_\mathbf{l}^\mathbf{K}\right)\right)\right)\\ \mu_g^{-1}\cdot\nabla\cdot\left(\mathbf{K}_g\left(1-\overline{S}\right)\cdot\left(1-\overline{S}\right)^{-1}\left(\nabla\cdot\left(\left(1-\overline{S}\right)\cdot F_g^P\right)+\dfrac{\partial}{\partial t}\left(\left(1-\overline{S}\right)\cdot\mathbf{F}_\mathbf{g}^\mathbf{K}\right)\right)\right)\end{pmatrix}$$

$$p_1^g - p_1^l = \frac{\partial J^{dr}\left(\overline{S}\right)}{\partial \overline{S}} s_1 + T \cdot \frac{\partial}{\partial t} s_1 \quad \text{for drainage} \left(\frac{\partial}{\partial t}\overline{S} < 0\right)$$

and

$$p_1^g - p_1^l = \frac{\partial J^{imb}\left(\overline{S}\right)}{\partial \overline{S}} s_1 + T \cdot \frac{\partial}{\partial t} s_1 \quad \text{for imbibition} \left(\frac{\partial}{\partial t}\overline{S} > 0\right)$$

As it is clear from the expressions for forces $F_{l,g}^{K,P}$ their time and space averages are zero in the first order in λ^1. It follows then that in order $\left\{s_i(\mathbf{x},t), p_i^l(\mathbf{x},t), p_i^g(\mathbf{x},t)\right\}$ have zero time and space averages the following choice must be made:

$$\mathbf{K}_1^l\left(\overline{S},\overline{P_l},\overline{P_g}\right) = 0; \quad \mathbf{K}_1^g\left(\overline{S},\overline{P_l},\overline{P_g}\right) = 0$$
$$\overline{P}_1^l\left(\overline{S},\overline{P_l},\overline{P_g}\right) = 0; \quad \overline{P}_1^g\left(\overline{S},\overline{P_l},\overline{P_g}\right) = 0$$
$$J_1^{imb}\left(\overline{S}\right) = 0; \quad J_1^{dr}\left(\overline{S}\right) = 0$$

The following set of linear equations describes then small vibrations of pressures and saturations in the first order in λ^1:

For λ^1

$$\frac{\partial}{\partial t}\begin{pmatrix} s_1 \\ -s_1 \end{pmatrix} = \frac{K_0}{\varepsilon} \cdot$$

$$\begin{pmatrix} \mu_l^{-1} \cdot \nabla \cdot \left(\frac{\partial \mathbf{K}_l}{\partial \overline{S}} s_1 \cdot \left(\overline{S}\right)^{-1} \nabla\left(\overline{S} \cdot \overline{P}_l\right) + \mathbf{K}_l \cdot \left(\nabla \frac{s_1}{\overline{S}} \right) \overline{P}_l + \mathbf{K}_l \cdot \left(\overline{S}\right)^{-1} \nabla \cdot \left(\overline{S} \cdot p_1^l\right) \right) \\ \mu_g^{-1} \cdot \nabla \cdot \left(\frac{\partial \mathbf{K}_g}{\partial \overline{S}} s_1 \cdot \left(1-\overline{S}\right)^{-1} \nabla\left(\left(1-\overline{S}\right) \cdot \overline{P}_g\right) - \mathbf{K}_g \cdot \left(\nabla \frac{s_1}{1-\overline{S}} \right) \overline{P}_g + \mathbf{K}_g \cdot \left(1-\overline{S}\right)^{-1} \nabla \cdot \left(\left(1-\overline{S}\right) \cdot p_1^g\right) \right) \end{pmatrix} +$$

$$-\frac{K_0}{\varepsilon} \cdot \begin{pmatrix} \mu_l^{-1} \cdot \nabla \cdot \left(\mathbf{K}_l \cdot \left(\overline{S}\right)^{-1} \left(\nabla\left(\overline{S} \cdot \widetilde{F_l^P}\right) + \frac{\partial}{\partial t}\left(\overline{S} \cdot \widetilde{\mathbf{F}_1^K}\right) \right) \right) \\ \mu_g^{-1} \cdot \nabla \cdot \left(\mathbf{K}_g \cdot \left(1-\overline{S}\right)^{-1} \left(\nabla\left(\left(1-\overline{S}\right) \cdot \widetilde{F_g^P}\right) + \frac{\partial}{\partial t}\left(\left(1-\overline{S}\right) \cdot \widetilde{\mathbf{F}_\mathbf{g}^K}\right) \right) \right) \end{pmatrix}$$

$$p_1^g - p_1^l = \frac{\partial J^{dr}\left(\overline{S}\right)}{\partial \overline{S}} s_1 + T \cdot \frac{\partial}{\partial t} s_1 \quad \text{for drainage} \left(\frac{\partial}{\partial t}\overline{S} < 0\right)$$

and

$$p_1^g - p_1^l = \frac{\partial J^{imb}\left(\overline{S}\right)}{\partial \overline{S}} s_1 + T \cdot \frac{\partial}{\partial t} s_1 \quad \text{for imbibition} \left(\frac{\partial}{\partial t}\overline{S} > 0\right)$$

So far no non-zero contribution to the averaged equations for non-periodic motion caused by external vibration has been obtained. To get the first non-zero terms one needs to calculate the second order contribution in λ^2.

For λ^2

$$p_2^g - p_2^l = \frac{\partial^2 J^{dr}\left(\overline{S}\right)}{\partial \overline{S}^2} \frac{\left(s_1\right)^2}{2} + \frac{\partial J^{dr}\left(\overline{S}\right)}{\partial \overline{S}} s_2 + T \cdot \frac{\partial}{\partial t} s_2 \quad \text{for drainage} \left(\frac{\partial}{\partial t}\overline{S} < 0\right)$$

and

$$p_2^g - p_2^l = \frac{\partial^2 J^{imb}\left(\overline{S}\right)}{\partial \overline{S}^2} \frac{\left(s_1\right)^2}{2} + \frac{\partial J^{imb}\left(\overline{S}\right)}{\partial \overline{S}} s_2 + T \cdot \frac{\partial}{\partial t} s_2 \quad \text{for imbibition} \left(\frac{\partial}{\partial t}\overline{S} > 0\right)$$

$$\frac{\partial}{\partial t}\begin{pmatrix} s_2\left(\overline{S},\overline{P_l},\overline{P_g},\mathbf{x},t\right) \\ -s_2\left(\overline{S},\overline{P_l},\overline{P_g},\mathbf{x},t\right) \end{pmatrix} + \frac{K_0}{\varepsilon} \cdot \begin{pmatrix} \mu_l^{-1} \cdot \nabla \cdot \begin{pmatrix} \mathbf{K}_0^l\left(\overline{S},\overline{P_l},\overline{P_g}\right) \cdot \left(\overline{S}\right)^{-1} \left(\nabla \cdot \left(\overline{S}\right) P_2^l\left(\overline{S},\overline{P_l},\overline{P_g}\right)\right) + \\ \mathbf{K}_2^l\left(\overline{S},\overline{P_l},\overline{P_g}\right) \cdot \left(\overline{S}\right)^{-1} \left(\nabla \cdot \left(\overline{S}\right) \overline{P}_0^l\left(\overline{S},\overline{P_l},\overline{P_g}\right)\right) \end{pmatrix} \\ \mu_g^{-1} \cdot \nabla \cdot \begin{pmatrix} \mathbf{K}_0^g\left(\overline{S},\overline{P_l},\overline{P_g}\right) \cdot \left(1-\overline{S}\right)^{-1} \left(\nabla \cdot \left(1-\overline{S}\right) P_2^g\left(\overline{S},\overline{P_l},\overline{P_g}\right)\right) + \\ \mathbf{K}_2^g\left(\overline{S},\overline{P_l},\overline{P_g}\right) \cdot \left(1-\overline{S}\right)^{-1} \left(\nabla \cdot \left(1-\overline{S}\right) \overline{P}_0^g\left(\overline{S},\overline{P_l},\overline{P_g}\right)\right) \end{pmatrix} \end{pmatrix}$$

=

$$\frac{K_0}{\varepsilon} \cdot \begin{pmatrix} \mu_l^{-1} \cdot \nabla \cdot \left[\left(\frac{\partial \mathbf{K}_l\left(\overline{S}\right)}{\partial \overline{S}} s_2 \right) \left(\overline{S}\right)^{-1} \nabla\left(\overline{S} \cdot \overline{P_l}\right) + \mathbf{K}_l\left(\overline{S}\right) \nabla\left(\frac{s_2}{\overline{S}}\right) \overline{P_l} + \mathbf{K}_l\left(\overline{S}\right) \left(\overline{S}\right)^{-1} \nabla\left(\overline{S} \cdot p_2^l\right) \right] \\ \mu_g^{-1} \cdot \nabla \cdot \left[\left(\frac{\partial \mathbf{K}_g\left(1-\overline{S}\right)}{\partial \overline{S}} s_2 \right) \left(1-\overline{S}\right)^{-1} \nabla\left(\left(1-\overline{S}\right) \cdot \overline{P_g}\right) - \mathbf{K}_g\left(1-\overline{S}\right) \nabla\left(\frac{s_2}{1-\overline{S}}\right) \overline{P_g} + \right. \\ \left. \mathbf{K}_g\left(1-\overline{S}\right) \left(1-\overline{S}\right)^{-1} \nabla\left(\left(1-\overline{S}\right) \cdot p_2^g\right) \right] \end{pmatrix} +$$

$$\frac{K_0}{\varepsilon}\cdot\left(\begin{array}{c}\mu_l^{-1}\cdot\nabla\cdot\left[\begin{array}{l}\left(\frac{1}{2}\frac{\partial^2\mathbf{K}_l\left(\overline{S}\right)}{\partial\overline{S}^2}+\frac{\mathbf{K}_l\left(\overline{S}\right)}{\overline{S}}\right)\frac{\left(s_1\right)^2}{\overline{S}^2}\nabla\left(\overline{S}\cdot\overline{P}_l\right)+\left(\frac{\partial\mathbf{K}_l\left(\overline{S}\right)}{\partial\overline{S}}-\frac{\mathbf{K}_l\left(\overline{S}\right)}{\overline{S}}\right)\left(s_1\cdot p_1^l\right)\frac{\nabla\overline{S}}{\overline{S}}+\\ \frac{\partial\mathbf{K}_l\left(\overline{S}\right)}{\partial\overline{S}}s_1\nabla p_1^l+\frac{\mathbf{K}_l\left(\overline{S}\right)}{\overline{S}}p_1^l\nabla s_1+\left(\frac{\partial\mathbf{K}_l\left(\overline{S}\right)}{\partial\overline{S}}-\frac{\mathbf{K}_l\left(\overline{S}\right)}{\overline{S}}\right)\frac{s_1}{\overline{S}}\nabla\left(\frac{s_1}{\overline{S}}\right)\cdot\overline{P}_l\end{array}\right]\\ \mu_g^{-1}\cdot\nabla\cdot\left[\begin{array}{l}\left(\frac{1}{2}\frac{\partial^2\mathbf{K}_g\left(1-\overline{S}\right)}{\partial\overline{S}^2}+\frac{\mathbf{K}_g\left(1-\overline{S}\right)}{1-\overline{S}}\right)\frac{\left(s_1\right)^2}{\left(1-\overline{S}\right)^2}\nabla\left(\overline{S}\cdot\overline{P}_g\right)+\left(\frac{\partial\mathbf{K}_g\left(1-\overline{S}\right)}{\partial\overline{S}}+\frac{\mathbf{K}_g\left(1-\overline{S}\right)}{1-\overline{S}}\right)\left(s_1\cdot p_1^g\right)\frac{\nabla\overline{S}}{\overline{S}}+\\ \frac{\partial\mathbf{K}_g\left(1-\overline{S}\right)}{\partial\overline{S}}s_1\nabla p_1^g-\frac{\mathbf{K}_g\left(1-\overline{S}\right)}{1-\overline{S}}p_1^g\nabla s_1-\left(\frac{\partial\mathbf{K}_g\left(1-\overline{S}\right)}{\partial\overline{S}}-\frac{\mathbf{K}_g\left(1-\overline{S}\right)}{1-\overline{S}}\right)\frac{s_1}{1-\overline{S}}\nabla\left(\frac{s_1}{1-\overline{S}}\right)\cdot\overline{P}_g\end{array}\right]\end{array}\right)+$$

$$\left(\begin{array}{c}\mu_l^{-1}\cdot\nabla\cdot\left[-\mathbf{K}_l\left(\overline{S}\right)\left[\nabla\left(\frac{s_1}{\overline{S}}\right)F_l^P+\frac{\partial}{\partial t}\left(\frac{s_1}{\overline{S}}\right)\mathbf{F}_\mathbf{l}^\mathbf{K}+\left(\overline{S}\right)^{-1}\nabla\left(\overline{S}\cdot{}^1F_l^P\right)+\left(\overline{S}\right)^{-1}\frac{\partial}{\partial t}\left(\overline{S}\cdot{}^1\mathbf{F}_\mathbf{l}^\mathbf{K}\right)\right]-\frac{\partial\mathbf{K}_l\left(\overline{S}\right)}{\partial\overline{S}}s_1\left(\overline{S}\right)^{-1}\left[\nabla\left(\overline{S}\cdot F_l^P\right)+\frac{\partial}{\partial t}\left(\overline{S}\cdot\mathbf{F}_\mathbf{l}^\mathbf{K}\right)\right]\right]\\ \mu_g^{-1}\cdot\nabla\cdot\left[\begin{array}{l}-\mathbf{K}_g\left(1-\overline{S}\right)\left[-\nabla\left(\frac{s_1}{1-\overline{S}}\right)F_g^P-\frac{\partial}{\partial t}\left(\frac{s_1}{1-\overline{S}}\right)\mathbf{F}_\mathbf{g}^\mathbf{K}+\left(1-\overline{S}\right)^{-1}\nabla\left(\left(1-\overline{S}\right)\cdot{}^1F_g^P\right)+\left(1-\overline{S}\right)^{-1}\frac{\partial}{\partial t}\left(\left(1-\overline{S}\right)\cdot{}^1\mathbf{F}_\mathbf{g}^\mathbf{K}\right)\right]\\ -\frac{\partial\mathbf{K}_g\left(1-\overline{S}\right)}{\partial\overline{S}}s_1\left(1-\overline{S}\right)^{-1}\left[\nabla\left(\left(1-\overline{S}\right)\cdot F_g^P\right)+\frac{\partial}{\partial t}\left(\left(1-\overline{S}\right)\cdot\mathbf{F}_\mathbf{g}^\mathbf{K}\right)\right]\end{array}\right]\end{array}\right)$$

The same way as for λ^1, $\left\{s_2\left(\overline{S},\overline{P_l},\overline{P_g},\mathbf{x},t\right),p_2^l\left(\overline{S},\overline{P_l},\overline{P_g},\mathbf{x},t\right),p_2^2\left(\overline{S},\overline{P_l},\overline{P_g},\mathbf{x},t\right)\right\}$ should not possess slow non-periodic component. To satisfy that, one requests:

$$\left(\begin{array}{c}\mathbf{K}_0^l\left(\overline{S},\overline{P_l},\overline{P_g}\right)\cdot\left(\overline{S}\right)^{-1}\left(\nabla\cdot\left(\overline{S}\right)P_2^l\left(\overline{S},\overline{P_l},\overline{P_g}\right)\right)+\mathbf{K}_2^l\left(\overline{S},\overline{P_l},\overline{P_g}\right)\cdot\left(\overline{S}\right)^{-1}\left(\nabla\cdot\left(\overline{S}\right)\overline{P}_0^l\left(\overline{S},\overline{P_l},\overline{P_g}\right)\right)\\ \mathbf{K}_0^g\left(\overline{S},\overline{P_l},\overline{P_g}\right)\cdot\left(1-\overline{S}\right)^{-1}\left(\nabla\cdot\left(1-\overline{S}\right)P_2^g\left(\overline{S},\overline{P_l},\overline{P_g}\right)\right)+\mathbf{K}_2^g\left(\overline{S},\overline{P_l},\overline{P_g}\right)\cdot\left(1-\overline{S}\right)^{-1}\left(\nabla\cdot\left(1-\overline{S}\right)\overline{P}_0^g\left(\overline{S},\overline{P_l},\overline{P_g}\right)\right)\end{array}\right)=$$

=

$$
\left(
\begin{array}{l}
\left(\frac{1}{2}\frac{\partial^2 \mathbf{K}_l(\bar{S})}{\partial \bar{S}^2}S+\frac{\mathbf{K}_l(\bar{S})}{\bar{S}}\right)\frac{\overline{(s_1)^2}}{\bar{S}^2}\nabla\left(\bar{S}\cdot\bar{P}_l\right)+\left(\frac{\partial \mathbf{K}_l(\bar{S})}{\partial \bar{S}}-\frac{\mathbf{K}_l(\bar{S})}{\bar{S}}\right)\left(\overline{s_1\cdot p_1^l}\right)\frac{\nabla\bar{S}}{\bar{S}}+ \\
\frac{\partial \mathbf{K}_l(\bar{S})}{\partial \bar{S}}\overline{s_1\nabla p_1^l}+\frac{\mathbf{K}_l(\bar{S})}{\bar{S}}\overline{p_1^l\nabla s_1}+\left(\frac{\partial \mathbf{K}_l(\bar{S})}{\partial \bar{S}}-\frac{\mathbf{K}_l(\bar{S})}{\bar{S}}\right)\overline{\frac{s_1}{\bar{S}}\nabla\left(\frac{s_1}{\bar{S}}\right)\cdot\bar{P}_l}
\end{array}
\right)
$$

$$
\left[
\begin{array}{l}
\left(\frac{1}{2}\frac{\partial^2 \mathbf{K}_g(1-\bar{S})}{\partial \bar{S}^2}(1-\bar{S})+\frac{\mathbf{K}_g(1-\bar{S})}{1-\bar{S}}\right)\frac{\overline{(s_1)^2}}{(1-\bar{S})^2}\nabla\left(\bar{S}\cdot\bar{P}_g\right)+\left(\frac{\partial \mathbf{K}_g(1-\bar{S})}{\partial \bar{S}}+\frac{\mathbf{K}_g(1-\bar{S})}{1-\bar{S}}\right)\left(\overline{s_1\cdot p_1^g}\right)\frac{\nabla\bar{S}}{\bar{S}}+ \\
\frac{\partial \mathbf{K}_g(1-\bar{S})}{\partial \bar{S}}\overline{s_1\nabla p_1^g}-\frac{\mathbf{K}_g(1-\bar{S})}{1-\bar{S}}\overline{p_1^g\nabla s_1}-\left(\frac{\partial \mathbf{K}_g(1-\bar{S})}{\partial \bar{S}}-\frac{\mathbf{K}_g(1-\bar{S})}{1-\bar{S}}\right)\overline{\frac{s_1}{1-\bar{S}}\nabla\left(\frac{s_1}{1-\bar{S}}\right)\cdot\bar{P}_g}
\end{array}
\right]
$$

+

$$
\left(
\begin{array}{l}
\left[-\mathbf{K}_l(\bar{S})\left[\nabla\overline{\left(\frac{s_1}{\bar{S}}\right)F_l^P}+\frac{\partial}{\partial t}\overline{\left(\frac{s_1}{\bar{S}}\right)\mathbf{F}_1^{\mathbf{K}}}+(\bar{S})^{-1}\nabla\left(\bar{S}\cdot\overline{{}^1F_l^P}\right)+(\bar{S})^{-1}\frac{\partial}{\partial t}\left(\bar{S}\cdot\overline{{}^1\mathbf{F}_1^{\mathbf{K}}}\right)\right]\right] \\
-\frac{\partial \mathbf{K}_l(\bar{S})}{\partial \bar{S}}\overline{s_1(\bar{S})^{-1}\left[\nabla\left(\bar{S}\cdot F_l^P\right)+\frac{\partial}{\partial t}\left(\bar{S}\cdot\mathbf{F}_1^{\mathbf{K}}\right)\right]}
\end{array}
\right]
$$

$$
\left[
\begin{array}{l}
\left[-\mathbf{K}_g(1-\bar{S})\left[-\nabla\overline{\left(\frac{s_1}{1-\bar{S}}\right)F_g^P}-\frac{\partial}{\partial t}\overline{\left(\frac{s_1}{1-\bar{S}}\right)\mathbf{F}_{\mathbf{g}}^{\mathbf{K}}}+(1-\bar{S})^{-1}\nabla\left((1-\bar{S})\cdot\overline{{}^1F_g^P}\right)+(1-\bar{S})^{-1}\frac{\partial}{\partial t}\left((1-\bar{S})\cdot\overline{{}^1\mathbf{F}_{\mathbf{g}}^{\mathbf{K}}}\right)\right]\right] \\
-\frac{\partial \mathbf{K}_g(1-\bar{S})}{\partial \bar{S}}\overline{s_1(1-\bar{S})^{-1}\left[\nabla\left((1-\bar{S})\cdot F_g^P\right)+\frac{\partial}{\partial t}\left((1-\bar{S})\cdot\mathbf{F}_{\mathbf{g}}^{\mathbf{K}}\right)\right]}
\end{array}
\right]
$$

$$J_2^{dr}(\bar{S})=\frac{\partial J^{dr}(\bar{S})}{\partial \bar{S}}\frac{(s_1)^2}{2}\quad\text{for drainage}\left(\frac{\partial}{\partial t}\bar{S}<0\right)$$

and

$$J_2^{imb}(\bar{S})=\frac{\partial J^{imb}(\bar{S})}{\partial \bar{S}}\frac{(s_1)^2}{2}\quad\text{for imbibition}\left(\frac{\partial}{\partial t}\bar{S}>0\right)$$

Equations for $\left\{s_2\left(\bar{S},\bar{P}_l,\bar{P}_g,\mathbf{x},t\right),p_2^l\left(\bar{S},\bar{P}_l,\bar{P}_g,\mathbf{x},t\right),p_2^2\left(\bar{S},\bar{P}_l,\bar{P}_g,\mathbf{x},t\right)\right\}$ are fully similar to the case for λ^1 and look as follows:

$$\frac{\partial}{\partial t}\begin{pmatrix} s_2 \\ -s_2 \end{pmatrix} = \frac{K_0}{\varepsilon}\cdot$$

$$\left(\begin{array}{l} \mu_l^{-1}\cdot\nabla\cdot\left[\left(\dfrac{\partial \mathbf{K}_l(\overline{S})}{\partial \overline{S}}s_2\right)(\overline{S})^{-1}\nabla(\overline{S}\cdot\overline{P}_l)+\mathbf{K}_l(\overline{S})\nabla\left(\dfrac{s_2}{\overline{S}}\right)\overline{P}_l+\mathbf{K}_l(\overline{S})(\overline{S})^{-1}\nabla(\overline{S}\cdot p_2^l)\right] \\ \\ \mu_g^{-1}\cdot\nabla\cdot\left[\begin{array}{l}\left(\dfrac{\partial \mathbf{K}_g(1-\overline{S})}{\partial \overline{S}}s_2\right)(1-\overline{S})^{-1}\nabla((1-\overline{S})\cdot\overline{P}_g)-\mathbf{K}_g(1-\overline{S})\nabla\left(\dfrac{s_2}{1-\overline{S}}\right)\overline{P}_g+ \\ \mathbf{K}_g(1-\overline{S})(1-\overline{S})^{-1}\nabla((1-\overline{S})\cdot p_2^g)\end{array}\right] \end{array}\right)+$$

$$\frac{K_0}{\varepsilon}\cdot\left(\begin{array}{l} \mu_l^{-1}\cdot\nabla\cdot\left[\begin{array}{l}\left(\dfrac{1}{2}\dfrac{\partial^2\mathbf{K}_l(\overline{S})}{\partial\overline{S}^2}\overline{S}+\dfrac{\mathbf{K}_l(\overline{S})}{\overline{S}}\right)\dfrac{\widetilde{(s_1)^2}}{\overline{S}^2}\nabla(\overline{S}\cdot\overline{P}_l)+\left(\dfrac{\partial\mathbf{K}_l(\overline{S})}{\partial\overline{S}}-\dfrac{\mathbf{K}_l(\overline{S})}{\overline{S}}\right)\widetilde{(s_1\cdot p_1^l)}\dfrac{\nabla\overline{S}}{\overline{S}}+ \\ \dfrac{\partial\mathbf{K}_l(\overline{S})}{\partial\overline{S}}\widetilde{s_1\nabla p_1^l}+\dfrac{\mathbf{K}_l(\overline{S})}{\overline{S}}\widetilde{p_1^l\nabla s_1}+\left(\dfrac{\partial\mathbf{K}_l(\overline{S})}{\partial\overline{S}}-\dfrac{\mathbf{K}_l(\overline{S})}{\overline{S}}\right)\widetilde{\dfrac{s_1}{\overline{S}}\nabla\left(\dfrac{s_1}{\overline{S}}\right)}\cdot\overline{P}_l \\ -\mathbf{K}_l(\overline{S})\left[\widetilde{\nabla\left(\dfrac{s_1}{\overline{S}}\right)F_l^P}+\dfrac{\partial}{\partial t}\widetilde{\left(\dfrac{s_1}{\overline{S}}\right)\mathbf{F}_1^{\mathbf{K}}}+(\overline{S})^{-1}\nabla\widetilde{(\overline{S}\cdot{}^1F_l^P)}+(\overline{S})^{-1}\dfrac{\partial}{\partial t}\widetilde{(\overline{S}\cdot{}^1\mathbf{F}_1^{\mathbf{K}})}\right] \\ -\dfrac{\partial\mathbf{K}_l(\overline{S})}{\partial\overline{S}}\overline{s_1(\overline{S})^{-1}\left[\nabla(\overline{S}\cdot F_l^P)+\dfrac{\partial}{\partial t}(\overline{S}\cdot\mathbf{F}_1^{\mathbf{K}})\right]}\end{array}\right] \\ \\ \mu_g^{-1}\cdot\nabla\cdot\left[\begin{array}{l}\left(\dfrac{1}{2}\dfrac{\partial^2\mathbf{K}_g(1-\overline{S})}{\partial\overline{S}^2}(1-\overline{S})+\dfrac{\mathbf{K}_g(1-\overline{S})}{1-\overline{S}}\right)\dfrac{\widetilde{(s_1)^2}}{(1-\overline{S})^2}\nabla(\overline{S}\cdot\overline{P}_g)+\left(\dfrac{\partial\mathbf{K}_g(1-\overline{S})}{\partial\overline{S}}+\dfrac{\mathbf{K}_g(1-\overline{S})}{1-\overline{S}}\right)\widetilde{(s_1\cdot p_1^g)}\dfrac{\nabla\overline{S}}{\overline{S}}+ \\ \dfrac{\partial\mathbf{K}_g(1-\overline{S})}{\partial\overline{S}}\widetilde{s_1\nabla p_1^g}-\dfrac{\mathbf{K}_g(1-\overline{S})}{1-\overline{S}}\widetilde{p_1^g\nabla s_1}-\left(\dfrac{\partial\mathbf{K}_g(1-\overline{S})}{\partial\overline{S}}-\dfrac{\mathbf{K}_g(1-\overline{S})}{1-\overline{S}}\right)\widetilde{\dfrac{s_1}{1-\overline{S}}\nabla\left(\dfrac{s_1}{1-\overline{S}}\right)}\cdot\overline{P}_g \\ -\left[-\mathbf{K}_g(1-\overline{S})\widetilde{\nabla\left(\dfrac{s_1}{1-\overline{S}}\right)F_g^P}-\dfrac{\partial}{\partial t}\widetilde{\left(\dfrac{s_1}{1-\overline{S}}\right)\mathbf{F}_g^{\mathbf{K}}}+(1-\overline{S})^{-1}\nabla\widetilde{((1-\overline{S})\cdot{}^1F_g^P)}+(1-\overline{S})^{-1}\dfrac{\partial}{\partial t}\widetilde{((1-\overline{S})\cdot{}^1\mathbf{F}_g^{\mathbf{K}})}\right] \\ -\dfrac{\partial\mathbf{K}_g(1-\overline{S})}{\partial\overline{S}}\overline{s_1(1-\overline{S})^{-1}\left[\nabla((1-\overline{S})\cdot F_g^P)+\dfrac{\partial}{\partial t}((1-\overline{S})\cdot\mathbf{F}_g^{\mathbf{K}})\right]}\end{array}\right] \end{array}\right)$$

Here

$$\{\widetilde{\ldots}\}=\{\ \}-\widetilde{\{\ldots\}}=\{\ \}-\lim_{T,L\to\infty}\frac{1}{T\cdot L^3}\int_0^{T,L}dt\mathbf{dx}\{\ldots\}$$

Summarizing, the $\left\{\overline{S}(\mathbf{x},t),\overline{P_l}(\mathbf{x},t),\overline{P_g}(\mathbf{x},t)\right\}$ that describe slow non-periodic transport in second order in vibration amplitude λ^2 satisfy the following set of equations:

$$\left(\text{Here } \overline{\frac{s_1}{\overline{S}}\nabla\left(\frac{s_1}{\overline{S}}\right)} \text{ and } \overline{\frac{s_1}{1-\overline{S}}\nabla\left(\frac{s_1}{1-\overline{S}}\right)} = 0 \text{ as } s_1 \text{ being periodic.}\right)$$

$$\frac{\partial}{\partial t}\begin{pmatrix}\overline{S}\\ -\overline{S}\end{pmatrix} = \frac{K_0}{\varepsilon}\cdot\begin{pmatrix}\mu_l^{-1}\cdot\nabla\cdot\left(\mathbf{K}_l\overline{S}^{-1}\nabla\left(\overline{SP_l}\right)\right)\\ \mu_g^{-1}\cdot\nabla\cdot\left(\mathbf{K}_g\left(1-\overline{S}\right)^{-1}\nabla\left(\left(1-\overline{S}\right)\overline{P}_g\right)\right)\end{pmatrix} + \frac{K_0}{\varepsilon}\cdot$$

$$\begin{pmatrix}\mu_l^{-1}\cdot\nabla\cdot\left[\left(\frac{1}{2}\frac{\partial^2\mathbf{K}_l\left(\overline{S}\right)}{\partial\overline{S}^2}\overline{S}+\frac{\mathbf{K}_l\left(\overline{S}\right)}{\overline{S}}\right)\frac{\overline{(s_1)^2}}{\overline{S}^2}\nabla\left(\overline{S}\cdot\overline{P}_l\right)+\left(\frac{\partial\mathbf{K}_l\left(\overline{S}\right)}{\partial\overline{S}}-\frac{\mathbf{K}_l\left(\overline{S}\right)}{\overline{S}}\right)\overline{\left(s_1\cdot p_1^l\right)}\frac{\nabla\overline{S}}{\overline{S}}+\frac{\partial\mathbf{K}_l\left(\overline{S}\right)}{\partial\overline{S}}\overline{s_1\nabla p_1^l}+\frac{\mathbf{K}_l\left(\overline{S}\right)}{\overline{S}}\overline{p_1^l\nabla s_1}\right]\\ \mu_g^{-1}\cdot\nabla\cdot\left[\left(\frac{1}{2}\frac{\partial^2\mathbf{K}_g\left(1-\overline{S}\right)}{\partial\overline{S}^2}\left(1-\overline{S}\right)+\frac{\mathbf{K}_g\left(1-\overline{S}\right)}{1-\overline{S}}\right)\frac{\overline{(s_1)^2}}{\left(1-\overline{S}\right)^2}\nabla\left(\overline{S}\cdot\overline{P}_g\right)+\left(\frac{\partial\mathbf{K}_g\left(1-\overline{S}\right)}{\partial\overline{S}}+\frac{\mathbf{K}_g\left(1-\overline{S}\right)}{1-\overline{S}}\right)\overline{\left(s_1\cdot p_1^g\right)}\frac{\nabla\overline{S}}{\overline{S}}+\right.\\ \left.\frac{\partial\mathbf{K}_g\left(1-\overline{S}\right)}{\partial\overline{S}}\overline{s_1\nabla p_1^g}-\frac{\mathbf{K}_g\left(1-\overline{S}\right)}{1-\overline{S}}\overline{p_1^g\nabla s_1}\right]\end{pmatrix}+$$

$$\frac{K_0}{\varepsilon}\cdot\begin{pmatrix}\mu_l^{-1}\cdot\nabla\cdot\left[-\mathbf{K}_l\left(\overline{S}\right)\left[\nabla\overline{\left(\frac{s_1}{\overline{S}}\right)F_l^P}+\frac{\partial}{\partial t}\overline{\left(\frac{s_1}{\overline{S}}\right)\mathbf{F}_l^{\mathbf{K}}}+\left(\overline{S}\right)^{-1}\nabla\left(\overline{S}\cdot\overline{{}^1F_l^P}\right)+\left(\overline{S}\right)^{-1}\frac{\partial}{\partial t}\left(\overline{S}\cdot\overline{{}^1\mathbf{F}_l^{\mathbf{K}}}\right)\right]-\frac{\partial\mathbf{K}_l\left(\overline{S}\right)}{\partial\overline{S}}\overline{s_1\left(\overline{S}\right)^{-1}\left[\nabla\left(\overline{S}\cdot F_l^P\right)+\frac{\partial}{\partial t}\left(\overline{S}\cdot\mathbf{F}_l^{\mathbf{K}}\right)\right]}\right]\\ \mu_g^{-1}\cdot\nabla\cdot\left[\begin{array}{l}-\mathbf{K}_g\left(1-\overline{S}\right)\left[-\nabla\overline{\left(\frac{s_1}{1-\overline{S}}\right)F_g^P}-\frac{\partial}{\partial t}\overline{\left(\frac{s_1}{1-\overline{S}}\right)\mathbf{F}_g^{\mathbf{K}}}+\left(1-\overline{S}\right)^{-1}\nabla\left(\overline{\left(1-\overline{S}\right)\cdot{}^1F_g^P}\right)+\left(1-\overline{S}\right)^{-1}\frac{\partial}{\partial t}\left(\overline{\left(1-\overline{S}\right)\cdot{}^1\mathbf{F}_g^{\mathbf{K}}}\right)\right]\\ -\frac{\partial\mathbf{K}_g\left(1-\overline{S}\right)}{\partial\overline{S}}\overline{s_1\left(1-\overline{S}\right)^{-1}\left[\nabla\left(\left(1-\overline{S}\right)\cdot F_g^P\right)+\frac{\partial}{\partial t}\left(\left(1-\overline{S}\right)\cdot\mathbf{F}_g^{\mathbf{K}}\right)\right]}\end{array}\right]\end{pmatrix}$$

$$\overline{P}_g-\overline{P}_l = J^{dr}\left(\overline{S}\right)+\frac{\partial J^{dr}\left(\overline{S}\right)}{\partial\overline{S}}\frac{\overline{(s_1)^2}}{2}+T\cdot\frac{\partial}{\partial t}\overline{S} \text{ for drainage } \left(\frac{\partial}{\partial t}\overline{S}<0\right)$$

and

$$\overline{P}_g-\overline{P}_l = J^{imb}\left(\overline{S}\right)+\frac{\partial J^{imb}\left(\overline{S}\right)}{\partial\overline{S}}\frac{\overline{(s_1)^2}}{2}+T\cdot\frac{\partial}{\partial t}\overline{S} \text{ for imbibition } \left(\frac{\partial}{\partial t}\overline{S}>0\right)$$

Here

$$\begin{pmatrix} \overline{{}^1F_l^P} \\ \overline{{}^1F_g^P} \end{pmatrix} = \begin{pmatrix} +\varepsilon \cdot b \cdot \overline{s_1 \cdot \nabla \cdot \mathbf{u}_g} \\ -\varepsilon \cdot b \cdot \overline{s_1 \cdot \nabla \cdot \mathbf{u}_l} \end{pmatrix}; \quad \begin{pmatrix} \widetilde{{}^1F_l^P} \\ \widetilde{{}^1F_g^P} \end{pmatrix} = \begin{pmatrix} q \cdot \nabla \cdot {}^1\mathbf{u}_s + r \cdot \nabla \cdot {}^1\mathbf{u}_l + \varepsilon \cdot b \cdot \overline{S} \cdot \nabla \cdot {}^1\mathbf{u}_g \\ t \cdot \nabla \cdot {}^1\mathbf{u}_s + \varepsilon \cdot b \cdot \left(1 - \overline{S}\right) \cdot \nabla \cdot {}^1\mathbf{u}_l + s \cdot \nabla \cdot {}^1\mathbf{u}_g \end{pmatrix}$$

$$\begin{pmatrix} \overline{{}^1\mathbf{F}_\mathbf{l}^\mathbf{K}} \\ \overline{{}^1\mathbf{F}_\mathbf{g}^\mathbf{K}} \end{pmatrix} = \begin{pmatrix} -\rho_g \beta_{gl} \overline{\frac{s_1}{S^2} \frac{\partial}{\partial t}\left(\mathbf{u}_l - \mathbf{u}_s\right)} \\ +\rho_l \beta_{gl} \overline{\frac{s_1}{\left(1-S\right)^2} \frac{\partial}{\partial t}\left(\mathbf{u}_g - \mathbf{u}_s\right)} \end{pmatrix};$$

$$\begin{pmatrix} \widetilde{{}^1\mathbf{F}_\mathbf{l}^\mathbf{K}} \\ \widetilde{{}^1\mathbf{F}_\mathbf{g}^\mathbf{K}} \end{pmatrix} = \begin{pmatrix} \rho_l \cdot \frac{\partial}{\partial t} {}^1\mathbf{u}_l + \left(\rho_l \cdot \beta_l + \rho_g \cdot \left(S^{-1} - 1\right) \cdot \beta_{gl}\right) \frac{\partial}{\partial t}\left({}^1\mathbf{u}_l - {}^1\mathbf{u}_s\right) \\ \rho_g \cdot \frac{\partial}{\partial t} {}^1\mathbf{u}_g + \left(\rho_g \cdot \beta_g + \rho_l \cdot \left(\left(1-S\right)^{-1} - 1\right) \cdot \beta_{gl}\right) \frac{\partial}{\partial t}\left({}^1\mathbf{u}_g - {}^1\mathbf{u}_s\right) \end{pmatrix}$$

As it has been mentioned earlier, $\widetilde{{}^1F_{l,g}^{K,P}}$ requires next order correction for $\{\mathbf{u}_s, \mathbf{u}_l, \mathbf{u}_g\}$. They are not appear in the equations for slow variables in the second order in λ and therefore are not computed here.

Appendix II.

Approximate solution by method of harmonic balance.

Assume now that $\{\mathbf{u}_s, \mathbf{u}_l, \mathbf{u}_g\}$ is a harmonic wave:

$$\begin{Bmatrix} \mathbf{u}_s \\ \mathbf{u}_l \\ \mathbf{u}_g \end{Bmatrix} = \begin{Bmatrix} {}^c\mathbf{u}_s \\ {}^c\mathbf{u}_l \\ {}^c\mathbf{u}_g \end{Bmatrix} \cdot \cos(\omega \cdot t + \mathbf{k} \cdot \mathbf{x}) + \begin{Bmatrix} {}^s\mathbf{u}_s \\ {}^s\mathbf{u}_l \\ {}^s\mathbf{u}_g \end{Bmatrix} \cdot \sin(\omega \cdot t + \mathbf{k} \cdot \mathbf{x})$$

and calculate additional pressure and permeability that this simple vibration induces in porous material. First, a response to this driving force needs to be calculated:

$$\begin{Bmatrix} s_l \\ p_l^l \\ p_l^g \end{Bmatrix} = \begin{Bmatrix} {}^c s_l \\ {}^c p_l^l \\ {}^c p_l^g \end{Bmatrix} \cdot \cos(\omega \cdot t + \mathbf{k} \cdot \mathbf{x}) + \begin{Bmatrix} {}^s s_l \\ {}^s p_l^l \\ {}^s p_l^g \end{Bmatrix} \cdot \sin(\omega \cdot t + \mathbf{k} \cdot \mathbf{x})$$

Substituting this into equations for $\{s_l(\mathbf{x},t), p_l^l(\mathbf{x},t), p_l^g(\mathbf{x},t)\}$ one finds the following linear system for amplitudes $\{{}^c s_l, {}^s s_l, {}^c p_l^l, {}^s p_l^l, {}^c p_l^g, {}^s p_l^g\}$:

Waves and structural vibrations.

Keeping the terms with the highest order in $\{\omega, \mathbf{k}\}$ one gets

$$\left(\begin{array}{c|c|cccc} D_l & \overline{S}^{-1} \cdot \overline{P_l} & 0 & 1 & 0 & 0 \\ \hline -\overline{S}^{-1} \cdot \overline{P_l} & D_l & -1 & 0 & 0 & 0 \\ \hline D_g & \left(1-\overline{S}\right)^{-1} \cdot \overline{P_g} & 0 & 0 & 0 & 1 \\ \hline -\left(1-\overline{S}\right)^{-1} \cdot \overline{P_g} & D_g & 0 & 0 & -1 & 0 \\ \hline -\partial J / \partial \overline{S} & T \cdot \omega & -1 & 0 & 1 & 0 \\ \hline -T \cdot \omega & -\partial J / \partial \overline{S} & 0 & -1 & 0 & 1 \end{array}\right) \cdot \begin{pmatrix} {}^c s_l \\ {}^s s_l \\ {}^c p_l^l \\ {}^s p_l^l \\ {}^c p_l^g \\ {}^s p_l^g \end{pmatrix} = -\begin{pmatrix} {}^c F^l \\ {}^s F^l \\ {}^c F^g \\ {}^s F^g \\ 0 \\ 0 \end{pmatrix}$$

where

$$\begin{pmatrix} D_l \\ D_g \end{pmatrix} = \begin{pmatrix} \dfrac{\mathbf{k}}{\mathbf{k}\cdot\mathbf{K}_1\cdot\mathbf{k}}\cdot\left[2\left(\dfrac{\partial\mathbf{K}_1}{\partial\overline{S}}-\dfrac{\mathbf{K}_1}{\overline{S}}\right)\cdot\dfrac{\nabla\overline{S}}{\overline{S}}\overline{P_l}+\left(\dfrac{\partial\mathbf{K}_1}{\partial\overline{S}}+\dfrac{\mathbf{K}_1}{\overline{S}}\right)\cdot\nabla\overline{P_l}\right]-\dfrac{\varepsilon\cdot\mu_l}{K_0}\cdot\dfrac{\omega}{\mathbf{k}\cdot\mathbf{K}_1\cdot\mathbf{k}} \\ \dfrac{\mathbf{k}}{\mathbf{k}\cdot\mathbf{K}_g\cdot\mathbf{k}}\cdot\left[2\left(\dfrac{\partial\mathbf{K}_g}{\partial\overline{S}}+\dfrac{\mathbf{K}_g}{1-\overline{S}}\right)\cdot\dfrac{\nabla\overline{S}}{1-\overline{S}}\overline{P_g}-\left(\dfrac{\partial\mathbf{K}_1}{\partial\overline{S}}-\dfrac{\mathbf{K}_1}{1-\overline{S}}\right)\cdot\nabla\overline{P_g}\right]+\dfrac{\varepsilon\cdot\mu_g}{K_0}\cdot\dfrac{\omega}{\mathbf{k}\cdot\mathbf{K}_g\cdot\mathbf{k}} \end{pmatrix}$$

and

$$\begin{pmatrix} {}^cF^l \\ {}^sF^l \\ {}^cF^g \\ {}^sF^g \end{pmatrix} = \begin{pmatrix} q\cdot\mathbf{k}\cdot{}^c\mathbf{u}_s + r\cdot\mathbf{k}\cdot{}^c\mathbf{u}_l + \varepsilon\cdot b\cdot\overline{S}\cdot\mathbf{k}\cdot{}^c\mathbf{u}_g \\ q\cdot\mathbf{k}\cdot{}^s\mathbf{u}_s + r\cdot\mathbf{k}\cdot{}^s\mathbf{u}_l + \varepsilon\cdot b\cdot\overline{S}\cdot\mathbf{k}\cdot{}^s\mathbf{u}_g \\ t\cdot\mathbf{k}\cdot{}^c\mathbf{u}_s + \varepsilon\cdot b\cdot\left(1-\overline{S}\right)\cdot\mathbf{k}\cdot{}^c\mathbf{u}_l + s\cdot\mathbf{k}\cdot{}^c\mathbf{u}_g \\ t\cdot\mathbf{k}\cdot{}^s\mathbf{u}_s + \varepsilon\cdot b\cdot\left(1-\overline{S}\right)\cdot\mathbf{k}\cdot{}^s\mathbf{u}_l + s\cdot\mathbf{k}\cdot{}^s\mathbf{u}_g \end{pmatrix} +$$

$$+\begin{pmatrix} \dfrac{\omega^2}{\mathbf{k}\cdot\mathbf{K}_1\cdot\mathbf{k}}\cdot\left(\rho_l\cdot\mathbf{k}\cdot\mathbf{K}_1\cdot{}^c\mathbf{u}_l+\left(\rho_l\cdot\beta_l+\rho_g\cdot\left(\overline{S}^{-1}-1\right)\cdot\beta_{gl}\right)\cdot\mathbf{k}\cdot\mathbf{K}_1\cdot\left({}^c\mathbf{u}_l-{}^c\mathbf{u}_s\right)\right) \\ \dfrac{\omega^2}{\mathbf{k}\cdot\mathbf{K}_1\cdot\mathbf{k}}\cdot\left(\rho_l\cdot\mathbf{k}\cdot\mathbf{K}_1\cdot{}^s\mathbf{u}_l+\left(\rho_l\cdot\beta_l+\rho_g\cdot\left(\overline{S}^{-1}-1\right)\cdot\beta_{gl}\right)\cdot\mathbf{k}\cdot\mathbf{K}_1\cdot\left({}^s\mathbf{u}_l-{}^s\mathbf{u}_s\right)\right) \\ \dfrac{\omega^2}{\mathbf{k}\cdot\mathbf{K}_g\cdot\mathbf{k}}\cdot\left(\rho_l\cdot\mathbf{k}\cdot\mathbf{K}_g\cdot{}^c\mathbf{u}_g+\left(\rho_g\cdot\beta_g+\rho_l\cdot\left(\left(1-\overline{S}\right)^{-1}-1\right)\cdot\beta_{gl}\right)\cdot\mathbf{k}\cdot\mathbf{K}_g\cdot\left({}^c\mathbf{u}_g-{}^c\mathbf{u}_s\right)\right) \\ \dfrac{\omega^2}{\mathbf{k}\cdot\mathbf{K}_g\cdot\mathbf{k}}\cdot\left(\rho_l\cdot\mathbf{k}\cdot\mathbf{K}_g\cdot{}^s\mathbf{u}_g+\left(\rho_g\cdot\beta_g+\rho_l\cdot\left(\left(1-\overline{S}\right)^{-1}-1\right)\cdot\beta_{gl}\right)\cdot\mathbf{k}\cdot\mathbf{K}_g\cdot\left({}^s\mathbf{u}_g-{}^s\mathbf{u}_s\right)\right) \end{pmatrix}$$

Eliminating $\left\{{}^cp_1^l, {}^sp_1^l, {}^cp_1^g, {}^sp_1^g\right\}$ from the equations above one gets the system for $\left\{{}^cs_1, {}^ss_1\right\}$ only:

$$\left(\begin{array}{c|c} -\dfrac{\partial J}{\partial\overline{S}}+\dfrac{\overline{P_l}}{\overline{S}}-\dfrac{\overline{P_g}}{1-\overline{S}} & T\cdot\omega-D_l+D_g \\ \hline -T\cdot\omega+D_l-D_g & -\dfrac{\partial J}{\partial\overline{S}}+\dfrac{\overline{P_l}}{\overline{S}}-\dfrac{\overline{P_g}}{1-\overline{S}} \end{array}\right)\cdot\begin{pmatrix} {}^cs_1 \\ {}^ss_1 \end{pmatrix} = \begin{pmatrix} {}^sF^l - {}^sF^g \\ {}^cF^g - {}^cF^l \end{pmatrix}$$

and $\overline{s^2} = \left({}^cs_1\right)^2 + \left({}^ss_1\right)^2 = \left({}^sF^l - {}^sF^g\right)^2 + \left({}^cF^g - {}^cF^l\right)^2$

Shaking.

Spatial wave dependencies are neglected in this case. Keeping only the terms with the highest order in ω one gets:

$$\left(\begin{array}{c|c|cccc}
D_l & -\omega\cdot\dfrac{\varepsilon\cdot\mu}{K_0}\cdot\dfrac{1}{\nabla\left(\mathbf{K}_l S^{-1}\nabla S\right)} & 1 & 0 & 0 & 0 \\
\hline
\omega\cdot\dfrac{\varepsilon\cdot\mu}{K_0}\cdot\dfrac{1}{\nabla\left(\mathbf{K}_l S^{-1}\nabla S\right)} & D_l & 0 & 1 & 0 & 0 \\
\hline
D_g & \omega\cdot\dfrac{\varepsilon\cdot\mu}{K_0}\cdot\dfrac{1}{\nabla\left(\mathbf{K}_g (1-S)^{-1}\nabla S\right)} & 0 & 0 & -1 & 0 \\
\hline
-\omega\cdot\dfrac{\varepsilon\cdot\mu}{K_0}\cdot\dfrac{1}{\nabla\left(\mathbf{K}_g (1-S)^{-1}\nabla S\right)} & D_g & 0 & 0 & 0 & -1 \\
\hline
-\partial J/\partial\bar{S} & T\cdot\omega & -1 & 0 & 1 & 0 \\
\hline
-T\cdot\omega & -\partial J/\partial\bar{S} & 0 & -1 & 0 & 1
\end{array}\right)\cdot\begin{pmatrix} {}^{c}s_1 \\ {}^{s}s_1 \\ {}^{c}p_1^{l} \\ {}^{s}p_1^{l} \\ {}^{c}p_1^{g} \\ {}^{s}p_1^{g} \end{pmatrix} = -\begin{pmatrix} {}^{c}F^{l} \\ {}^{s}F^{l} \\ {}^{c}F^{g} \\ {}^{s}F^{g} \\ 0 \\ 0 \end{pmatrix}$$

where

$$\begin{pmatrix} D_l \\ D_g \end{pmatrix} = \begin{pmatrix} \dfrac{\nabla\left[\left(\dfrac{\partial\mathbf{K}_1}{\partial\bar{S}}-\dfrac{\mathbf{K}_1}{\bar{S}}\right)\cdot\dfrac{\nabla\bar{S}}{\bar{S}}\bar{P}_l+\dfrac{\partial\mathbf{K}_1}{\partial\bar{S}}\cdot\nabla\bar{P}_l\right]}{\nabla\left(\mathbf{K}_1\cdot\dfrac{\nabla\bar{S}}{\bar{S}}\right)} \\ \dfrac{\nabla\left[\left(\dfrac{\partial\mathbf{K}_g}{\partial\bar{S}}+\dfrac{\mathbf{K}_g}{1-\bar{S}}\right)\cdot\dfrac{\nabla\bar{S}}{1-\bar{S}}\bar{P}_g+\dfrac{\partial\mathbf{K}_g}{\partial\bar{S}}\cdot\nabla\bar{P}_g\right]}{\nabla\left(\mathbf{K}_g\cdot\dfrac{\nabla\bar{S}}{1-\bar{S}}\right)} \end{pmatrix}$$

and

$$\begin{pmatrix} {}^{c}F^{l} \\ {}^{s}F^{l} \\ {}^{c}F^{g} \\ {}^{s}F^{g} \end{pmatrix} = \begin{pmatrix} \rho_l \cdot \omega^2 \cdot \dfrac{\nabla \cdot \mathbf{K}_l \cdot \left({}^{c}\mathbf{u}_l + \left(\beta_l + \beta_{gl} \cdot \dfrac{\rho_g}{\rho_l} \cdot \left(\overline{S}^{-1} - 1 \right) \right) \cdot \left({}^{c}\mathbf{u}_s - {}^{c}\mathbf{u}_l \right) \right)}{\nabla \left(\mathbf{K}_l \cdot \dfrac{\nabla \overline{S}}{\overline{S}} \right)} \\ \rho_l \cdot \omega^2 \cdot \dfrac{\nabla \cdot \mathbf{K}_l \cdot \left({}^{s}\mathbf{u}_l + \left(\beta_l + \beta_{gl} \cdot \dfrac{\rho_g}{\rho_l} \cdot \left(\overline{S}^{-1} - 1 \right) \right) \cdot \left({}^{s}\mathbf{u}_s - {}^{s}\mathbf{u}_l \right) \right)}{\nabla \left(\mathbf{K}_l \cdot \dfrac{\nabla \overline{S}}{\overline{S}} \right)} \\ \rho_g \cdot \omega^2 \cdot \dfrac{\nabla \cdot \mathbf{K}_g \cdot \left({}^{c}\mathbf{u}_g + \left(\beta_g + \beta_{gl} \cdot \dfrac{\rho_l}{\rho_g} \cdot \left(\left(1 - \overline{S} \right)^{-1} - 1 \right) \right) \cdot \left({}^{c}\mathbf{u}_s - {}^{c}\mathbf{u}_g \right) \right)}{\nabla \left(\mathbf{K}_g \cdot \dfrac{\nabla \overline{S}}{1 - \overline{S}} \right)} \\ \rho_g \cdot \omega^2 \cdot \dfrac{\nabla \cdot \mathbf{K}_g \cdot \left({}^{s}\mathbf{u}_g + \left(\beta_g + \beta_{gl} \cdot \dfrac{\rho_l}{\rho_g} \cdot \left(\left(1 - \overline{S} \right)^{-1} - 1 \right) \right) \cdot \left({}^{s}\mathbf{u}_s - {}^{s}\mathbf{u}_g \right) \right)}{\nabla \left(\mathbf{K}_g \cdot \dfrac{\nabla \overline{S}}{1 - \overline{S}} \right)} \end{pmatrix}$$

Eliminating $\left\{ {}^{c}p_1^l, {}^{s}p_1^l, {}^{c}p_1^g, {}^{s}p_1^g \right\}$ from the equations above one gets the system for $\left\{ {}^{c}s_1, {}^{s}s_1 \right\}$ only:

$$\left(\begin{array}{c|c} -\dfrac{\partial J}{\partial \overline{S}} + D_l + D_g & \omega \cdot \left(T + \dfrac{\varepsilon \cdot \mu}{K_0} \left[\dfrac{1}{\nabla \left(\mathbf{K}_l \left(1 - S \right)^{-1} \nabla S \right)} - \dfrac{1}{\nabla \left(\mathbf{K}_l S^{-1} \nabla S \right)} \right] \right) \\ \hline -\omega \cdot \left(T + \dfrac{\varepsilon \cdot \mu}{K_0} \left[\dfrac{1}{\nabla \left(\mathbf{K}_l \left(1 - S \right)^{-1} \nabla S \right)} - \dfrac{1}{\nabla \left(\mathbf{K}_l S^{-1} \nabla S \right)} \right] \right) & -\dfrac{\partial J}{\partial \overline{S}} + D_l + D_g \end{array} \right) \cdot \begin{pmatrix} {}^{c}s_1 \\ {}^{s}s_1 \end{pmatrix} = -\begin{pmatrix} {}^{c}F^{g} + {}^{c}F^{l} \\ {}^{s}F^{l} + {}^{s}F^{g} \end{pmatrix}$$

and

$$\overline{s^2} = \left({}^{c}s_1 \right)^2 + \left({}^{s}s_1 \right)^2 = \frac{\left({}^{s}F^{l} + {}^{s}F^{g} \right)^2 + \left({}^{c}F^{g} + {}^{c}F^{l} \right)^2}{\left(-\dfrac{\partial J}{\partial \overline{S}} + D_l + D_g \right)^2 + \omega^2 \cdot \left(T + \dfrac{\varepsilon \cdot \mu}{K_0} \left[\dfrac{1}{\nabla \left(\mathbf{K}_l \left(1 - S \right)^{-1} \nabla S \right)} - \dfrac{1}{\nabla \left(\mathbf{K}_l S^{-1} \nabla S \right)} \right] \right)^2}$$

Correlations of induced saturation and pressure.

Rewriting equations for $\left\{{}^{c}s_1, {}^{s}s_1, {}^{c}p_1^l, {}^{s}p_1^l, {}^{c}p_1^g, {}^{s}p_1^g\right\}$ in matrix notations,

$$\mathbf{L}^w \cdot \mathbf{s}_1 + \mathbf{J} \cdot \mathbf{p}_1^l = \mathbf{f}_l^w$$

$$\mathbf{G}^w \cdot \mathbf{s}_1 + \mathbf{J} \cdot \mathbf{p}_1^g = \mathbf{f}_g^w$$

$$\mathbf{C} \cdot \mathbf{s}_1 - \mathbf{I} \cdot \mathbf{p}_1^l + \mathbf{I} \cdot \mathbf{p}_1^g = 0$$

for waves and

$$\mathbf{L}^{sh} \cdot \mathbf{s}_1 + \mathbf{I} \cdot \mathbf{p}_1^l = \mathbf{f}_l^{sh}$$

$$\mathbf{G}^{sh} \cdot \mathbf{s}_1 - \mathbf{I} \cdot \mathbf{p}_1^g = \mathbf{f}_g^{sh}$$

$$\mathbf{C} \cdot \mathbf{s}_1 - \mathbf{I} \cdot \mathbf{p}_1^l + \mathbf{I} \cdot \mathbf{p}_1^g = 0$$

for shaking.

Here:

$\mathbf{J} = \begin{pmatrix} 0 & 1 \\ -1 & 0 \end{pmatrix}; \mathbf{I} = \begin{pmatrix} 1 & 0 \\ 0 & 1 \end{pmatrix}$ with the obvious property $\mathbf{J}^T \cdot \mathbf{J} = \mathbf{I}$;

$$\mathbf{L}^{w,sh} = \begin{pmatrix} D_l & N_l \\ -N_l & D_l \end{pmatrix}^{w,sh}; \mathbf{G}^{w,sh} = \begin{pmatrix} D_g & N_g \\ -N_g & D_g \end{pmatrix}^{w,sh}; \mathbf{C} = \begin{pmatrix} -\partial J/\partial S & T \cdot \omega \\ -T \cdot \omega & -\partial J/\partial S \end{pmatrix}$$

and

$$\mathbf{f}_{l,g}^{w,sh} = -\begin{pmatrix} {}^{c}F^{l,g} \\ {}^{c}F^{l,g} \end{pmatrix}^{w,sh}$$

From this, first, expressions for $\left\{\mathbf{s}_1, \mathbf{p}_1^l, \mathbf{p}_1^g\right\}$ can be found:

$$\mathbf{s}_1 = \left(\mathbf{C} + \mathbf{J} \cdot \mathbf{L}^w - \mathbf{J} \cdot \mathbf{G}^w\right)^{-1} \left(\mathbf{f}_l^w - \mathbf{f}_g^w\right)$$

$$\mathbf{p}_1^l = \mathbf{J} \cdot \left(\mathbf{f}_l^w - \mathbf{L}^w \cdot \left(\mathbf{C} + \mathbf{J} \cdot \mathbf{L}^w - \mathbf{J} \cdot \mathbf{G}^w\right)^{-1} \left(\mathbf{f}_l^w - \mathbf{f}_g^w\right)\right)$$

$$\mathbf{p}_1^g = \mathbf{J} \cdot \left(\mathbf{f}_g^w - \mathbf{G}^w \cdot \left(\mathbf{C} + \mathbf{J} \cdot \mathbf{L}^w - \mathbf{J} \cdot \mathbf{G}^w\right)^{-1} \left(\mathbf{f}_l^w - \mathbf{f}_g^w\right)\right)$$

for waves and

$$\mathbf{s}_1 = \left(\mathbf{C} + \mathbf{L}^{sh} + \mathbf{G}^{sh}\right)^{-1} \left(\mathbf{f}_l^{sh} + \mathbf{f}_g^{sh}\right)$$

$$\mathbf{p}_1^l = \mathbf{f}_l^{sh} - \mathbf{L}^{sh} \cdot \left(\mathbf{C} + \mathbf{L}^{sh} + \mathbf{G}^{sh}\right)^{-1} \left(\mathbf{f}_l^{sh} + \mathbf{f}_g^{sh}\right)$$

$$\mathbf{p}_1^g = -\mathbf{f}_g^{sh} + \mathbf{G}^{sh} \cdot \left(\mathbf{C} + \mathbf{L}^{sh} + \mathbf{G}^{sh}\right)^{-1} \left(\mathbf{f}_l^{sh} + \mathbf{f}_g^{sh}\right)$$

for shaking.

And then the correlations entering equations for the second order might be expressed:

$$\overline{s_1^2} = {}^T\mathbf{s}_1 \cdot \mathbf{s}_1 = \frac{{}^T\left(\mathbf{f}_l^w - \mathbf{f}_g^w\right)\cdot\left(\mathbf{f}_l^w - \mathbf{f}_g^w\right)}{\det\left(\mathbf{C} + \mathbf{J}\cdot\mathbf{L}^w - \mathbf{J}\cdot\mathbf{G}^w\right)}$$

$$\overline{s_1 \cdot p_1^l} = {}^T\mathbf{s}_1 \cdot \mathbf{p}_1^l = {}^T\left(\mathbf{f}_l^w - \mathbf{f}_g^w\right)\cdot {}^T\left(\mathbf{C} + \mathbf{J}\cdot\mathbf{L}^w - \mathbf{J}\cdot\mathbf{G}^w\right)^{-1}\cdot\mathbf{J}\cdot\left(\mathbf{f}_l^w - \mathbf{L}^w\cdot\left(\mathbf{C} + \mathbf{J}\cdot\mathbf{L}^w - \mathbf{J}\cdot\mathbf{G}^w\right)^{-1}\cdot\left(\mathbf{f}_l^w - \mathbf{f}_g^w\right)\right)$$

$$\overline{s_1 \cdot p_1^g} = {}^T\mathbf{s}_1 \cdot \mathbf{p}_1^g = {}^T\left(\mathbf{f}_l^w - \mathbf{f}_g^w\right)\cdot {}^T\left(\mathbf{C} + \mathbf{J}\cdot\mathbf{L}^w - \mathbf{J}\cdot\mathbf{G}^w\right)^{-1}\cdot\mathbf{J}\cdot\left(\mathbf{f}_l^w - \mathbf{G}^w\cdot\left(\mathbf{C} + \mathbf{J}\cdot\mathbf{L}^w - \mathbf{J}\cdot\mathbf{G}^w\right)^{-1}\cdot\left(\mathbf{f}_l^w - \mathbf{f}_g^w\right)\right)$$

$$\overline{s_1 \cdot \nabla p_1^l} = \overline{\nabla s_1 \cdot p_1^l} = {}^T\mathbf{s}_1 \cdot \mathbf{J}\cdot\mathbf{p}_1^l \cdot \mathbf{k} =$$

$${}^T\left(\mathbf{f}_l^w - \mathbf{f}_g^w\right)\cdot {}^T\left(\mathbf{C} + \mathbf{J}\cdot\mathbf{L}^w - \mathbf{J}\cdot\mathbf{G}^w\right)^{-1}\cdot\left(\mathbf{f}_l^w - \mathbf{L}^w\cdot\left(\mathbf{C} + \mathbf{J}\cdot\mathbf{L}^w - \mathbf{J}\cdot\mathbf{G}^w\right)^{-1}\cdot\left(\mathbf{f}_l^w - \mathbf{f}_g^w\right)\right)\cdot\mathbf{k}$$

$$\overline{s_1 \cdot \nabla p_1^g} = \overline{\nabla s_1 \cdot p_1^g} = {}^T\mathbf{s}_1 \cdot \mathbf{J}\cdot\mathbf{p}_1^g \cdot \mathbf{k} =$$

$${}^T\left(\mathbf{f}_l^w - \mathbf{f}_g^w\right)\cdot {}^T\left(\mathbf{C} + \mathbf{J}\cdot\mathbf{L}^w - \mathbf{J}\cdot\mathbf{G}^w\right)^{-1}\cdot\left(\mathbf{f}_l^w - \mathbf{G}^w\cdot\left(\mathbf{C} + \mathbf{J}\cdot\mathbf{L}^w - \mathbf{J}\cdot\mathbf{G}^w\right)^{-1}\cdot\left(\mathbf{f}_l^w - \mathbf{f}_g^w\right)\right)\cdot\mathbf{k}$$

for waves and

$$\overline{s_1^2} = {}^T\mathbf{s}_1 \cdot \mathbf{s}_1 = \frac{{}^T\left(\mathbf{f}_l^w + \mathbf{f}_g^w\right)\cdot\left(\mathbf{f}_l^w + \mathbf{f}_g^w\right)}{\det\left(\mathbf{C} + \mathbf{L}^{sh} + \mathbf{G}^{sh}\right)}$$

$$\overline{s_1 \cdot p_1^l} = {}^T\mathbf{s}_1 \cdot \mathbf{p}_1^l = {}^T\left(\mathbf{f}_l^w + \mathbf{f}_g^w\right)\cdot {}^T\left(\mathbf{C} + \mathbf{L}^{sh} + \mathbf{G}^{sh}\right)^{-1}\cdot\left(\mathbf{f}_l^{sh} - \mathbf{L}^{sh}\cdot\left(\mathbf{C} + \mathbf{L}^{sh} + \mathbf{G}^{sh}\right)^{-1}\left(\mathbf{f}_l^w + \mathbf{f}_g^w\right)\right)$$

$$\overline{s_1 \cdot p_1^g} = {}^T\mathbf{s}_1 \cdot \mathbf{p}_1^g = {}^T\left(\mathbf{f}_l^w + \mathbf{f}_g^w\right)\cdot {}^T\left(\mathbf{C} + \mathbf{L}^{sh} + \mathbf{G}^{sh}\right)^{-1}\cdot\left(\mathbf{f}_l^{sh} - \mathbf{G}^{sh}\cdot\left(\mathbf{C} + \mathbf{L}^{sh} + \mathbf{G}^{sh}\right)^{-1}\left(\mathbf{f}_l^w + \mathbf{f}_g^w\right)\right)$$

for shaking.

Appendix III

Dynamics of saturation

Detailed sequence of snapshots demontsrating the change of watert saturation with time is shown below.

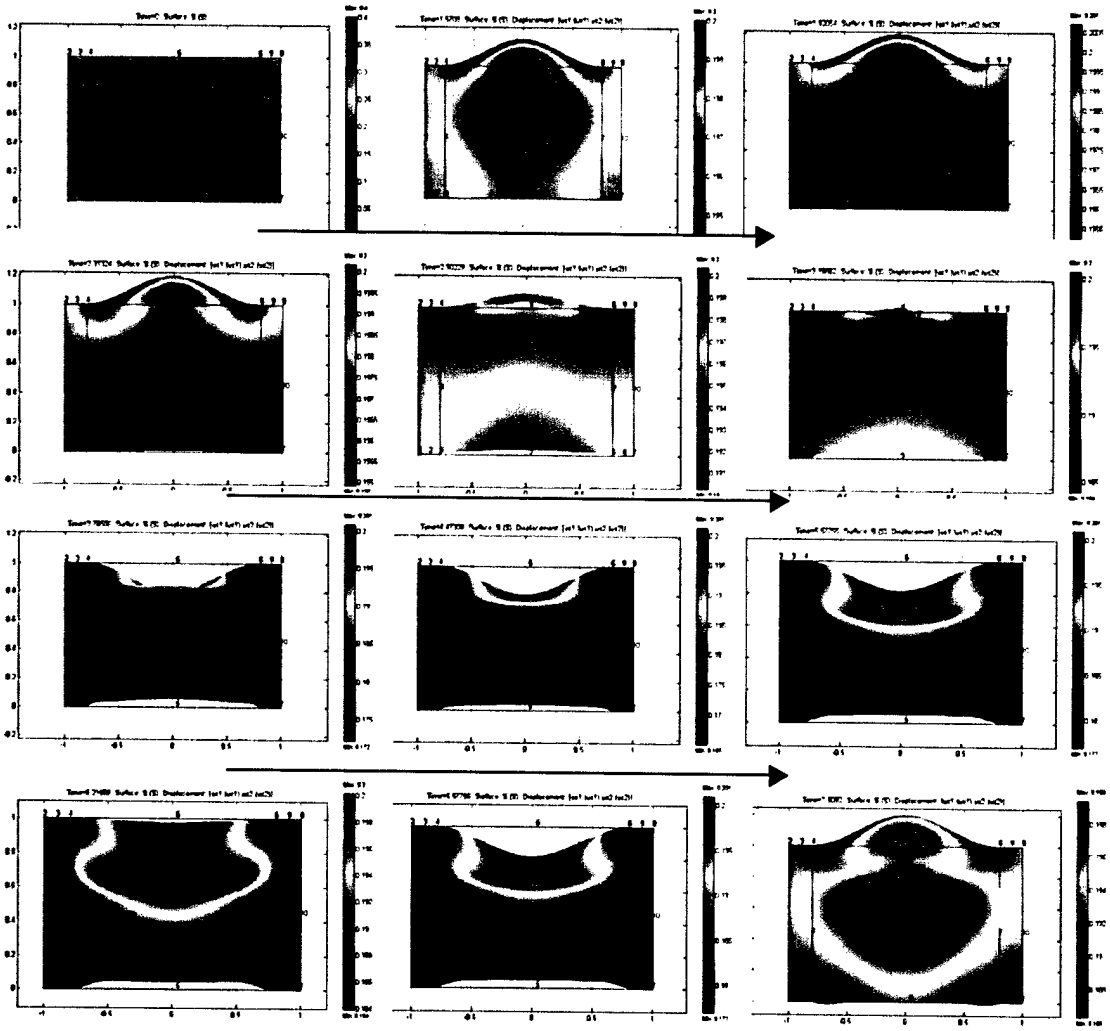

Gas and liquid pressure.

Comparison between gas and liquid pressure with structural vibrations is shown in figures below. One can see the degree of in-phase oscillations.

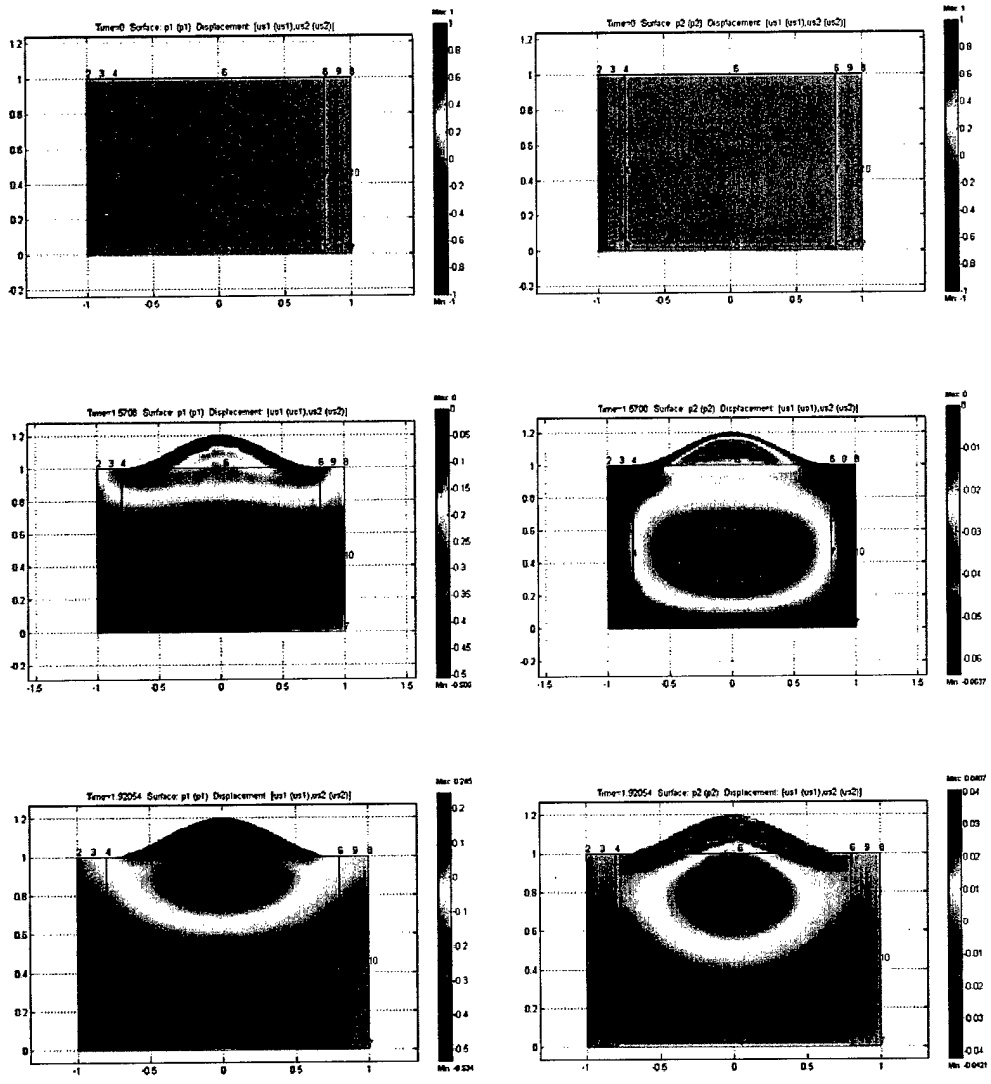

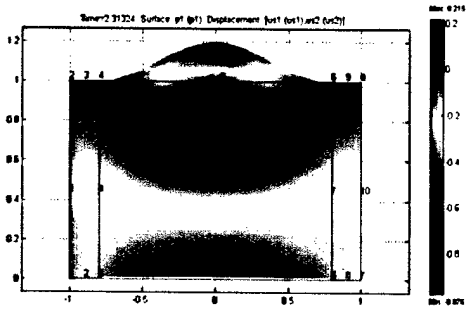

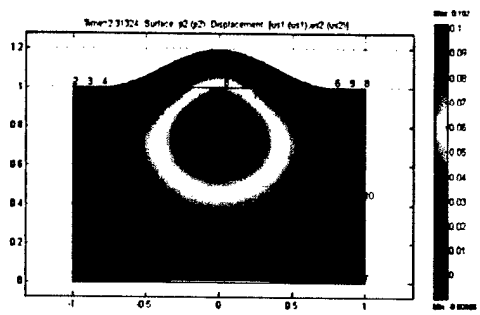

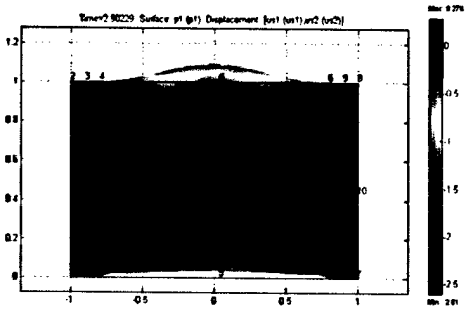

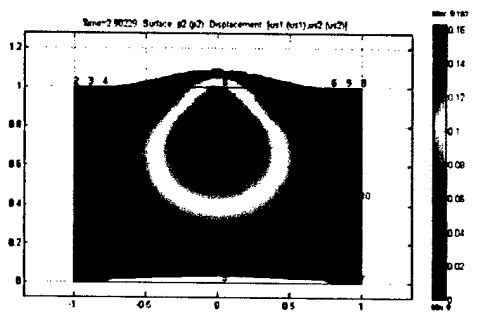

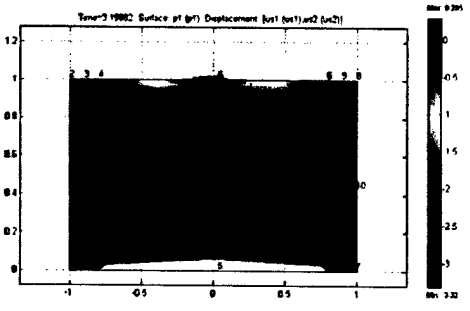

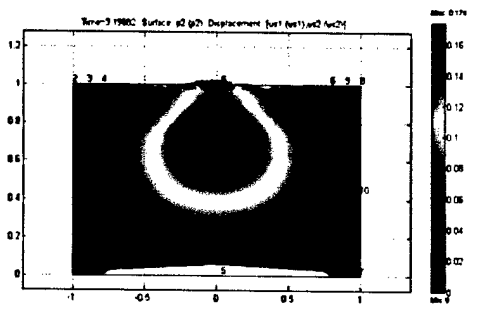

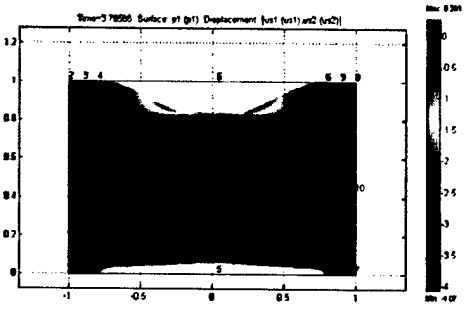

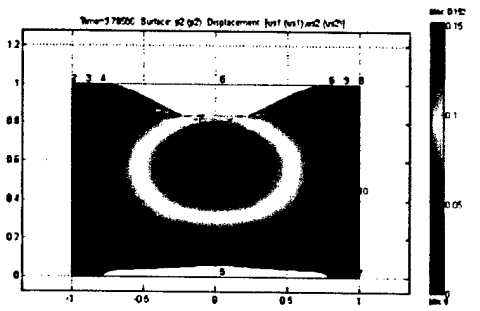

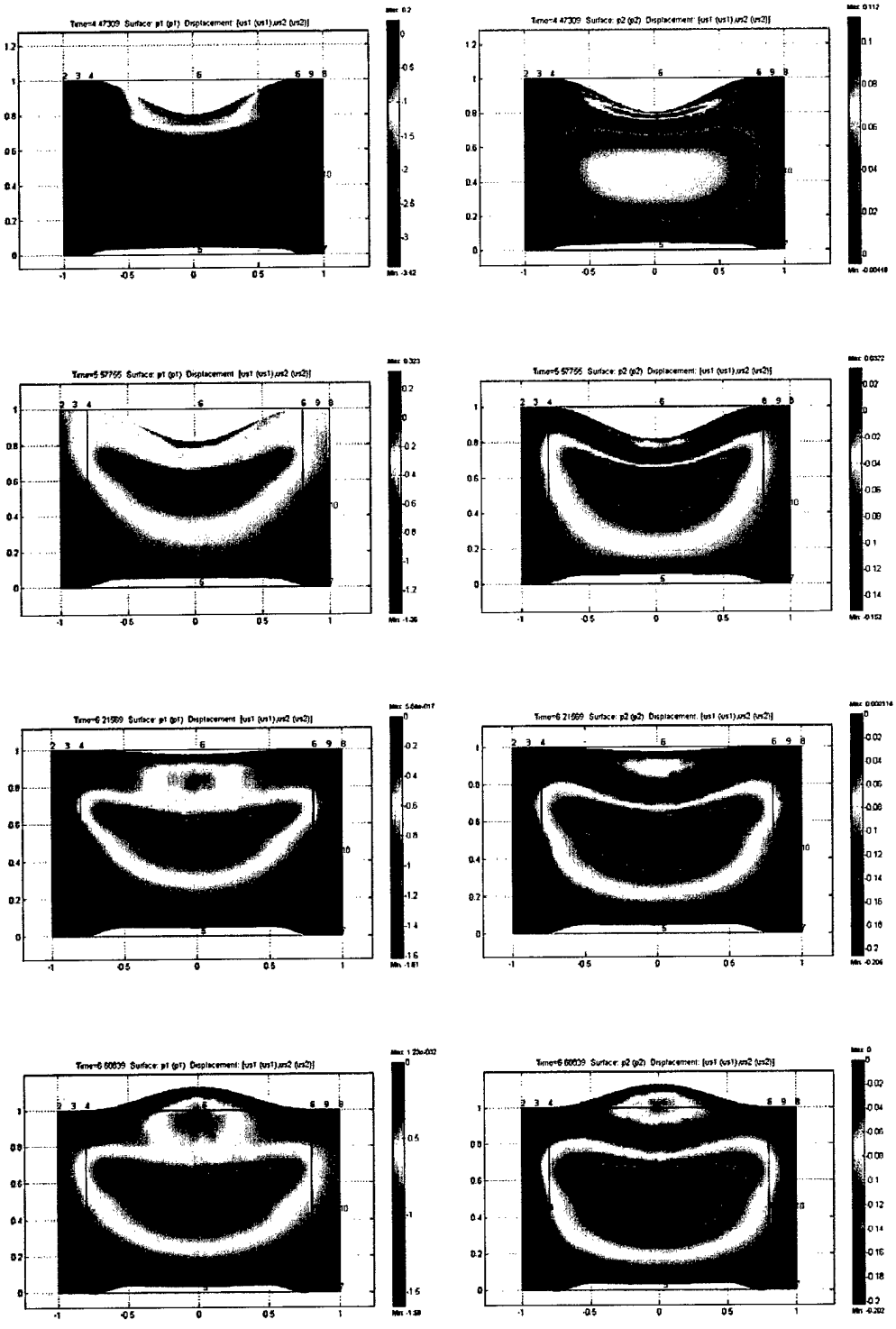

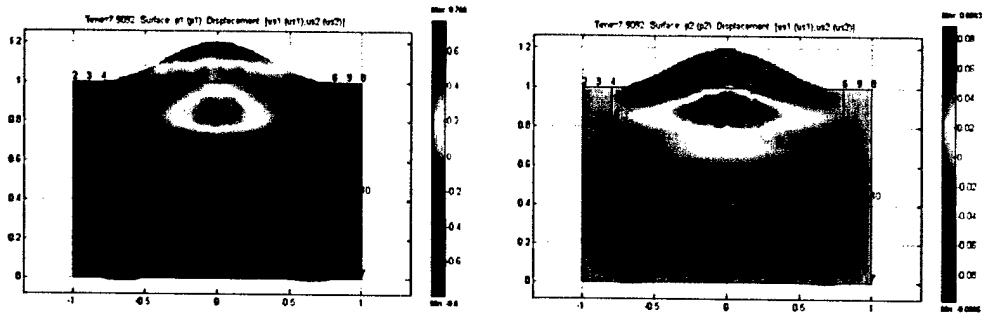

Liquid versus solid displacement: the mode perpendicular to the excitation.

Figures below illustrate x-displacement of solid and liquid phases with time

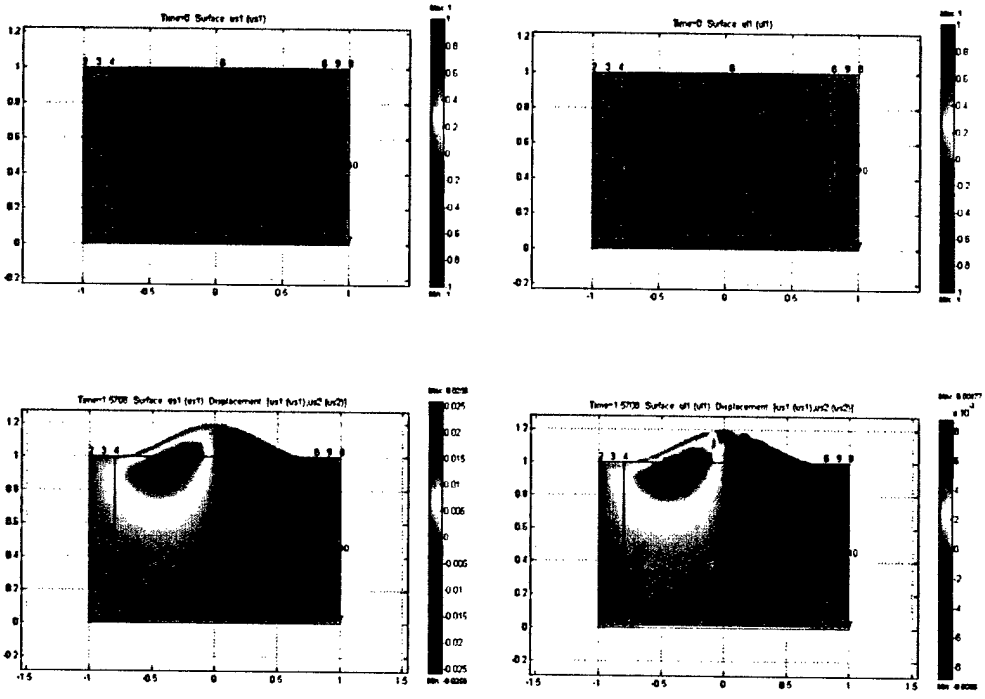

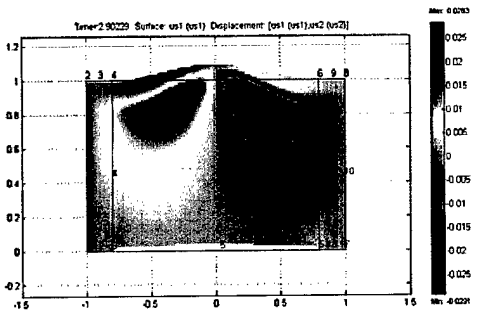

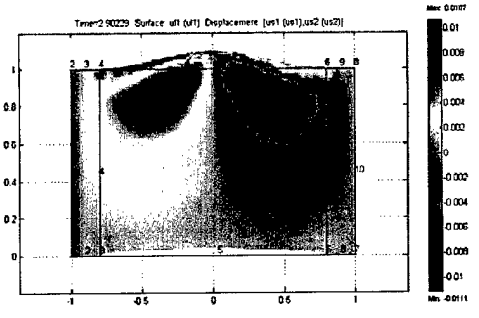

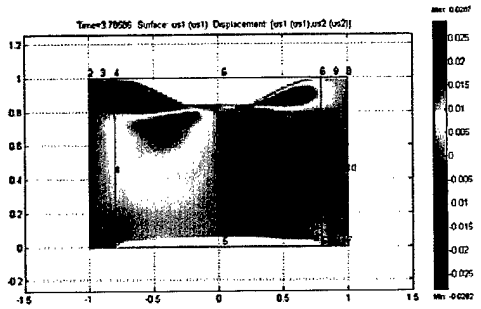

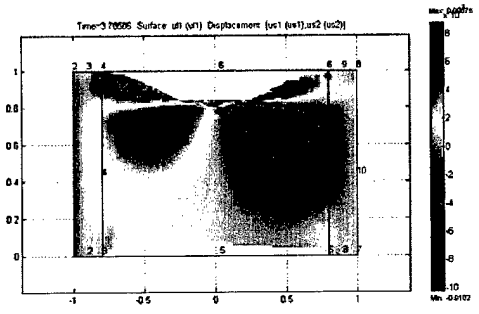

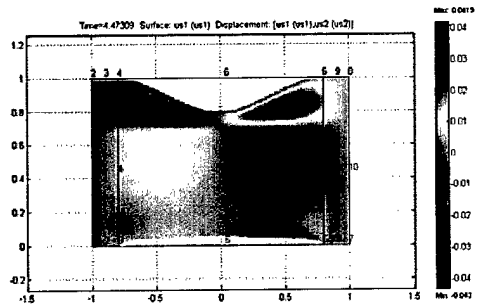

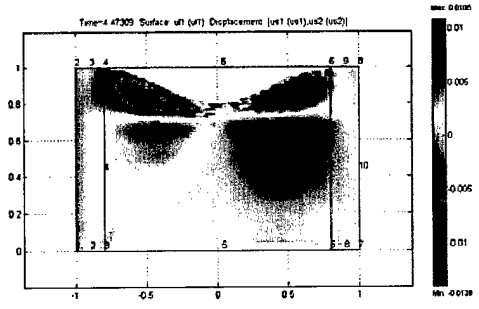

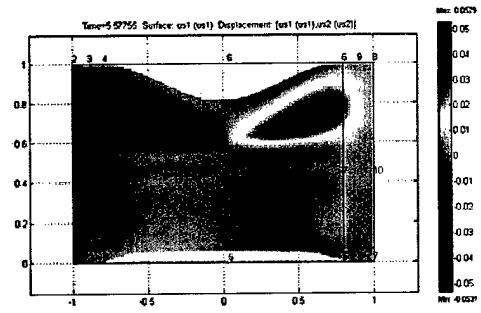

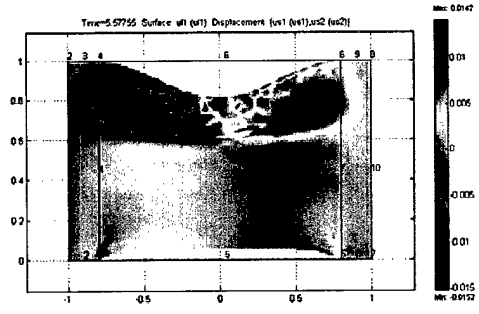

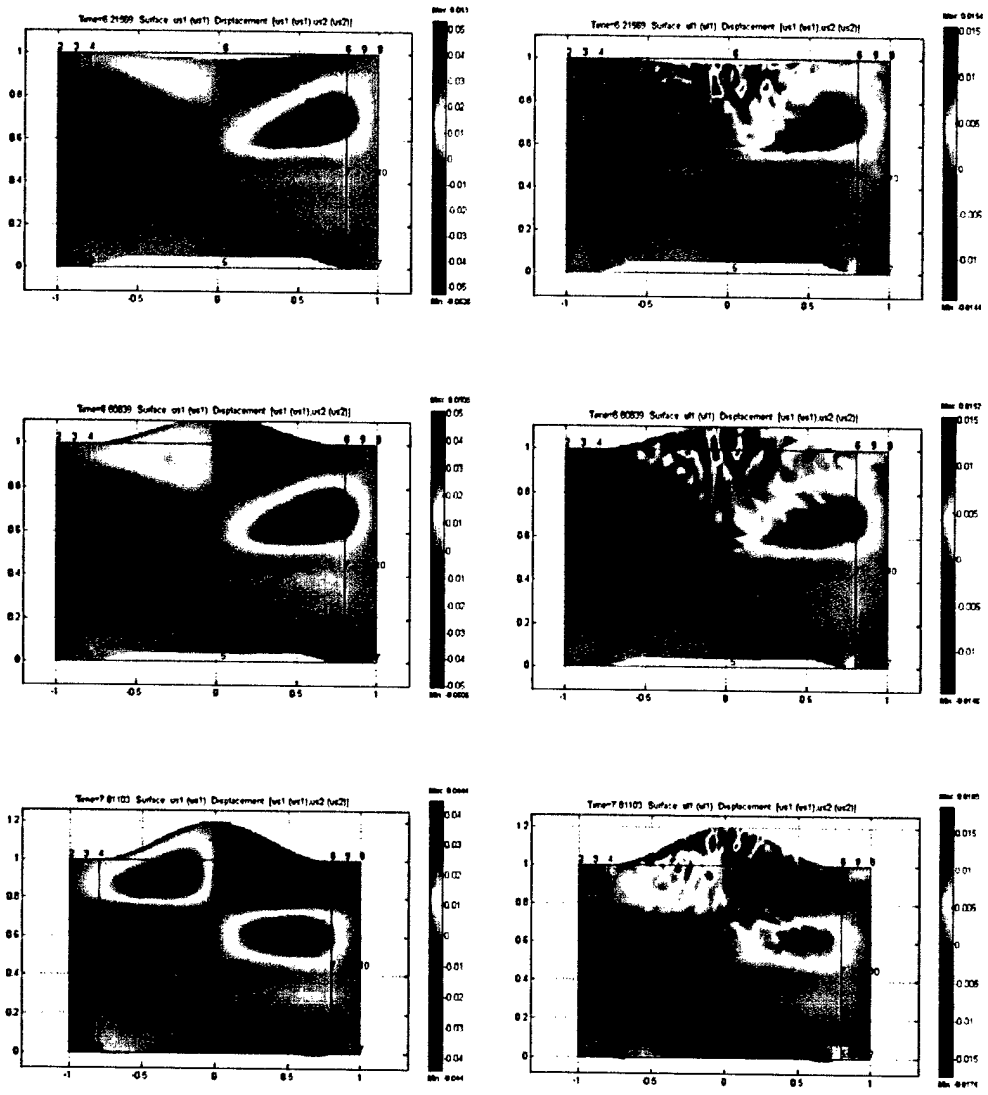

Solid versus liquid displacement: the mode collinear with the excitation.

Next set of figures illustrates the comparison between displacement of solid and liquid phases in y-direction, along the plate thickness.